A STUDY OF SOME CAMBRIAN SEDIMENTS
FROM JASPER PARK,
ALBERTA.

BY

PHILIP CHARLES WALLER

MAY, 1959

For Reference

NOT TO BE TAKEN FROM THIS ROOM

Ex libris
universitatis
albertaensis

UNIVERSITY OF ALBERTA
QUAECUMQUE VERA

Digitized by the Internet Archive
in 2018 with funding from
University of Alberta Libraries

https://archive.org/details/studyofsomecambr00phil

THESIS
1959(F)
#48

THE UNIVERSITY OF ALBERTA

A STUDY OF SOME CAMBRIAN SEDIMENTS FROM JASPER PARK, ALBERTA

A DISSERTATION

SUBMITTED TO THE FACULTY OF GRADUATE STUDIES

IN PARTIAL FULFILMENT OF THE REQUIREMENTS FOR THE DEGREE

MASTER OF SCIENCE

DEPARTMENT OF GEOLOGY

by

PHILIP CHARLES WALLER

EDMONTON, ALBERTA

MAY, 1959

Frontispiece

Sunset Peak Area. - Photograph taken from location 6 looking southeast toward massive westerly-dipping Cambrian quartzites (ridges) and limy or shaly beds (saddles). Edith Cavell quartzites on left, Bosche(?) formation on far right (photo by R. E. Folinsbee).

ACKNOWLEDGMENT

The writer wishes to extend his sincere gratitude to Dr. R. E. Folinsbee, Department of Geology, under whose direction this study was undertaken, for his guidance and assistance. Grateful acknowledgment for advice and constructive criticism is made to Dr. H. Baadsgaard, for his assistance with the glauconite analysis and potassium-argon age determinations; to Dr. C. R. Stelck, for his assistance on palaeontology; to Drs. J. F. Lerbekmo, S. J. Nelson and F. A. Campbell for critically reviewing various portions of the manuscript; and finally, to all other members of the Department of Geology for their suggestions and criticisms.

The writer would like to thank Mr. N. G. Koch for able assistance rendered in collecting outcrop samples from the Nigel Pass Area.

The University of Minnesota kindly forwarded samples of glauconites KA-113 and KA-114.

The Department of Mining and Metallurgy kindly permitted the writer the use of their specialized x-ray equipment.

The Department of Geology was very generous in providing for the plates and thin-sections.

ABSTRACT

Cambrian sediments from the Nigel Pass and Sunset Peak Areas of Jasper Park, Alberta, are the subject of this study. Twenty-six thin-sections and three suites of heavy minerals are described.

Cambrian sediments were deposited on a shallow, slowly subsiding shelf area flanking the craton. Lower Cambrian sediments were derived from the craton and Precambrian Beltian sediments.

The presence of glauconite in the Sunset Peak calcareous quartzitic sediments indicates slow deposition in a nearly neutral environment. X-ray and chemical analysis of this glauconite indicate it is ordered and rich in potassium. It has the chemical formula $K_{1.63}(Na,Rb,Ca)_{.06}(Al_{2.44}Fe^{+3}_{.76}Fe^{+2}_{.22}Mg_{.60})(Si_{7.00}Al_{1.00})O_{20}(OH)_4$. The chemical composition shows this glauconite to be a representative of the aluminum-rich glauconites, which are rare.

Potassium-argon dating of this authigenic glauconite and what appears to be a detrital microcline feldspar from these Lower Cambrian sediments yielded ages of 359, 413 and 344 million years respectively. The glauconite age is slightly low because of argon leakage; the feldspar (probably Precambrian) age is close to the 360 million year figure obtained at the University of Alberta for a biotite from the Ice River Complex of the Rocky Mountains and Yukon granites intruded at the time of the Cariboo orogeny. There is a distinct possibility that this feldspar age may reflect in some way the influence of the Cariboo orogeny which White (1959) postulates to have taken place from Late Ordovician through Devonian time.

TABLE OF CONTENTS

PAGE

CHAPTER ONE 1

Introduction 1

Previous Work 2

Material Used 3

CHAPTER TWO - STRATIGRAPHY, PALAEONTOLOGY AND PALAEOGEOGRAPHY 7

General Statement 7

Stratigraphy 7

Nigel Pass Area 7

Sunset Peak Area 12

Distribution of Cambrian 15

Palaeontology 16

Nigel Pass Area 16

Sunset Peak Area 16

Palaeogeography 17

CHAPTER THREE - PETROGRAPHY 23

General Description 23

Nigel Pass Area 23

Jonas Creek formation 23

Mount Whyte formation 24

Sunset Peak Area 25

Edith Cavell quartzite 25

Beds Overlying the Edith Cavell quartzite.............. 25

Heavy Accessory Minerals 26

General Statement 26

PAGE

Procedure 26

Opaque Heavy Minerals 28

Non-Opaque Heavy Minerals 29

Provenance 32

CHAPTER FOUR - MECHANICAL ANALYSIS 36

Procedure 36

Histograms and Frequency Polygons 36

Cumulative Curves 38

Interpretations and Results 39

CHAPTER FIVE - X-RAY ANALYSIS.......... 47

Glauconite 47

General Statement 47

Unorientated Powder Mounts 47

Procedure 47

Results 48

Orientated Powder Mounts 48

Preparation of X-ray Diffraction Slides 48

Results 53

Comparison of Results 53

Feldspar 53

CHAPTER SIX - CHEMICAL ANALYSIS AND DEPOSITIONAL ENVIRONMENT OF GLAUCONITE 55

General Statement 55

Separation of Glauconite 56

Results of Glauconite Analysis 57

PAGE

Reliability 58

Comparison and Discussion of Data 61

Calculation of the Chemical Formula of Glauconite 61

Comparison of Glauconite Formulae 65

Origin of Glauconite 67

General Statement 67

Discussion of Major Theories of Glauconite Formation 69

Biotite Mica 69

Gelatinized Substances 70

Colloidal Silicate Lattices 71

Depositional Environment 71

CHAPTER SEVEN - GEOCHRONOLOGY 74

Introduction 74

Separation of Material 74

Results 75

Interpretations 75

CHAPTER EIGHT - SUMMARY AND CONCLUSIONS 82

BIBLIOGRAPHY 84

APPENDIX A - LOCATION OF OUTCROP SAMPLES I

Sunset Peak Area I

Nigel Pass Area I

PAGE

APPENDIX B - THIN SECTION DESCRIPTIONS III

Nigel Pass Area III

Sunset Peak Area XII

APPENDIX C - ANALYTICAL METHODS.................................. XXIV

LIST OF PLATES, FIGURES AND TABLES

Plate 1 Photomicrographs of Heavy Minerals XXIX

Plate 2 " " " " XXX

Plate 3 " " " " XXXI

Plate 4 Photomicrographs of Glauconite XXXII

Plate 5 Photomicrographs of Thin Sections XXXIII

Plate 6 " " " " XXXIV

Plate 7 " " " " XXXV

Plate 8 " " " " XXXVI

Plate 9 " " " " XXXVII

Plate 10 " " " " XXXVIII

Plate 11 Photomicrographs of Thin Sections and Photographs of Outcrop Samples XXXIX

Figure 1 Index Map 4

Figure 2 Late Beltian sea outlining the craton 19

Figure 3 Late Lower Cambrian seas 20

Figure 4 Mid-Middle Cambrian seas 21

Figure 5 Mid-Upper Cambrian seas 22

Figure 6 Histogram and Frequency Polygon of sample 3462-8 42

Figure 7 Histogram and Frequency Polygon of sample 3461-1 43

PAGE

Figure 8 Cumulative Curve, sample 3462-8 44

Figure 9 Cumulative Curve, sample 3461-1 45

Figure 10 Cumulative Curves of samples 3462-8 and 3461-1 46

Figure 11 X-Ray Diffraction Patterns of Palaeozoic Glauconites ... 52

Figure 12 Schematic presentation of the crystal structure of illite 66

Figure 13 Holmes B Time Scale 79

Figure 14 Palaeographic extent of Palaeozoic Orogenies in the Canadian Western Cordillera 80

Figure 15 Time and Intensity of Orogenies in the Canadian Western Cordillera 81

Aerial Photograph 1 Nigel Pass Area 5

Aerial Photograph 2 Sunset Peak Area 6

Table 1 Correlation Table 8

Table 2 Relative Abundance of Heavy Minerals 35

Table 3 Sample Weight Percentages from Sieve Analysis 37

Table 4 Unorientated X-Ray Powder Mounts of Glauconite 49

Table 5 Orientated X-Ray Powder Mounts of Glauconite 51

Table 6 Unorientated X-Ray Powder Mounts of Feldspar 54

Table 7 Results of Glauconite Analysis 57

Table 8 Glauconite Analyses 60

Table 9 Results of Calculations of the Chemical Formula of Glauconite 62

Table 10 Comparison of Glauconite Formulae 65

Table 11 Chemical Analysis of Biotite 69

CHAPTER ONE

INTRODUCTION

This study was undertaken for two reasons. Firstly, to determine the composition and provenance of some Lower Cambrian sediments in Jasper Park, Alberta. Secondly, to obtain an absolute age for a Lower (?) Cambrian glauconite occurring in the Sunset Peak Area of Jasper Park. Attempts to find glauconite-bearing beds in the Nigel Pass Area were unsuccessful. Instead, the only datable mineral obtained was a microcline feldspar contained in basal beds of the Lower Cambrian Jonas Creek formation.

Thin sections made from outcrop samples of Cambrian beds in each area were examined petrographically.

One sample of Lower Cambrian quartzite from each area, both from similar stratigraphic positions was studied in detail. For each of these samples a mechanical analysis and heavy mineral study was made.

From a chemical analysis of the glauconite used for age-dating, a chemical formula was constructed. It was hoped that the analysis might shed some light on the environmental conditions prevailing at the time the glauconite formed.

X-ray powder photographs were taken of both the glauconite and feldspar samples used in potassium-argon dating in an attempt to evaluate impurities. For comparative work the glauconite was run on an x-ray diffractometer with an attached wide angle goniometer with a geiger counter pick-up and recorder.

Ages of 359 and 413 million years were obtained for the glauconite,

and 344 million years for the feldspar. These dates suggest argon leakage, but are comparable with Cambrian glauconite ages from other areas (Hurley, 1958).

This study therefore, has been a partial success in that the relative amounts and variety of detrital minerals contained in the Lower Cambrian quartzites have been determined, while the mechanical analyses have indicated the mode of formation. From the chemical analysis of the glauconite some conclusions can be drawn regarding its depositional environment. The ages of the glauconite and feldspar add more data to the field of geochronology.

PREVIOUS WORK

In 1900 James McEvoy made the earliest geologic report on the central Canadian Rocky Mountains. He described the geology along the Miette River in the vicinity of Yellowhead Pass.

In 1912 D. B. Dowling, and subsequently L. D. Burling, C. D. Walcott, E. M. Kindle, C. Deiss, P. E. Raymond, J. A. Allan, R. L. Rutherford, P. S. Warren, F. Rasetti, R. D. Hughes and others have reported on the Jasper Park Area. Recently, F. K. North and G. G. L. Henderson (1954) and V. J. Okulitch (1956) have given further accounts of the geology of the Southern Rocky Mountains of Canada, and have attempted to straighten out the entangled nomenclature.

In 1957 Cormier published the results of a glauconite study using the rubidium-strontium method of age dating. He gives a glauconite, collected from the Mount Whyte formation along the Brazeau River, an age of 465 ± 65 million years. This is stratigraphically the Sunset Peak glauconite horizon; the ages agree within the limits

of error.

C. W. Hunt (1957, personal communication to R. E. Folinsbee) gave a brief description of the formations outcropping in the Sunset Peak Area of Jasper Park. He collected glauconite from Lower (?) Cambrian beds. Subsequent potassium-argon age-dating carried out by H. Baadsgaard at the University of Alberta yielded an age of 432 million years for this glauconite.

Aside from the above mentioned work, no mechanical analyses, petrographic studies or age-dating results known to the writer have been published concerning Cambrian formations in Jasper Park, Alberta.

MATERIAL USED

The material used in procuring the data presented in this thesis was obtained from three sources:

(1) Outcrop samples collected by R. E. Folinsbee through the courtesy of Imperial Oil Company. These samples are listed in Appendix A, page I.

(2) Outcrop samples collected by the writer, and are listed in Appendix A, page I and II.

(3) Glauconite samples KA-113 and KA-114 from the University of Minnesota, U. S. A.

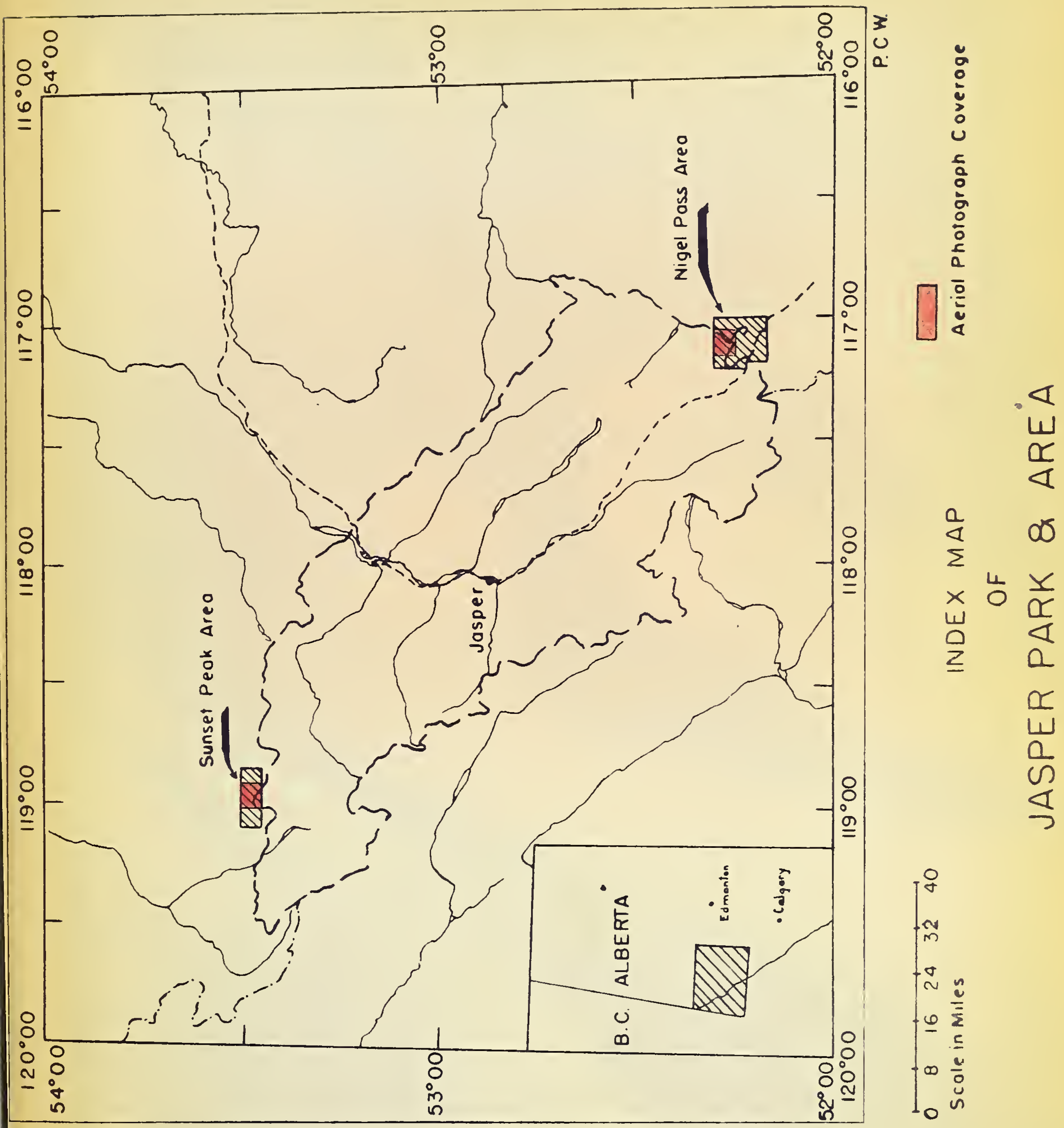
116°00
117°00
118°00
119°00
120°00
54°00
53°00
52°00
Sunset Peak Area
Nigel Pass Area
Jasper
B.C.
ALBERTA
Edmonton
Calgary
0 8 16 24 32 40
Scale in Miles
🟥 Aerial Photograph Coverage
P.C.W.
INDEX MAP
OF
JASPER PARK & AREA

Figure 1.

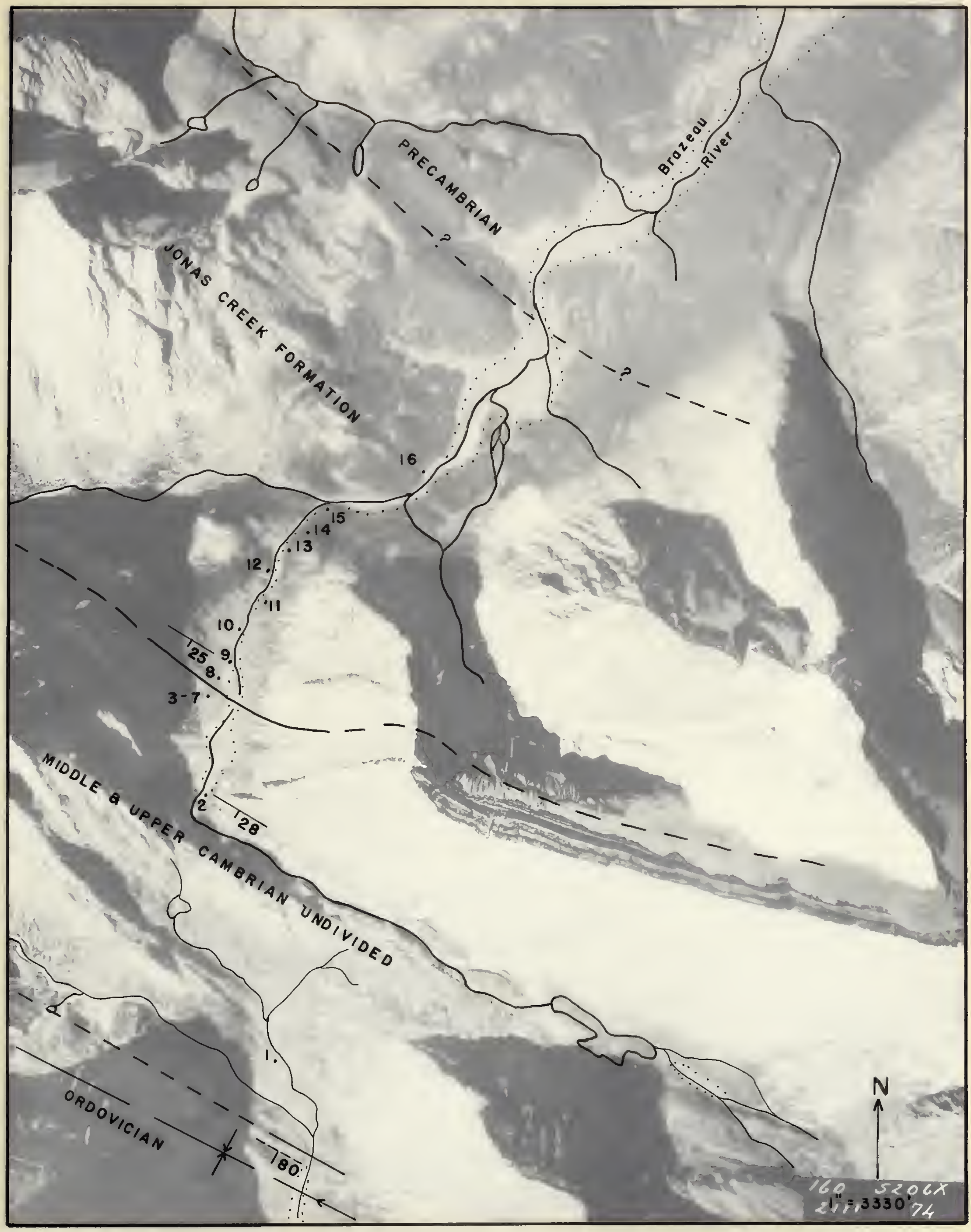
PRECAMBRIAN
Brazeau
River
?
?
JONAS CREEK FORMATION
16
15
14
13
12
11
10
9
25
8
3-7
2
28
MIDDLE & UPPER CAMBRIAN UNDIVIDED
1
ORDOVICIAN
80
N
160 5206X
1" = 3330'
74

Aerial Photograph I.- NIGEL PASS AREA

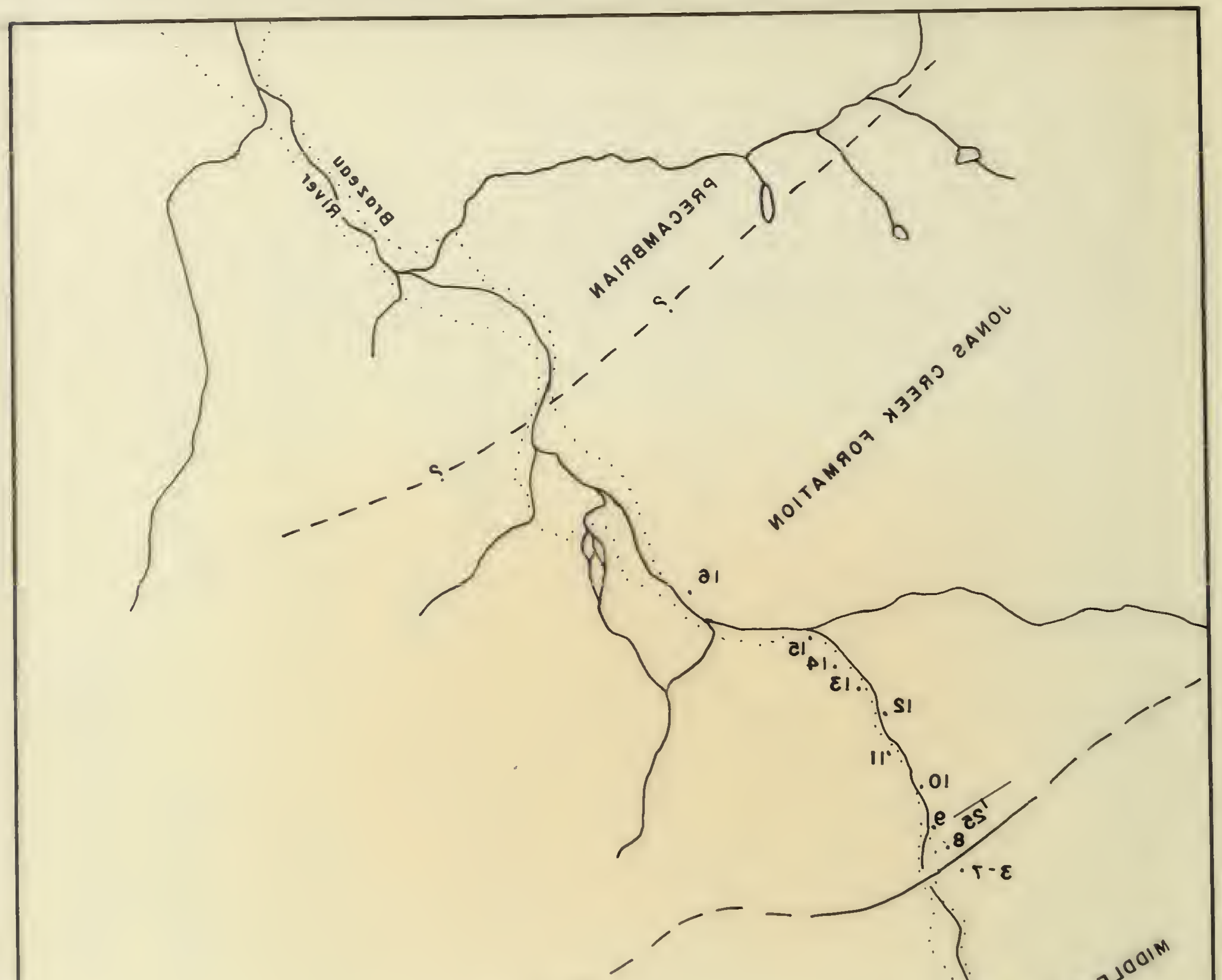
Brazeau River
PRECAMBRIAN
?
JONAS CREEK FORMATION
16
15
14
13
12
11
10
9
25
8
3-7
2
28
MIDDLE & UPPER CAMBRIAN UNDIVIDED
1
ORDOVICIAN
180
N
1" = 3330'

Aerial Photograph 1- NIGEL PASS AREA

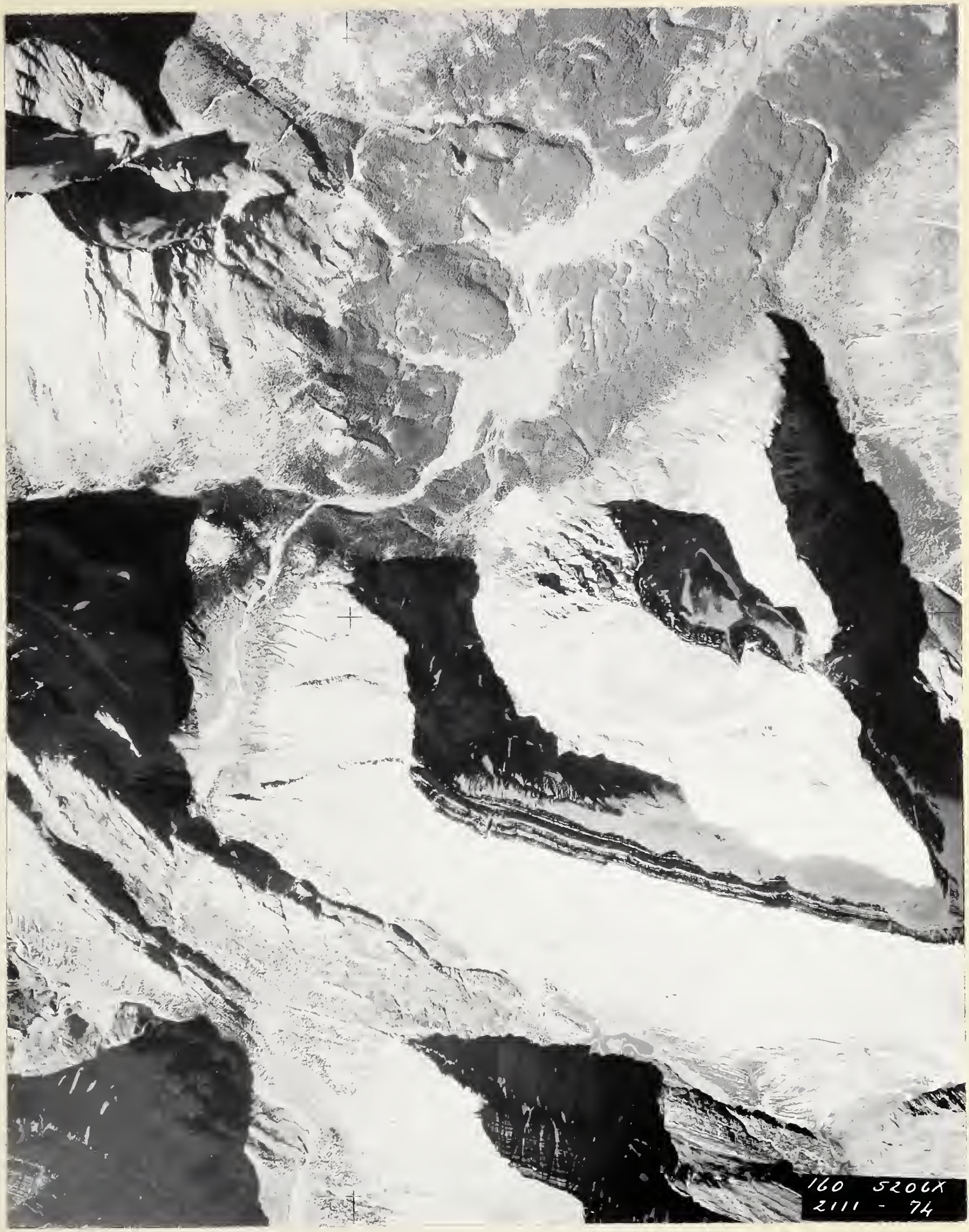
160 5206X
2111 - 74

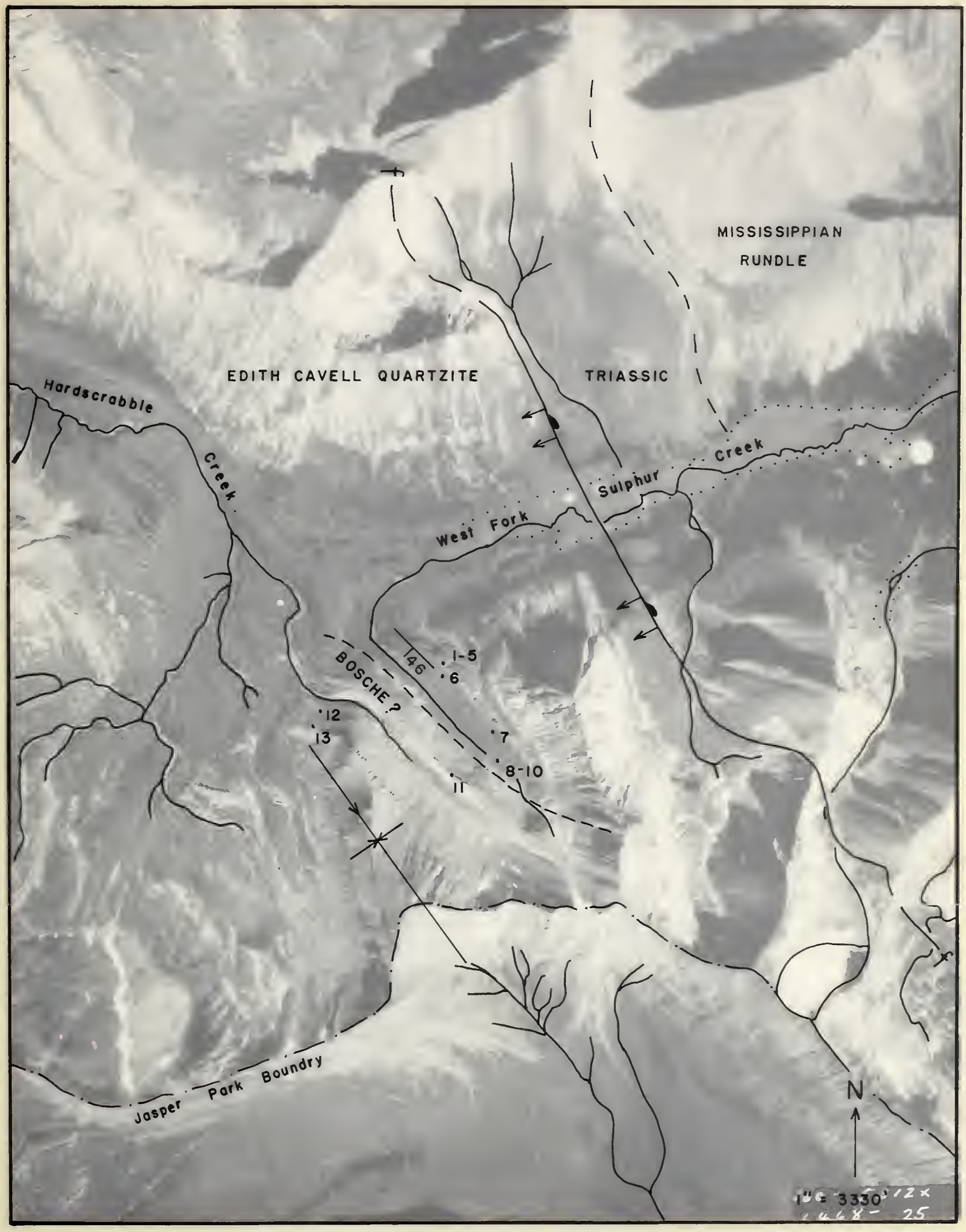
MISSISSIPPIAN
RUNDLE
EDITH CAVELL QUARTZITE
TRIASSIC
Hardscrabble
Creek
Sulphur
Creek
West Fork
BOSCHE ?
146
1-5
6
7
8-10
11
12
13
Jasper Park Boundry
N
1" = 3330'
12x
1448-
25

Aerial Photograph 2.- SUNSET PEAK AREA

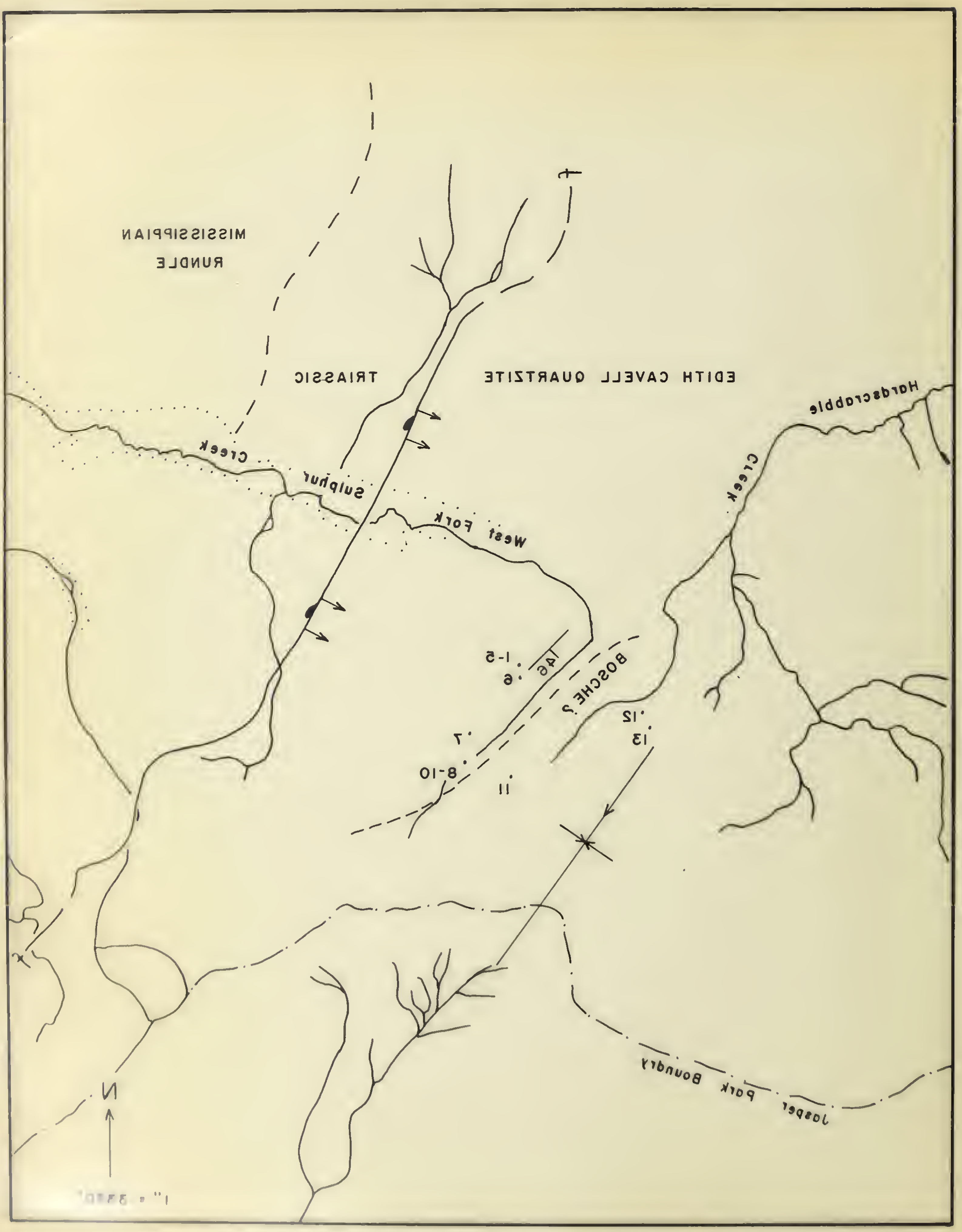
MISSISSIPPIAN
RUNDLE
TRIASSIC
EDITH CAVELL QUARTZITE
Sulphur Creek
West Fork
Hardscrabble Creek
f
BOSCHE 2
146
1-5
6
7
8-10
11
12
13
Jasper Park Boundary
N
1" = 3300'

Aerial Photograph 2.- SUNSET PEAK AREA

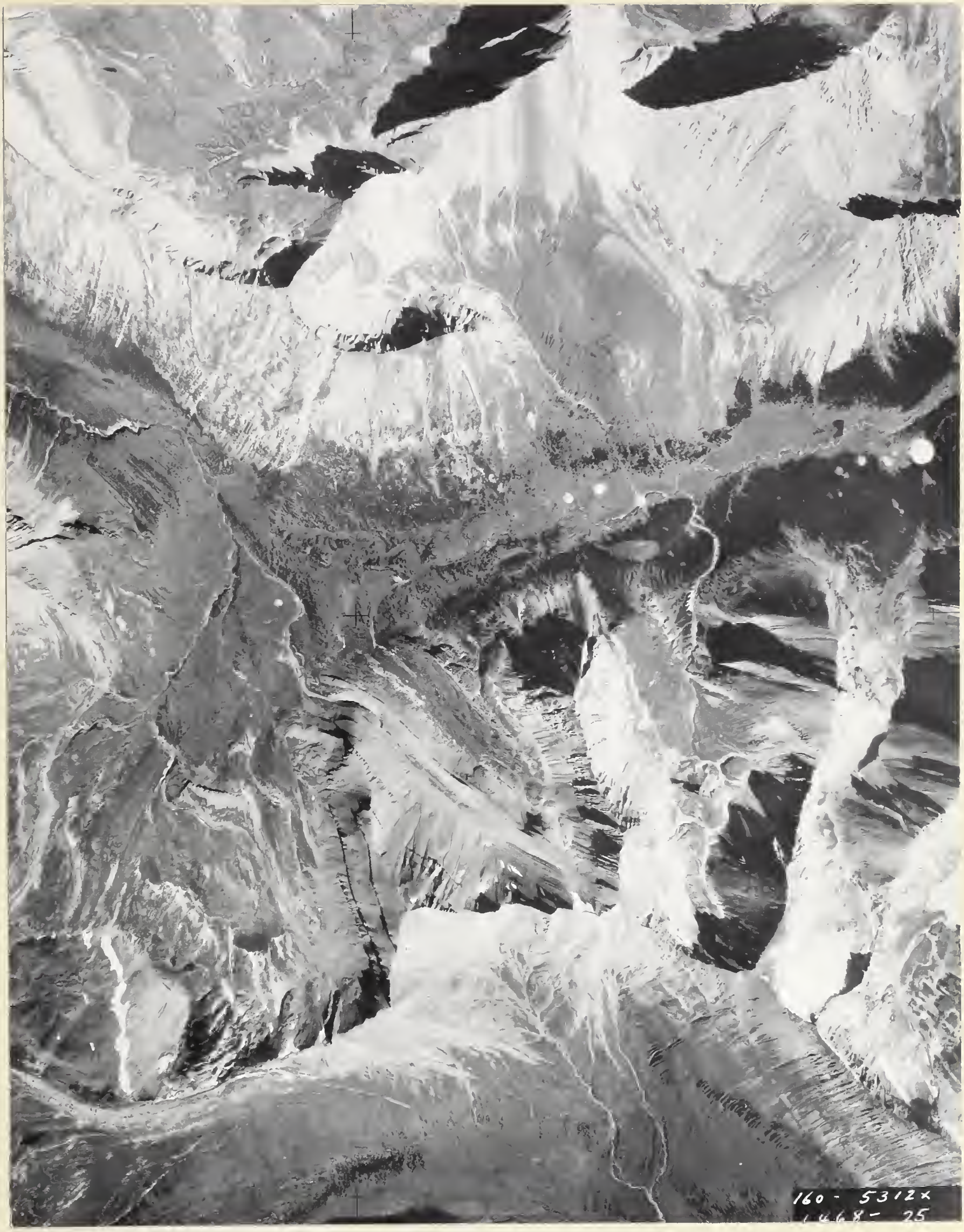
160 - 5312x
1468 - 25

CHAPTER TWO

STRATIGRAPHY, PALAEONTOLOGY AND PALAEOGEOGRAPHY

General Statement

Although this thesis is not primarily concerned with the detailed stratigraphy of the area, it is felt that a brief discussion of some of the most recent stratigraphic work is necessary. A correlation chart (Table 1) has been compiled from the literature, incorporating the most recent data obtainable.

The two areas involved in this study are separated by approximately 110 miles. The southern, Nigel Pass Area, is located in twp. 38, rge. 22 W5th Meridian (52° 15' north latitude, 117° 6' west longitude). The northern, Sunset Peak Area, is located in twp 52, rge. 7 W6th Meridian (53° 30' north latitude, 119° 00' west longitude).

STRATIGRAPHY

Nigel Pass Area (see Figure 1, and Aerial Photograph 1).

The Nigel Pass Area lies just southeast of the Sunwapta and Southesk Map areas where Hughes (1953) divided the Precambrian into two formations; the Hector formation and the overlying Jonas Creek formation. Hughes considered the upper part of the Jonas Creek formation to be Lower Cambrian in age. However, Okulitch (1956) states categorically that the Jonas Creek formation is Lower Cambrian in age and is equivalent to Deiss's (1940) Gog formation in the Mount Assiniboine area.

CAMBRIAN CORRELATION CHART FOR THE MAIN RANGES OF THE CANADIAN ROCKY MOUNTAINS

Standard Section	Main Ranges and Bow River Valley C.D. Walcott (1928) F.K. North et al (1954) F. Rasetti (1951, 1956) V.J. Okulitch (1956)		Sunwapta River Area J.A. Allan (1938) R.D. Hughes (1953) V.J. Okulitch (1956)		Mount Robson Area C.D. Walcott (1928) P.E. Raymond (1930) L.D. Burling (1923,1955) V.J. Okulitch (1956)	
Upper Cambrian	Lower Goodsir sh.		Tangle Ridge sh. & ls.		Lynx ls. & sh.	
	Lyell ls.					
	Sullivan ls.					
	Arctomys ls. & sh.					
Middle Cambrian	Pika ls. & sh.		Sunwapta Peak ls., dol. & sh.		Bosche ls. & sh.	? Titkana ls.
	Eldon dol.					
	Stephen sh.					
	Cathedral dol.					Tatei ls.
	Ross Lake sh.					? Chetang ls.
	Mount Whyte ls.		Mount Whyte ls. & metarg.			Hota-Adolphus ls.
Lower Cambrian	Gog (St. Piran)	Peyto ls. mem.	Gog (St.Piran)	Peyto ls. mem.		Mahto ss.
						Tah-Mural ls.
		St. Piran ss. mem.		Jonas Creek formation	Edith Cavell quartzites	McNaughton ss(?)
		Lake Louise sh.mem.				
		Fort Mountain ss. mem.				Miette ss.
Precambrian	Hector, siliceous shales with interbedded conglomerate.		Hector shales, quartzite, conglomerate		Jasper Series, quartzites, argillites, breccias, slates, etc.	

Table 1.

The Middle Cambrian is divided into two formations; the Mount Whyte formation overlain by the Sunwapta Peak formation. The Mount Whyte was originally defined by Walcott (1908), and later divided by Rasetti (1951) into the Mount Whyte formation and a lower unit called the Peyto limestone member (Lower Cambrian).

The Sunwapta Peak formation was first named by Hughes (1953). Its type locality is at Sunwapta Peak. A partial section was measured by Hughes on the northwest face of Tangle Ridge, and its description follows in descending order:

LITHOLOGIC DESCRIPTIONS	THICKNESS IN FEET	HEIGHT ABOVE BASE IN FEET
Overlying Tangle Ridge formation Top of section obscured. Limestone, dark blue-gray, massive, rounded weathering, buff weathering.	15.0	647.0
Limestone, dark blue-gray, dirty-gray weathering, irregularly platy, chunky to nodular platy at base, more massive upwards.	105.0	542.0
Limestone, dark blue-gray, weathers pitted, shot with calcite nodules, massive to irregularly platy, local ripple marks, contains intraformational conglomerate beds ranging up to three inches in thickness, becomes harder and denser upwards.	80.0	462.0
Limestone, dark blue-gray, buff weathering, nodular bedded and weathering.	15.0	447.0
Limestone, dark blue-gray, ribbed and furrowed to flat-surfaced, massive, becomes more platy toward the top.	95.0	352.0

Limestone, dark blue-gray, dense, fine crystalline, nodular bedding, weathers rusty and gray into sharp blocky fragments becomes thin-bedded to platy upwards. Sparse worm trails.	130.0	222.0
Limestone, dark blue-gray, platy nodular; weathers rusty, gray and light buff; weathers ribbed and furrowed. Bedding ranges from one-half to 1½ inches thick. Trace of trilobite fragments.	60.0	162.0
Obscured. Probably shaly limestone.	15.0	147.0
Limestone, very dark blue-gray, weathers into sharp square blocky fragments, becomes nodular weathering upwards. Thin shaly break near base forms a small terrace.	75.0	72.0
Limestone, buff and gray streaked, nodular weathering, rough platy. Weathers very buff to rusty on bedding planes.	45.0	27.0
Limestone, buff to gray weathering, nodular, somewhat platy to laminated, hackly weathering upwards.	27.0	
Mount Whyte formation.		

Hughes (1953) assigned a new formational name, Tangle Ridge, to a sequence of shale and limestone beds between the Middle Cambrian Sunwapta Peak formation and Ordovician limestone beds. The north ridge of Tangle Ridge between altitudes of 6,900 and 8,760 feet was designated as its type locality. A summary of his description follows:

LITHOLOGIC DESCRIPTIONS	THICKNESS IN FEET	HEIGHT ABOVE BASE IN FEET
Overlying Ordovician beds. Shale, green, and interbedded limestones.	470	1325
Shale, green, with lenses of limestone coquina ranging to six inches in thickness.	305	1020
Limestone, dark-gray, shot with fine limonite specks, weathers very finely pitted.	25	995
Limestone, dark-gray, contains one-quarter inch limonite spots, weathers pseudo-pisolitic.	125	870
Limestone, gray with slight brown cast, irregular buff and dark-gray stripes, weathers nodular, beomes denser upwards.	275	595
Limestone, very dark-gray, extremely hackly weathering, tough, when acidized releases fine pebble-shapes sub-rounded inclusions.	60	535
Shale, green and ochrous, friable.	60	475
Shale, fine sandy, overlain by limestone, buff, slightly argillaceous, wavy-banded, buff-weathering.	20	445
Base of more continuous outcrops Limestone, buff, argillaceous, platy.	50	405
Limestone, gray-brown, dense, matt, wavy irregular banding.	10	395
Sandstone, and siltstone, very fine grained, calcareous, light rich-buff weathering, platy, becomes shaly, green, 25 feet above base.	70	325

Limestone, dark-gray, matt, hard, dense, slightly shaly, trace of a nodular habit, one-quarter to five inch bandings, becomes very dark-gray and "slaty" at top.	30	295
Obscured, probably shale.	40	255
Limestone, light brown, dolomitic, dense almost matt, hard, one-half to eight inch beds.	10	245
Shale, thin-bedded, green, with fossil rain imprints; and shale, red, becoming buff, dolomitic, granular, massive upwards.	40	205
Shale, variegated green and red, splintery, platy, hard but friable, becomes very ochrous and locally mauve upwards. Interbedded with thin sandstones, buff, platy, locally cross-bedded.	205	0
Discontinuous outcrops.		

The writer collected samples in this area during late September. Because of bad weather he had little opportunity to measure outcrop distances, except by pacing. Samples 3462-16 to 3462-8 are definitely from the Jonas Creek formation. Samples 3462-7 to 3462-3 are from the Mount Whyte formation; sample 3462-2 is from either the Sunwapta Peak or Tangle Ridge formations; and sample 3462-1 is from the Tangle Ridge formation or overlying Ordovician. Except for algae all outcrops are unfossiliferous.

SUNSET PEAK AREA (See Figure 1 and Aerial Photograph 2)

The nearest sequence of Cambrian rocks described lies approximately 27 miles southwest in the Mount Robson area. Burling (1923, 1955) has done most of the work in this area and his formation

names are listed in the stratigraphic table (Table 1).

Allan, Warren and Rutherford (1932) named the Precambrian rocks found in the Jasper area as the Jasper Series. These are overlain by the Miette sandstones described by Walcott (1913) as "... massive bedded grey sandstone with thick bands of grey and greenish siliceous shales".

The McNaughton sandstones were named by Walcott (1913) and described as "... light grey, massive bedded quartzitic sandstone". These sandstones overly the Miette sandstones. According to Walcott (1928) there is an unconformity between the McNaughton sandstones and the underlying Miette sandstones. However, Okulitch (1956, p. 712) stated:

> "Burling was unable to locate the McNaughton-Miette boundary. It is entirely possible that the Miette sandstone is part of the Lower Cambrian sedimentary sequence, and that the boundary lies at the base of the Miette sandstone on top of the more argillaceous Jasper Series."

The Edith Cavell quartzite is exposed on the eastern cliff of Mount Edith Cavell (Raymond, 1930), and is composed of thick-bedded hard grey quartzites. Talus debris contains both feldspar and fragments with Scolithus borings. The feldspar suggested to Raymond that a considerable thickness of arkosic beds was present that may represent the Miette sandstone. A considerable portion of the mountain is covered by snow, but grey quartzites are exposed on the summit (S.J. Nelson, personal communication). The presence of Scolithus borings in the talus suggests the possibility that the Edith Cavell quartzite may be correlated with the Jonas Creek formation.

For the purpose of description only, the lower sandstone unit in the Sunset Peak Area is designated the Edith Cavell quartzite. Samples obtained from this sequence contain no phenoclasts of feldspar. This suite is representative of only the top of the massive quartzite section. From the same area C.W. Hunt (1957, personal communication to R.E. Folinsbee) reported that the quartzite: "Is exposed in a thickness of about 3800 feet... with many pebble beds in its lower part... The top [of the quartzite]... occurs where the quartzites suddenly become more thin-bedded, earthy, glauconitic; and generally show evidence of muddier deposition". A compilation by the writer of Hunt's estimated thickness of the section follows:

Top	Feet
Lower Ordovician Mons dolomite forming high cliffs	800
Interbedded variegated shale and limestone . . .	1000
Limestone and interbedded shales with fossils near the top (Bosche(?) formation)	650
Interbedded variegated shales and glauconitic sandstones	500
Oolitic limestone	200
Glauconitic sandstones interbedded with gritstones and thin shales	1250
Edith Cavell quartzite (overthrust on Triassic rocks)	3800
Bottom	

Samples used in this study (see Appendix A, p. I) show that the Edith Cavell quartzite is overlain by a thin-bedded, richly glauconitic limy bed containing a few trilobites and/or other arthropod fragments. This limy bed is followed by a thick limy

sequence containing Lower Cambrian Archaeocyathids.

In suite 3461, samples 1 to 3 are from the Edith Cavell quartzite; samples 4 and 5 from the overlying glauconitic sequence; and sample 6 from the fossiliferous Archaeocyathid beds. Samples 7 to 13 may either be from equivalents of Burling's (1923) Adolphus formation or the Bosche (?) formation mentioned by Hunt (ibid). Sample 3461-12 contains algae and Gogia (?). Such forms as the latter are known to occur in Middle Cambrian strata on Mount Kitchener. (Harker and Hutchinson, 1953).

Distribution of Cambrian

The general distribution of Cambrian rocks has been discussed by Allan (1938, p. 115), as follows:

> "The most easterly band of Cambrian is exposed along the north-east face of Miette Range south of the Athabasca (Loc. 3), and in the Bosche Range north of the same valley. The second band is exposed in the Snaring Valley (Loc. 4) and along the north-east base of the Palisade six miles north of Jasper. The third band occurs in the upper part of Pyramid Mountain (Loc. 5) five miles north of Jasper and for an undetermined distance to the west. The most westerly band, and possibly the largest, occurs in the vicinity of the Continental Divide west of Jasper and in the Mount Robson area to the north-west (Loc. 6). These last two bands of Cambrian with the exposed pre-Cambrian between form largely the older or western belt of the Rocky Mountains east of the watershed. It appears that these two western bands unite south of Jasper to form one broad band extending from the east side of Athabasca Valley westward."

Thus sample suites 3461 and 3462 from the Sunset Peak and Nigel Pass areas appear to be from the same band of Cambrian sediments, outcropping in the main ranges of the Rocky Mountains.

PALAEONTOLOGY

Nigel Pass Area

The top of the Jonas Creek formation contains numerous Scolithus borings (suite 3462, samples 6, 8, 9, 10). Scolithus borings are present in formations ranging from Cambrian to Devonian in age and have little stratigraphic value (Shimer and Schrock, 1944).

A very short distance stratigraphically above the Mount Whyte-Jonas Creek contact small algal concretions were collected (plate 11, fig. 3). A layer of similar forms occurring at the same stratigraphic position was noted by Rasetti (1951) and R.D. Hughes (1953). Calcareous algae (?) were found by Raymond (1939, p. 31) in strata on one of the shoulders of Mount Edith Cavell. Raymond believes their origin to be inorganic.

Sunset Peak Area

Scolithus borings are present in the Edith Cavell quartzite (sample 3461-2).

The limy glauconite-rich sequence (sample 3461-5) contains numerous trilobite fragments, a few faecal (?) pellets and one small arthropod (?) showing internal segmentation.

In sample 3461-6 the following occur: poorly preserved Archaeocyathidae, trilobite spines, Helenia (?) or a similar pteropod. In North America Kawase and Okulitch (1957) apparently consider Archaeocyathids to be of Lower Cambrian age. However in Eurasia they seem to have persisted throughout most if not all of Middle Cambrian time (Okulitch, 1955).

Sample 3461-12 contains echinoderm fragments and an algae

assignable to the form-genus Pycnostroma. Walcott (1917) found the primitive echinoderm Gogia occurring 430 feet above the highest Olenellus fauna (Lower Cambrian). Similar echinoderms are known to occur in the Bathyuriscus-Elrathina zone (Harker and Hutchinson, 1953). On this basis sample 3461-12 has been assigned a Middle Cambrian age.

PALAEOGEOGRAPHY

The Pacific ocean had covered most of the Canadian Rocky Mountain area by Beltian (Late Precambrian) time. Between the Peace River "Arch" in the Peace River area and the highland of "Montania" in northern Montana, a broad, shallow embayment developed, which persisted into Cambrian time. In this sea were deposited Beltian sediments derived from the craton to the east (Warren, 1951).

A series of maps after Warren and Stelck (1958) depicting the extent of the sea on the craton from Beltian to Mid-Upper Cambrian time is shown in Figures 2 to 5.

At the beginning of Palaeozoic time the sea began to advance on the craton, flooding embayments and probably penetrating the craton most deeply along old drainage basins of major Precambrian river systems.

The basal beds of the Jonas Creek formation, consisting of arkose overlain by intraformational quartzite conglomerates represent the filling of Precambrian topographic lows. The arkose, composed of fresh angular alkalic feldspar associated with euhedral hyacinth zircon and angular tourmaline, was probably derived from the nearby craton to the east, though in appearance is quite out of keeping with other craton derived sediments and may have an entirely different source.

The conglomerate is composed of predominately well rounded quartz grains and a minor amount of subrounded feldspar. The conglomerate may have been derived from topographically high areas of Beltian sediments.

The remainder of the Jonas Creek formation and all of the Edith Cavell quartzites probably represent a beach or littoral deposit. These sands are classed as arenites (Williams, H. et al, 1958, p. 293). The absence of feldspar in these sands appears congruent with the paucity of the unstable heavy detritals.

Marine deposition of this sand took place on a shallow-water shelf which was fairly uniform over a large area. Lack of very coarse sand and interstitial fine material, plus the well rounded and sorted character of the quartz grains suggest that winnowing by wave action was persistent throughout the depositional period. Some ripple marking and low angle cross-bedding was observed in the Nigel Pass Area.

Overlying the Edith Cavell quartzites in the Sunset Peak Area is a limy bed containing glauconite and trilobite fragments, followed by a fossiliferous limestone containing Archaeocyathidae and Helenia (?) fragments. One of the prerequisites for glauconite formation is a stable depositional medium and fairly shallow water. Thus near the end of Lower Cambrian time the sea transgressed farther onto the craton, depositing limy muds and shallow water limestones. The sea continued to advance eastward throughout Middle and Upper Cambrian time, depositing thick limy shales and limestones. Consequent burial and intrastratal solutions have resulted in partial recrystallization of the limestones and limy muds, as well as the filling of void spaces in the sands with quartz and barite.

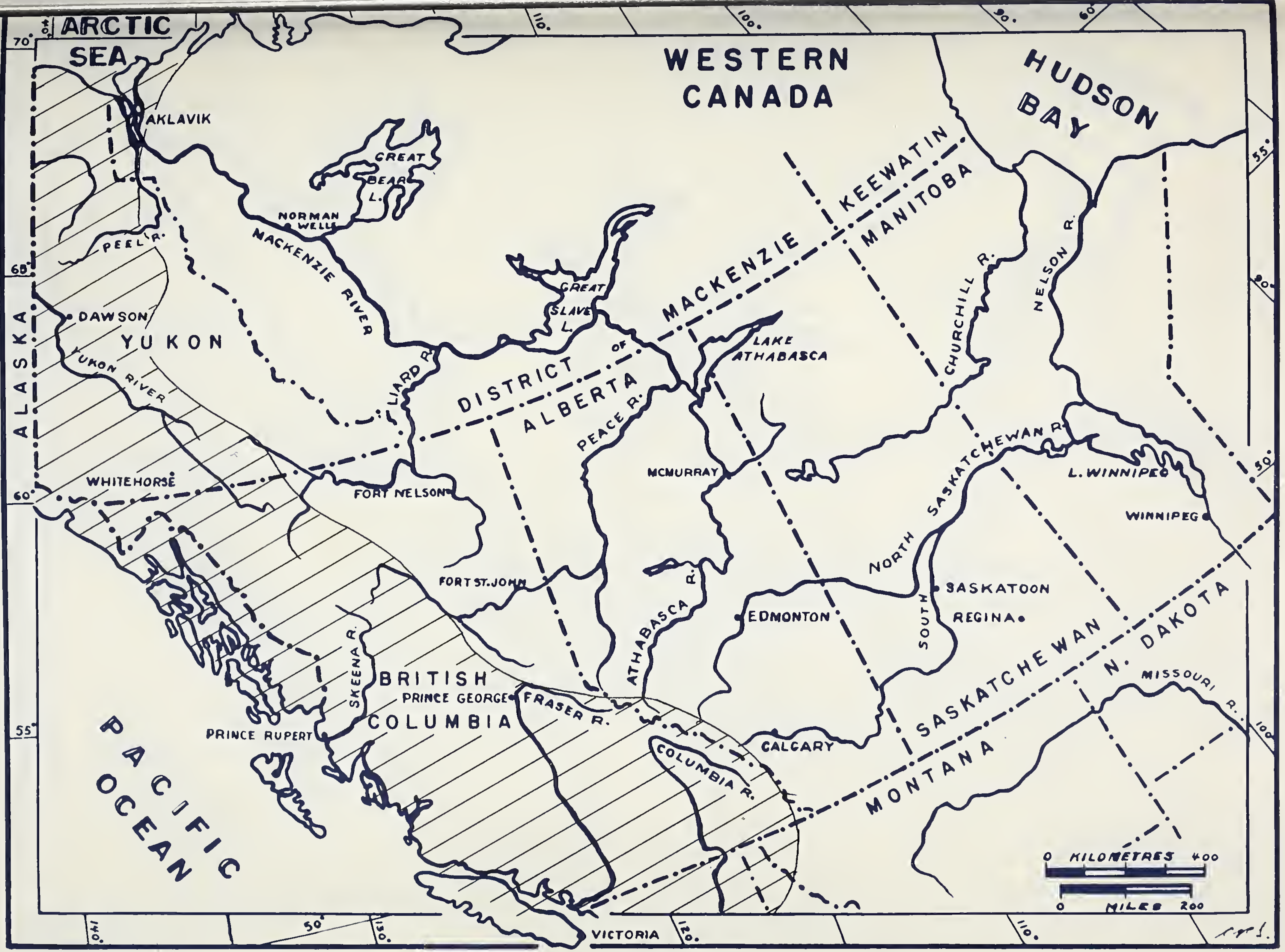
ARCTIC SEA
WESTERN CANADA
HUDSON BAY
AKLAVIK
GREAT BEAR L.
NORMAN WELLS
MACKENZIE RIVER
PEEL R.
DAWSON
YUKON
YUKON RIVER
ALASKA
GREAT SLAVE L.
MACKENZIE
KEEWATIN
MANITOBA
CHURCHILL R.
NELSON R.
LAKE ATHABASCA
DISTRICT OF ALBERTA
LIARD R.
PEACE R.
MCMURRAY
WHITEHORSE
FORT NELSON
SASKATCHEWAN R.
L. WINNIPEG
WINNIPEG
NORTH SASKATCHEWAN
FORT ST. JOHN
ATHABASCA R.
EDMONTON
SASKATOON
SOUTH
REGINA
SASKATCHEWAN
N. DAKOTA
MISSOURI R.
MONTANA
BRITISH COLUMBIA
PRINCE GEORGE
FRASER R.
SKEENA R.
PRINCE RUPERT
CALGARY
COLUMBIA R.
PACIFIC OCEAN
VICTORIA
0 KILOMETRES 400
0 MILES 200
70°
65°
60°
55°
50°
140°
130°
120°
110°
100°
90°
60°

Figure 2. - Late Beltian sea outlining the craton.

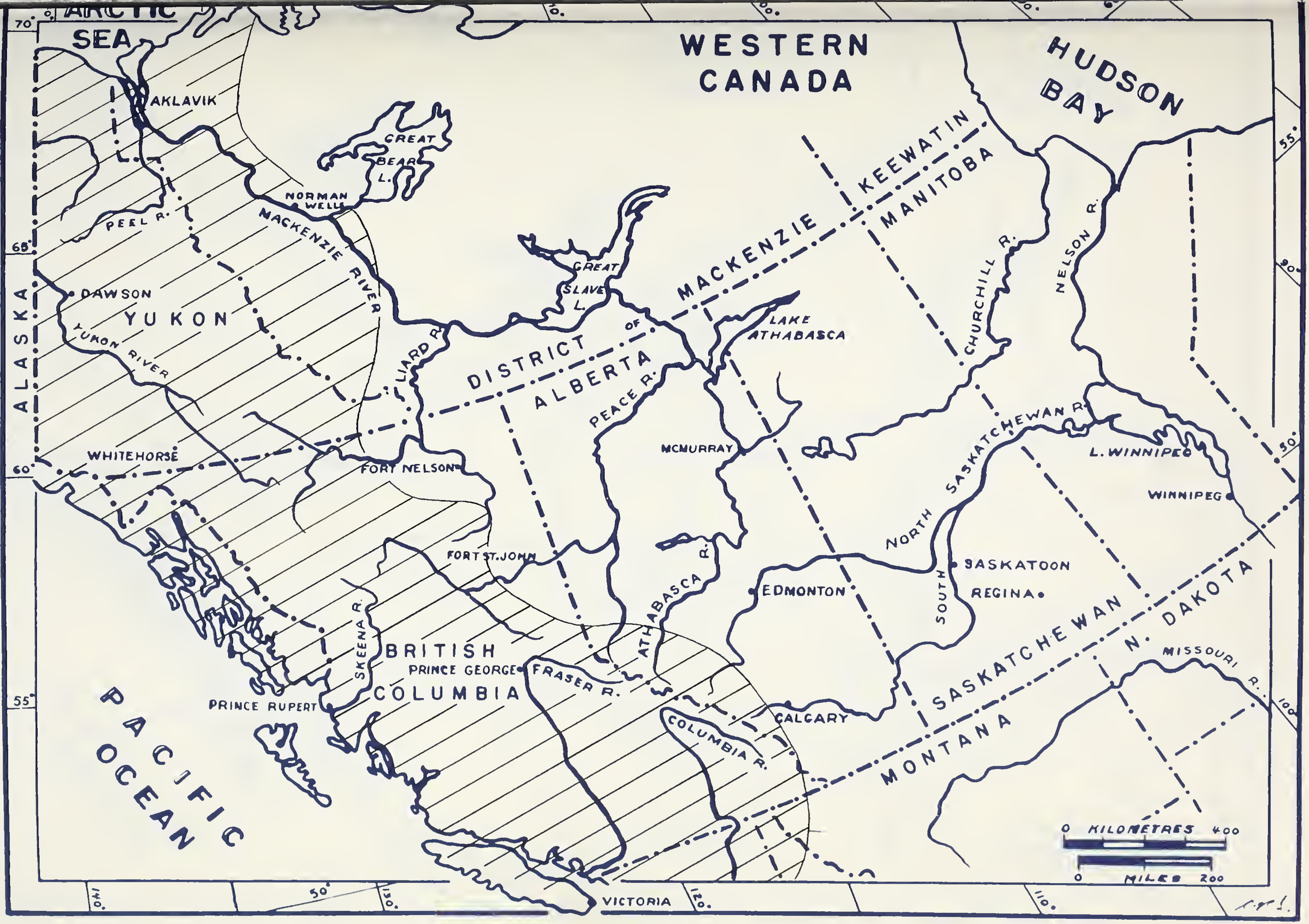
ARCTIC SEA
WESTERN CANADA
HUDSON BAY
AKLAVIK
GREAT BEAR L.
NORMAN WELLS
PEEL R.
MACKENZIE RIVER
MACKENZIE
KEEWATIN
MANITOBA
GREAT SLAVE L.
DISTRICT OF ALBERTA
LAKE ATHABASCA
CHURCHILL R.
NELSON R.
DAWSON
YUKON
YUKON RIVER
ALASKA
LIARD R.
PEACE R.
MCMURRAY
SASKATCHEWAN R.
L. WINNIPEG
WINNIPEG
WHITEHORSE
FORT NELSON
NORTH
SOUTH
SASKATOON
REGINA
FORT ST. JOHN
ATHABASCA R.
EDMONTON
SKEENA R.
BRITISH COLUMBIA
PRINCE GEORGE
FRASER R.
SASKATCHEWAN
N. DAKOTA
MISSOURI R.
PRINCE RUPERT
CALGARY
COLUMBIA R.
MONTANA
PACIFIC OCEAN
VICTORIA
0 KILOMETRES 400
0 MILES 200
70°
65°
60°
55°
50°
55°
90°
100°
110°
120°
130°
140°

Figure 3. - Late Lower Cambrian seas.

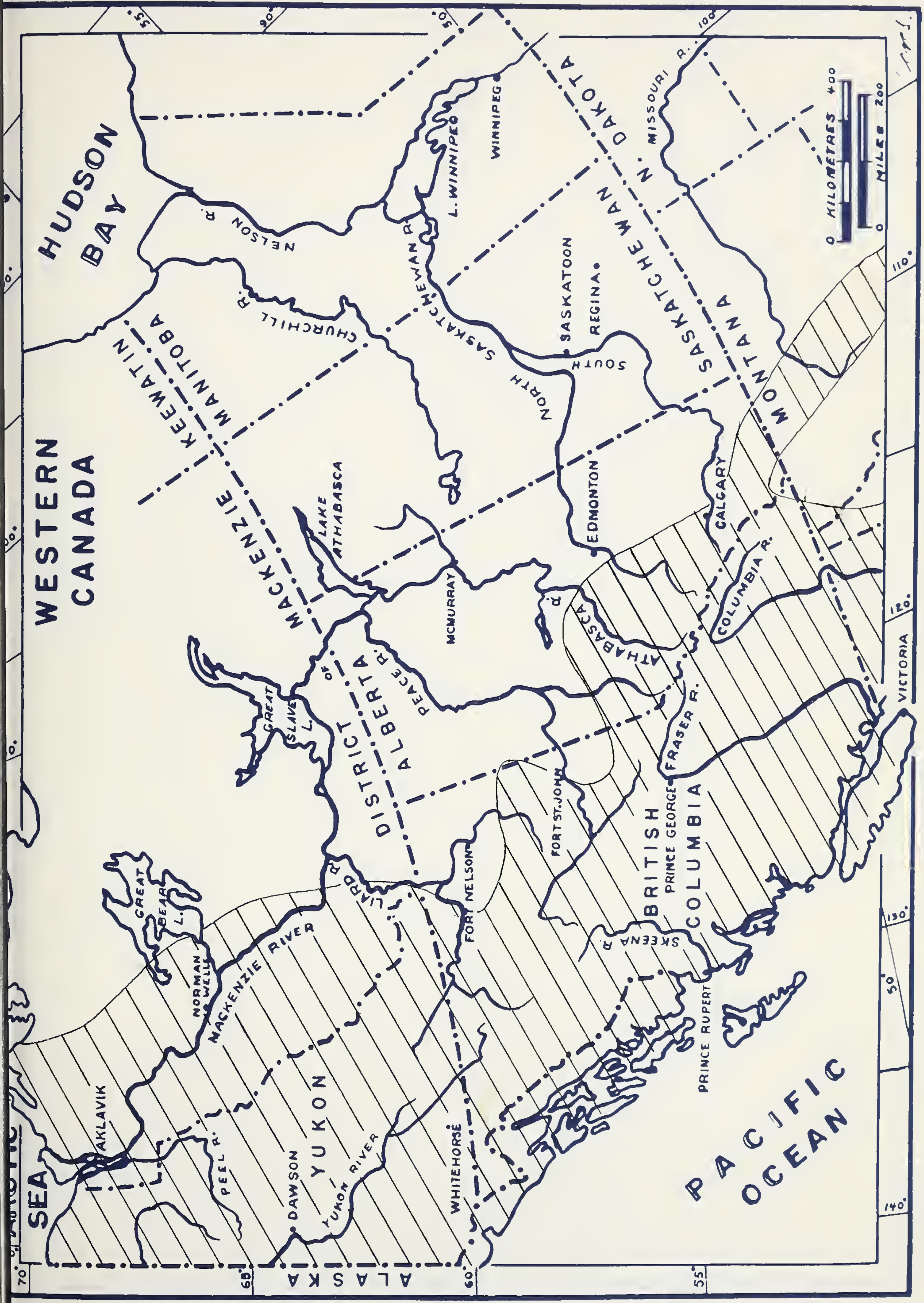
HUDSON BAY
WESTERN CANADA
KEEWATIN
MANITOBA
MACKENZIE
DISTRICT OF ALBERTA
SASKATCHEWAN
N. DAKOTA
MONTANA
BRITISH COLUMBIA
YUKON
ALASKA
PACIFIC OCEAN
SEA
NELSON R.
CHURCHILL R.
SASKATCHEWAN R.
NORTH
SOUTH
L. WINNIPEG
WINNIPEG
SASKATOON
REGINA
MISSOURI R.
LAKE ATHABASCA
McMURRAY
EDMONTON
CALGARY
ATHABASCA R.
PEACE R.
GREAT SLAVE L.
GREAT BEAR L.
NORMAN WELLS
MACKENZIE RIVER
LIARD R.
FORT NELSON
FORT ST. JOHN
PRINCE GEORGE
FRASER R.
COLUMBIA R.
SKEENA R.
PRINCE RUPERT
VICTORIA
AKLAVIK
PEEL R.
DAWSON
YUKON RIVER
WHITEHORSE
KILOMETRES
0
400
MILES
0
200
50°
55°
60°
65°
70°
90°
100°
110°
120°
130°
140°

Figure 4. - Mid-Middle Cambrian seas.

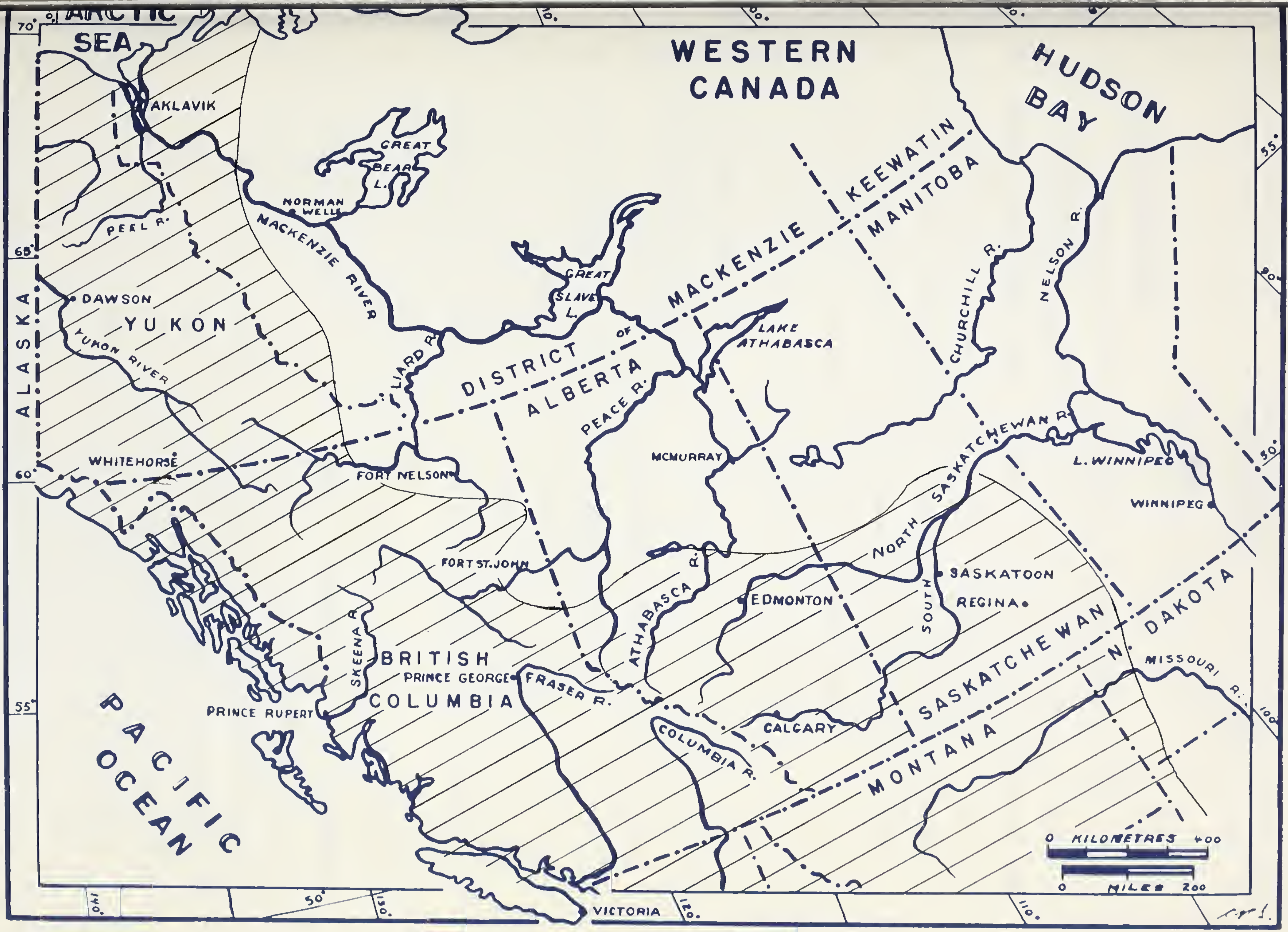
SEA
WESTERN CANADA
HUDSON BAY
AKLAVIK
GREAT BEAR L.
NORMAN WELLS
MACKENZIE RIVER
PEEL R.
DAWSON
YUKON
YUKON RIVER
ALASKA
WHITEHORSE
FORT NELSON
LIARD R.
GREAT SLAVE L.
DISTRICT OF MACKENZIE
KEEWATIN
MANITOBA
ALBERTA
PEACE R.
LAKE ATHABASCA
MCMURRAY
CHURCHILL R.
NELSON R.
SASKATCHEWAN R.
L. WINNIPEG
WINNIPEG
NORTH
SOUTH
SASKATOON
REGINA
EDMONTON
ATHABASCA R.
FORT ST. JOHN
SKEENA R.
BRITISH COLUMBIA
PRINCE GEORGE
FRASER R.
PRINCE RUPERT
PACIFIC OCEAN
CALGARY
COLUMBIA R.
SASKATCHEWAN
MONTANA
N. DAKOTA
MISSOURI R.
VICTORIA
0 KILOMETRES 400
0 MILES 200
70°
65°
60°
55°
50°
55°
90°
100°
110°
120°
130°
140°

Figure 5. - Mid-Upper Cambrian seas.

CHAPTER THREE

PETROGRAPHY

General Description

Outcrop samples were used for the study of thin sections from Cambrian sediments in the Nigel Pass and Sunset Peak Areas. A total of forty thin sections were prepared by Mr. F. Roberts, Petrographic Thin Section Service, Alhambra, California. More than one thin section was prepared from some samples and only the better ones are described.

A general description of twenty-six thin sections is given below. A detailed description of each slide is in appendix B.

The grade scale used is that of Wentworth (1922).

Nigel Pass Area:

Jonas Creek formation

Grain size varies from fine sand to coarse pebbles. Quartz grains and siliceous rock fragments (metaquartzite) are in the main well rounded; feldspar grains are subrounded to angular.

Packing of the grains is generally tight, but in some cases normal packing was observed. Packing of the grains plus subsequent cementation has eliminated porosity.

The cement is mostly silica in the form of quartz overgrowths, with minor amounts of calcite, barite and hematite. Most of the grains are partially bordered by minute rims of amorphous hematite and limonite, suggesting that iron oxides were deposited contemporaneously with silica, which was later partly replaced by calcite and barite. In sample 3462-12 hematite borders some of the quartz grains as subhedral hexagonal crystals.

Sorting ranges from poor to good with the poorest sorting

present in the basal arkose and conglomerate (3462-16 and 15).

Quartz and siliceous rock fragments are the principle components found in thin sections, with quartz dominant, the siliceous rock fragments subordinate. Some small liquid and solid inclusions (mostly apatite) are present in some of the quartz grains, but for the most part the inclusions are too minute to be determined petrographically.

All grains and the silica cement exhibit undulose extinction under crossed nicols. The metaquartzite grains are strongly strained. Strain shadows in the cement indicates that stress has occurred after deposition.

Mount Whyte formation

The formation grades from a quartz arenite at the base to a calcarenite at the top. Grain size varies from fine to medium quartz to cryptocrystalline calcite.

A short distance stratigraphically above the base of the formation an algal zone occurs composed of fine-to medium-crystalline dolomite and fine-grained angular quartz grains cemented with quartz, barite, dolomite and limonite.

Calcilutites overlying the algal beds contain fine to coarse well rounded quartz grains which "float" in the cryptocrystalline calcite. Numerous porphyroblasts and veins are composed of medium crystalline calcite. The porphyroblasts may have originally been pore spaces or small organic bodies, and the veins shrinkage cracks which existed in a limy mud before recrystallization to calcite.

Thin sections of samples obtained above the Mount Whyte

formation are all calcilutites composed of cryptocrystalline to very fine crystalline brownish-coloured calcite. The strata were probably originally deposited as limy muds.

Sunset Peak Area:

Edith Cavell quartzite

The Edith Cavell quartzite is petrographically similar to the Jonas Creek formation. Thin sections show the grain size varies from fine to coarse sand. Quartz and siliceous rock fragments (metaquartzite) are well rounded, well sorted, tightly to moderately packed, and cemented with hematite, barite, and authigenic silica. All grains and cement show undulose extinction under crossed nicols. Collophane is a constituent of phosphatic nodules which occur in the upper quartzites. Glauconite is present in minute amounts while feldspar is almost entirely lacking.

Beds Overlying the Edith Cavell quartzite

Most of these beds are composed of carbonates and interbedded quartz arenites. Grains vary from cryptocrystalline to coarse sand-size. Most of the carbonates are fossiliferous and glauconitic. The majority of fossil fragments are composed of collophane. The glauconite has an irregular rather than rounded outline and appears to be authigenic. It seems to have undergone little transportation other than probable agitation on the sea floor during the process of formation. Some grains in sample 3461-10 are partly replaced by hematite as a result of oxidation of pyrite (?) under present weathering conditions.

A thin sandy bed rich in hematite contains well developed hematitic pisoliths with well rounded quartz nuclei.

The upper part of the section is composed of interbedded calcilutites, pisolitic (algal) calcilutaceous siltstones and oolitic calcarenites.

Small structures, recognized in thin sections as well as in outcrop samples, are mainly the result of slumping, contorted bedding and stylolyte partings.

Heavy Accessory Minerals

General Statement

Heavy minerals were obtained from the Jonas Creek formation and Edith Cavell quartzite. The sample taken from the Edith Cavell quartzite (3461-1) is from the top of the unit. The two samples obtained from the Jonas Creek formation are from a large interval. One sample (3462-8) is from the top of the formation just below the Mount Whyte / Jonas Creek contact. The other sample (3462-16) is from a basal arkosic arenite bed approximately 2500' below the first sample, probably fairly close to the contact with the underlying Hector formation.

Procedure:

Samples 3461-1 and 3462-8 were ground fine enough to pass through a 16 mesh screen, and sieved using 18, 25, 35, 45, 60, 80, 100, 120, 140, 170, 200 and 325 mesh screens (U.S. Series). Sample 3462-16 was ground fine enough to pass through a 10 mesh screen, and sieved using 35, 60, 100, 120, 170, 200 and 270 mesh screens. For

all samples the fraction retained on the +200 mesh screen was collected and bottled for heavy mineral separation.

The heavy minerals were separated from the light minerals by the use of heavy liquids. Apparatus used consisted of two long-stemmed four-inch diameter funnels, four inches of rubber tubing, a pinch clamp and a stand. The upper funnel was one-third filled with tetrabromoethane ($CHBr_2CHBr_2$) which has a specific gravity of 2.950/20°C. Approximately 2 grams each of washed and dried sample from the interval -170 +200 mesh was used in samples 3461-1 and 3462-8, and over 10 grams from sample 3462-16. The heavy minerals were further separated by pouring them into methylene iodide (S.G. 3.33) liquid.

Sample 3462-16 contained large amounts of iron-stained quartz, feldspar and carbonate grains. The sample was passed through a Frantz Isodynamic Separator with setting of .35, .45 and 1.5 amperes. These fractions plus the non-magnetic fraction at 1.5 amperes were mounted in Aroclor (R.I. 1.66). The heavy mineral fractions of samples 3461-1 and 3462-8 were not run through the Frantz Separator, but mounted in Aroclor immediately after the tetrabromoethane separation.

Light fractions were mounted in Canada Balsam.

An examination was made of at least two slides from each interval sampled. Since the total number of heavy minerals on each slide was comparatively small a total count was made of minerals on each slide. All the non-opaque minerals were recorded. On all slides, except those run through the Frantz Separator at .45 and 1.5 amperes, the number of opaques greatly exceeded the remaining minerals present. The relative abundance of the heavy accessory minerals

contained in the samples is tabulated in Table 2. Photomicrographs of some of the heavy minerals found are shown in Plates 1, 2 and 3.

List of Heavy Accessory Minerals

Authigenic

Barite
Hematite
Pyrite

Detrital

Apatite
Hematite ?
Leucoxene
Magnetite
Monazite
Tourmaline
Zircon

Opaque Heavy Minerals

Abundant quartz and to a lesser extent feldspar, were brought down in the heavy mineral fractions because of hematite coatings, and were not considered in the counts.

Hematite - Irregular aggregates rounded to hexagonal shape, exhibiting a dull-red to blood-red lustre in reflected light. In most slides some hematite coats quartz and feldspar grains and is therefore considered to be authigenic.

Leucoxene - Occurs as rounded to oval shape grains, white to very dull-yellowish-white, having in some cases a minutely pitted surface. It is an alteration product of ilmenite.

Pyrite - Occurs as aggregates, or in some cases as euhedral crystals of

cubic habit, brass-yellow in reflected light. The pyrite is considered authigenic.

Magnetite - Occurs as angular to subrounded grains, bluish-black in reflected light, and is difficult to separate from ilmenite by reflected light alone.

Non-Opaque Heavy Minerals

Non-opaque heavy mineral suites in all cases were extremely simple, consisting mainly of barite and zircon. Tourmaline and apatite were present in some slides.

Barite - Colourless, tabular, irregular to ragged. Sharp angular cleavage fragments, with numerous colourless to red, round to rod-shaped inclusions. The grains in some slides are sprinkled with a dusty coating of hematite. Prismatic grains exhibit parallel extinction and bright interference colours. A mineral of authigenic origin.

Apatite - Colourless grains oval or nearly circular in plan, more rarely rounded elongate prisms. Some grains are subangular, which may be partly due to crushing. A few grains contain colourless inclusions arranged in rows or planes or distributed in a random fashion.

Monazite - Pale-yellow, very slightly pleochroic. Only a few grains were observed in the slides. All grains were rounded equidimensional, but one grain was subhedral and partially pitted. Monazite is marked by its pale-yellow colour, high relief, high birefringence and slight pleochroism. It has a very small optic angle.

Tourmaline - Colours predominating are yellow and green to various shades of brown, with minor amounts in shades of sky-blue to indigo-blue. Most grains are angular, irregularly fractured and strongly pleochroic. A few grains have slightly rounded corners with minute colourless inclusions. One grain observed was yellowish-brown, sub-rounded, with a small colourless smooth overgrowth on one edge. Commonly the blue variety shows maximum absorption and minimum pleochroism, the change in colour going from medium-blue to almost black. The orientation produces a slightly off-center uniaxial figure.

Krynine (1946) classified tourmaline as follows:

Type I Granitic - Formed as an end-phase product within large plutonic igneous bodies. Typical colour is dark-brown, green, or pink (with a greenish cast). Bubble inclusions and cavities are common.

Type II Pegmatitic - From pegmatites and veined rocks. Typical colour is blue, with pleochroism in shades of mauve and lavender. Inclusions are rare.

Type III Metamorphic - In pegmatized sandstones, or metaquartzites, quartz-schists, and quartz-mica-schists. Colour varies from brown and pinkish, less commonly green to more commonly deep-brown. Inclusions are rare.

In slates, phyllites, and non-quartzose mica schists, Colour varies from colourless to very pale-brown. Abundant dark carbonaceous inclusions are common.

Type IV Authigenic - Formed in sedimentary rocks during or after the

deposition of a sediment. Occurs as a clear, non-pleochroic overgrowth on one end of the grain.

Type V Sedimentary - Derived from the reworking of early formed sediments. Occurs as rounded grains with or without rounded overgrowths. Varieties found may be any of the four basic types.

All basic types are present, but not in all slides, with metamorphic, pegmatitic and granitic types being the most common. Only a few of the tourmaline grains showed evidence of rounding, and these were mostly of the metamorphic and granitic varieties. One metamorphic variety appeared to have a poorly developed colourless overgrowth at one end of the grain. In all cases the pegmatitic tourmaline was found as irregular fragments, which could be partially the result of crushing.

Zircon - Zircon was by far the most abundant detrital heavy mineral, and was present in all slides. Two main varieties were recognized; the well rounded hyacinth type present in all slides, and the dark-brown euhedral type, present only in sample 3462-16. Gradations between these two main varieties are many, and zircons accordingly are divided into the following catagories.

I Hyacinth, well rounded, no halos or inclusions.

II Hyacinth, well rounded, with colourless to dark, rounded to rod-shaped inclusions.

III Hyacinth, rounded, with dark-brown core.

IV Hyacinth to deep-purple, well rounded, with a dark core and radiating micro-fissures.

V Hyacinth to deep-purple to black, well rounded, no core or inclusions.

VI Dark-brown, rounded, with black core.

VII Deep red-brown, tabular, rounded bipyramids, no cores or inclusions.

VIII As above, with dark core, micro-fissured.

IX As above but zoned.

X As above but not fissured.

XI Dark brown, euhedral.

XII Deep red-brown, euhedral, zoned, dark core, micro-fissured.

XIII As above, not fissured or zoned.

XIV Any of the above types with overgrowths.

Provenance

The Lower Cambrian rocks studied have a marked paucity of detrital heavy minerals. The sediments are believed to be derived from a mixed igneous, metamorphic, and sedimentary source. Because only three rock samples were analyzed for their heavy mineral assemblages, the conclusions drawn are to be regarded as tentative.

The basal portion of the Jonas Creek formation (sample 3462-16) is composed of a mixed source mineral assemblage. Euhedral dark-brown zircon, angular tourmaline, partially rounded monazite and apatite are associated with subhedral microcline feldspar and well rounded quartz and siliceous rock fragments. The zircon and monazite are believed to be directly derived from igneous rocks. The hyacinth and dark-brown zircons are typical Precambrian varieties. Probably pegmatitic, granitic and metamorphic varieties of tourmaline are also

much more abundant than the authigenic or definitely sedimentary types. The apatite was also probably derived from igneous rocks, but there exists the possibility that it may have been derived in part from metamorphic limestones.

Except for the authigenic and sedimentary tourmaline, the writer believes the source of the heavy mineral and the feldspar to be from the craton to the east. The general lack of rounding of the constituents, especially the zircon and the feldspar, suggests that they have a short transportation history.

Subsurface studies of rocks of Precambrian age in Central Alberta by Burwash (1957) show the Canadian Shield is composed dominately of crystalline igneous and metamorphic rocks of granitic composition, with local areas of sedimentary and basic volcanic rocks.

The well rounded fine to coarse sand-size quartz and siliceous rock fragments, associated with sedimentary and authigenic tourmaline, clearly represent more than one cycle of deposition, and are probably derived from pre-existing Precambrian Beltian sediments. There exists the possibility that some of the multi-cycle material may also have been derived from the east. The Athabasca sandstone, of questionable age, contains tourmaline which commonly has overgrowths. The one or two grains of tourmaline observed with overgrowths in sample 3462-16 suggests that further studies on the distribution of this variety of tourmaline might be rewarding.

Samples examined from the upper portion of the quartzite sequence of both the Nigel Pass (3462-8) and the Sunset Peak Areas (3461-1) contained well rounded hyacinth zircon and well rounded, well

sorted fine-to medium-grained quartz. These sediments have undergone at least one, if not several cycles of deposition. They may have been derived originally from the craton as Precambrian Beltian sediments. According to Beveridge (1956) hyacinth zircons are known to occur in the Creston quartzite of Precambrian age which occurs in the general Kimberly area of southeastern British Columbia. Another known source is the Precambrian Purcell diorite sill, which occurs in the same area.

	3462-8 slide 1 S.G. > 3.33	3462-8 slide 2 S.G. > 3.33	3462-8 slide 3 S.G. > 3.33	3462-16-A (M.@.35A) S.G. > 2.89	3462-16-B (M.@.45A) S.G. > 2.89	3462-16-C (M.@1.5A) S.G. > 2.89	3462-16-D (N.M.@1.5A) S.G. > 2.89	3461-1 slide 1 S.G. > 3.33	3461-1 slide 2 S.G. > 3.33	3461-1 slide 3 S.G. > 2.89 < 3.3
Apatite							2			
Barite	9	9				3	8	6	5	3
Hematite	1	1	1	9	8	2		2	8	4
Leucoxene	2				2	2		1		
Pyrite								1	2	6
Magnetite				3	1					
Monazite					1					
* Tourmaline I				1	4					
* II				1	4			1		
* III					5					
* IV					1					
* V				1	1					
* Zircon I						1	1	7	1	7
* II							6	7		5
* III						4	2			
* IV						1	1			
* V		2	1			3	2			
* VI						4	3	1		
* VII						8	2			
* VIII						3	2			
* IX	2					1				
* X							2			
* XI						4				
* XII						3	3			
* XIII						3				
* XIV						3				

1. Less 1%
2. 1-3%
3. 3-6%
4. 6-9%
5. 10-15%
6. 15-25%
7. 25-40%
8. 40-70%
9. Greater than 70%

*For description of types see text pp. 30-32.

TABLE 2.

CHAPTER FOUR

MECHANICAL ANALYSIS

A mechanical analysis is the operation of determining the abundance or frequency of grain sizes within chosen classes or grades.

Mechanical analyses were made of samples 3461-1 and 3462-8. Both samples are from approximately the same stratigraphic position in each section Results are plotted on histograms, frequency polygons and cummulative curves.

Procedure:

Each sample was disaggregated in an iron mortar and thoroughly mixed. After coning and quartering, 100 grams of sample was screened through 18, 25, 35, 45, 60, 80, 100, 120, 140, 170, 200, and 325 mesh screens (U.S. Standard Sieve Series) using a RO-TAP Testing Sieve Shaker.

The weight percentages of the sample on each screen were calculated and plotted in the form of histograms (see Figure 6 and 7). Frequency polygons were drawn up on the same graphs. Cumulative weight percentages were plotted as cumulative curves on semi-logarithmic graph paper (Figures 8 to 10).

The weight percentages for each sample are given in Table 3.

Histograms and Frequency Polygons:

The histograms are plotted using the weight percentages as the ordinate and the Wentworth Grade Scale as the abscissa. Frequency polygons were constructed by plotting the frequency corresponding to a given grade size on a line midway between the grade limits.

Sample 3462-8 (A)

Weight of Sample 100 g. 12 minutes shaking on RO-TAP

Sieve No.	Screen Openings (mm)	Grade Size	Weight Retained (g.)	Weight Percent	Cumulative Percent
18	1.000	1.000 >	0.04	0.04	0.04
25	0.710	1.000-0.710	1.20	1.20	1.24
35	0.500	0.710-0.500	27.60	27.60	28.84
45	0.350	0.500-0.350	25.30	25.30	54.14
60	0.250	0.350-0.250	10.71	10.71	64.85
80	0.177	0.250-0.177	9.90	9.90	74.75
100	0.149	0.177-0.149	3.30	3.30	78.05
120	0.125	0.149-0.125	1.60	1.60	79.65
140	0.105	0.125-0.105	3.66	3.66	84.31
170	0.088	0.105-0.088	1.33	1.33	85.64
200	0.074	0.088-0.074	2.59	2.59	88.23
325	0.044	0.074-0.044	4.26	4.26	92.49
		less 0.044	7.65	7.65	100.14

Sample 3461-1 (B)

Weight of sample 100 g. 12 minutes shaking on RO-TAP

Sieve No.	Screen Openings (mm)	Grade Size	Weight Retained (g.)	Weight Percent	Cumulative Percent
18	1.000	1.000 >	0.35	0.35	0.35
25	0.710	1.000-0.710	3.38	3.38	3.73
35	0.500	0.710-0.500	32.56	32.56	36.29
45	0.350	0.500-0.350	24.11	24.11	60.46
60	0.250	0.350-0.250	13.74	13.74	74.14
80	0.177	0.250-0.177	10.05	10.05	84.19
100	0.149	0.177-0.149	3.30	3.30	87.49
120	0.125	0.149-0.125	1.11	1.11	88.60
140	0.105	0.125-0.105	3.19	3.19	91.79
170	0.088	0.105-0.088	1.00	1.00	92.79
200	0.074	0.088-0.074	1.91	1.91	94.70
325	0.044	0.074-0.044	2.73	2.73	97.43
		less 0.044	3.60	3.60	101.03

TABLE 3.

Cumulative Curves:

Graphs are constructed for each sample to express the cumulative weight percentages in going from coarse to fine material. The cumulative weight percentages are plotted along the ordinate axis and the Wentworth Grade Scale is plotted along the abscissa as the natural logarithm of the diameter. Thus the ordinate reading at any point on the graph gives the weight percentage of all the material coarser than the size represented.

The median size (Md) and the quartiles (Q_1 and Q_3) were read directly from the cumulative curves (see graphs) where:

$50\% < Md < 50\%$ of the diameters.
$25\% < Q_1 < 75\%$ of the diameters.
$75\% < Q_3 < 25\%$ of the diameters.

The coefficient of sorting was calculated for the samples using the following equation:

$$\text{Coeff. of sorting (So)} = \sqrt[2]{Q_3/Q_1}$$

Essentially, it is a measure of the spread of a cumulative curve and does not depend upon the size factor or units of measurement because it is a ratio between the quartiles.

Skewness was calculated using the equation:

$$\text{Skewness (Sk)} = \frac{Q_1 \times Q_3}{(Md)^2}$$

Skewness is a measure of the spread of a frequency curve. Skewness indicates on which side of the median diameter, and how far from it, the mode or peak of size distribution lies.

Kurtosis was calculated using the equation:

$$\text{Kurtosis (Kurt.)} = \frac{Q_3 - Q_1}{2(P_{90}-P_{10})}$$

where P_{90} and P_{10} are the sizes associated with the 90 and 10 percentile lines respectively and are read directly from the cumulative curve. Kurtosis may be thought of as the "peakedness" of a curve and involves a comparison of the spread of the central part of a curve to the spread of the curve as a whole.

Interpretations and Results:

Although the cumulative curve gives results similar to the histogram, the histogram may vary depending upon the class interval used, whereas the cumulative curve is more or less independent of class limits. A cumulative curve is therefore, generally a more reliable index of the nature of the continuous distribution than a histogram. The most abundant grains are associated with the maximum slope of the tangent of the cumulative curve. The degree to which the grains cluster about or spread away from the modal group, i.e., the group of greatest frequency, may be seen from the steepness of the curve. The approximate degree of sorting or sizing of the sediment may be read from the general slope of the curve and the range of sizes included within it.

The histograms show these samples to have a unimodal size distribution which is normal for marine sands according to Pettijohn (1957). Medium to coarse sand makes up the dominant portion of the samples, and fine sand predominates over very fine sand and coarse silt. In both samples very coarse sand and fine silt and clay are absent. The absence of fine silt to clay-size material would suggest that the sediment represents a lag deposit, or one which was well washed by wave action at the time of deposition.

Bimodal distributions are much more common in coarse fluvial sediments, such as gravels. Here the phenoclasts and matrix are of different grade sizes, each mode separated by perhaps four or five grades. This bimodal character of coarse fluvial sediments may be explained by the dual nature of the load carried by streams, i.e., suspension load and bed load. In torrential streams, the suspension load is mainly sand, while the bed load is in the coarse gravel range. Where the stream is more sluggish the suspension load is silt and clay, and the bed load is composed mostly of sand-size material. It was thought by Udden (1914) that bimodal distribution represented contemporaneous deposition of bed and suspended load of a stream. On the other hand Plumley (1948) interpreted the fines - the secondary mode in most instances - as materials having later filled the voids between the primary matrix - the principal mode.

Examination and comparison of the cumulative curves A(3462-8) and B(3461-1) shows that both curves tend to be somewhat unsymmetrical and are skewed toward the fine sized material. Although better shown by the histograms, the cumulative curves do show that the modal groups are quite well defined as can be seen from the steepness of the curves. The smoothness and regularity of the curves show the sediments are unimodal. Also, the steepness of the curves and the few grain sizes included within them shows the sediments are well sorted. Both curves are similar to a curve depicting a typical beach sand shown by Krumbein and Pettijohn (1938, fig. 102, p. 216). Therefore, both samples in this study probably represent beach or littoral deposits which have been cleaned and sorted by wave action.

On the cumulative curves of samples 3462-8 (A) and 3461-1 (B) results of calculations of the median, first and third quartiles, sorting, skewness and kurtosis have been tabulated. Sample B is on the whole, coarser grained than A. Both samples are well sorted, B better than A. According to Trask (1932, p. 72) a coefficient of sorting less than 2.5 indicates a well-sorted sediment; if it is greater than 4.5 a poorly sorted sediment; and if it is about 3.0 a normally sorted deposit. Hough (1940) and Stetson (quoted by Hough), point out that most near-shore marine sediments of sand-grade size have a coefficient of sorting between 1.0 and 2.0. Logarithmic values of the coefficient of sorting show that B is approximately one and one-half times better sorted than A.

Both samples have a negative logarithmic value of skewness, showing that the fine admixtures exceed the coarse admixtures in the sediments; A more than B. The finer sediments tend to become more negatively skewed according to Hough (1942).

The difference in kurtosis between the two samples is a reflection of difference in both P_{10} and P_{90} values and is difficult to evaluate.

According to Twenhofel (1941) the best that a graph can do is suggest an environment of deposition and an agent of deposition. The writer believes that a mechanical analysis of a sediment is helpful in obtaining a fuller background of information upon which to base an interpretation of the genesis of a rock.

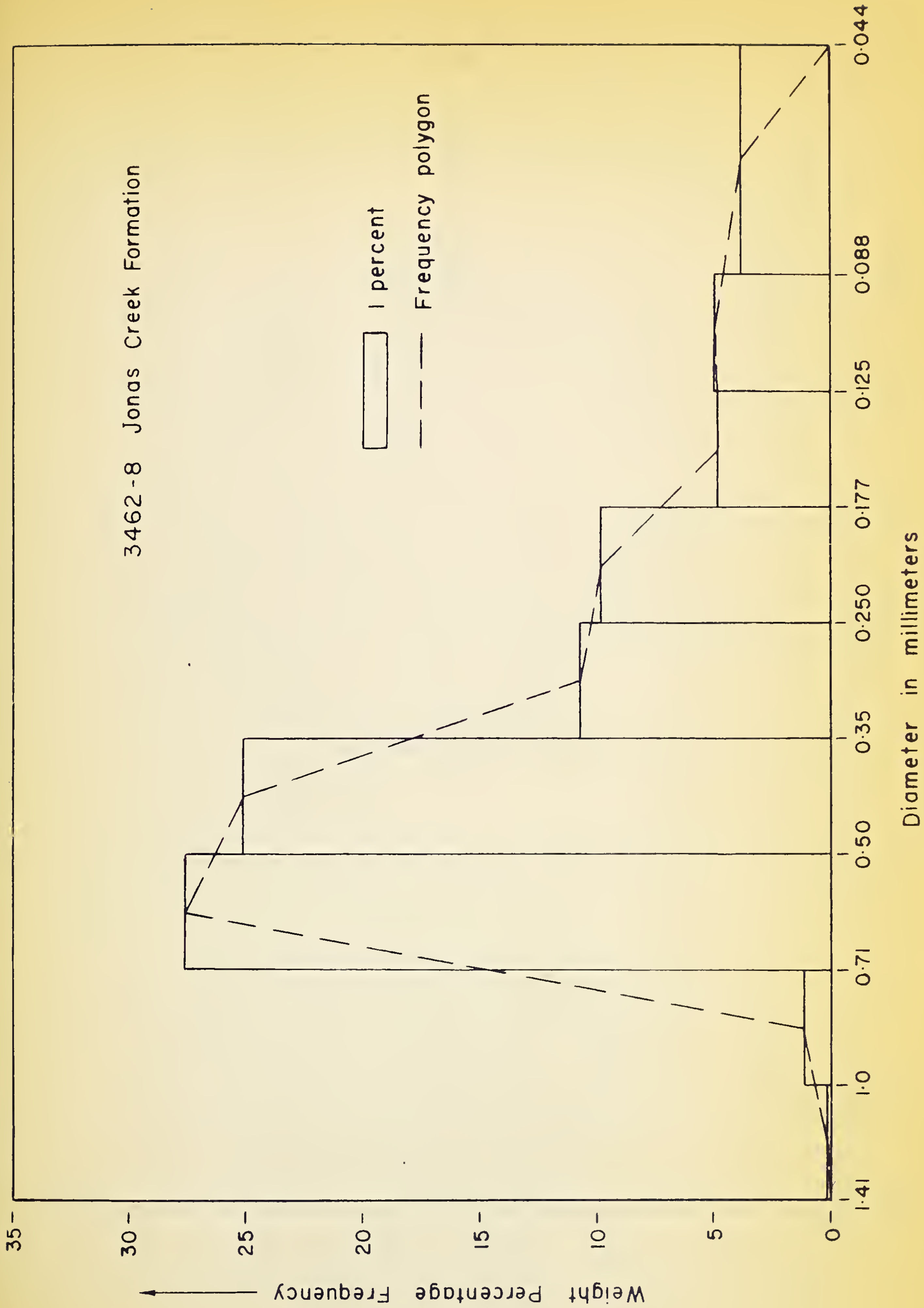
3462-8 Jonas Creek Formation
1 percent
Frequency polygon
Weight Percentage Frequency
0
5
10
15
20
25
30
35
1·41
1·0
0·71
0·50
0·35
0·250
0·177
0·125
0·088
0·044
Diameter in millimeters

Figure 6.

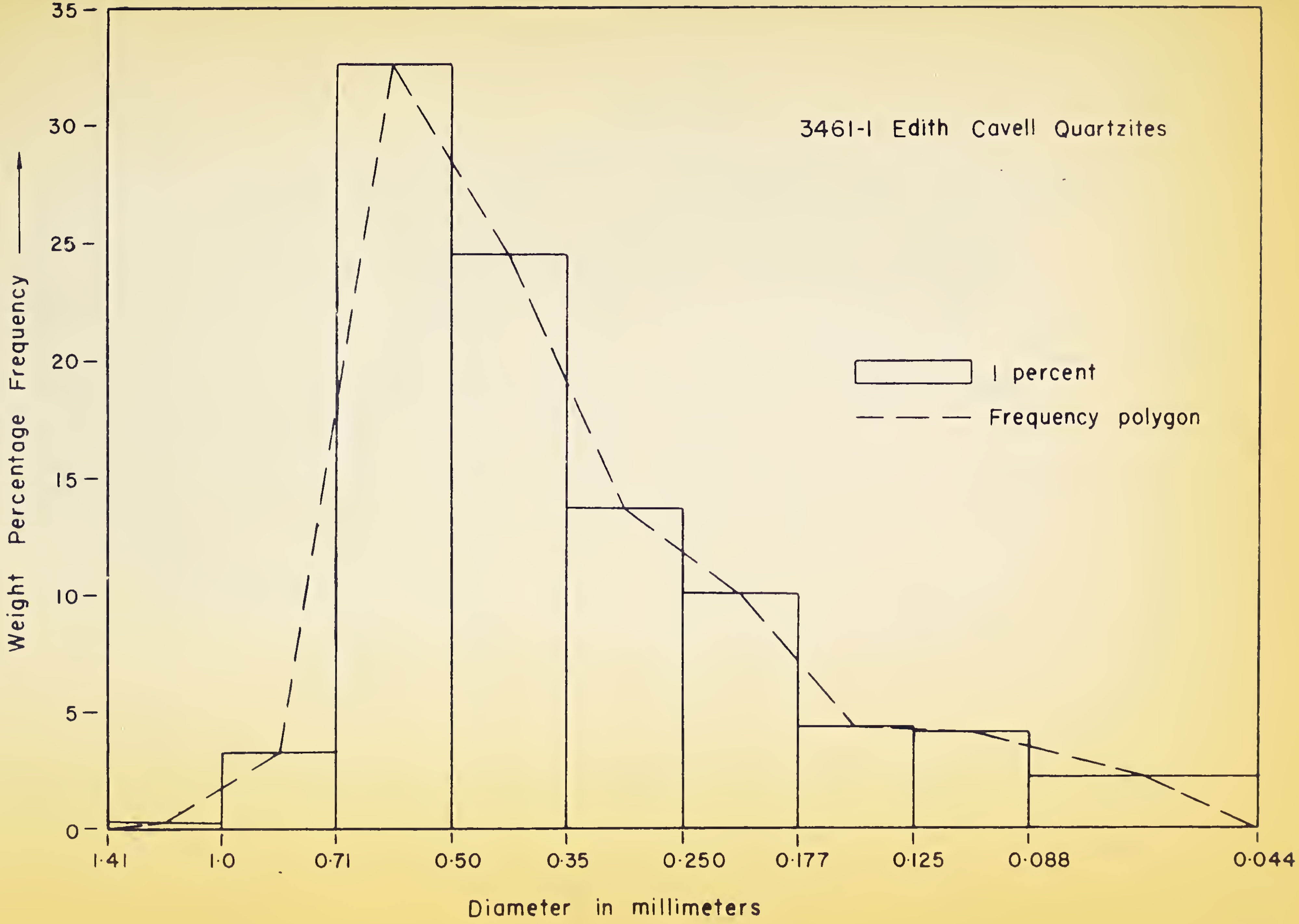
3461-1 Edith Cavell Quartzites
1 percent
Frequency polygon
Weight Percentage Frequency
35
30
25
20
15
10
5
0
1·41
1·0
0·71
0·50
0·35
0·250
0·177
0·125
0·088
0·044
Diameter in millimeters

Figure 7.

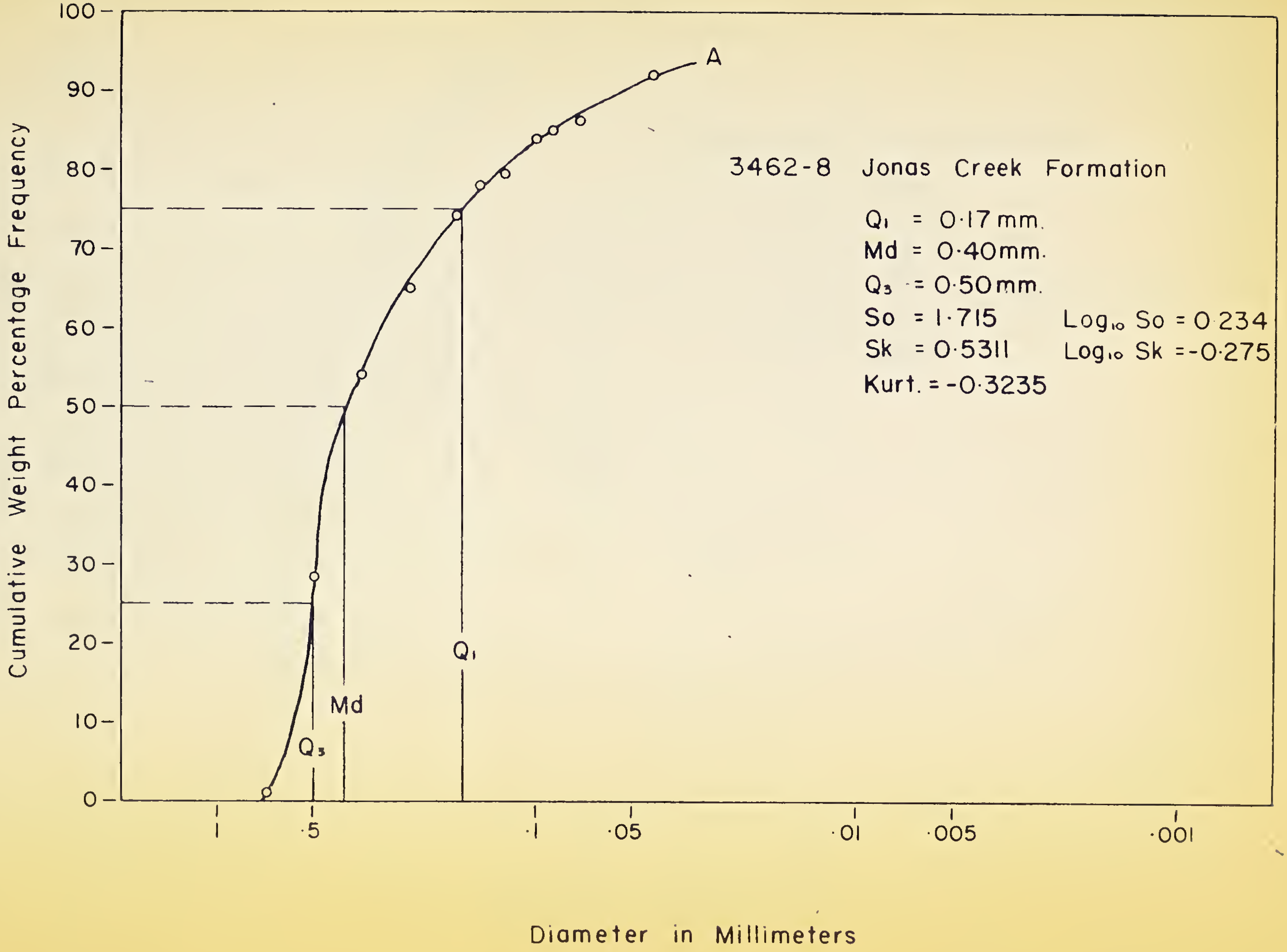
3462-8 Jonas Creek Formation
Q₁ = 0·17 mm.
Md = 0·40mm.
Q₃ = 0·50mm.
So = 1·715
Sk = 0·5311
Kurt. = -0·3235
Log₁₀ So = 0·234
Log₁₀ Sk = -0·275
A
Q₁
Md
Q₃
Cumulative Weight Percentage Frequency
100
90
80
70
60
50
40
30
20
10
0
1
·5
·1
·05
·01
·005
·001
Diameter in Millimeters

Figure 8.

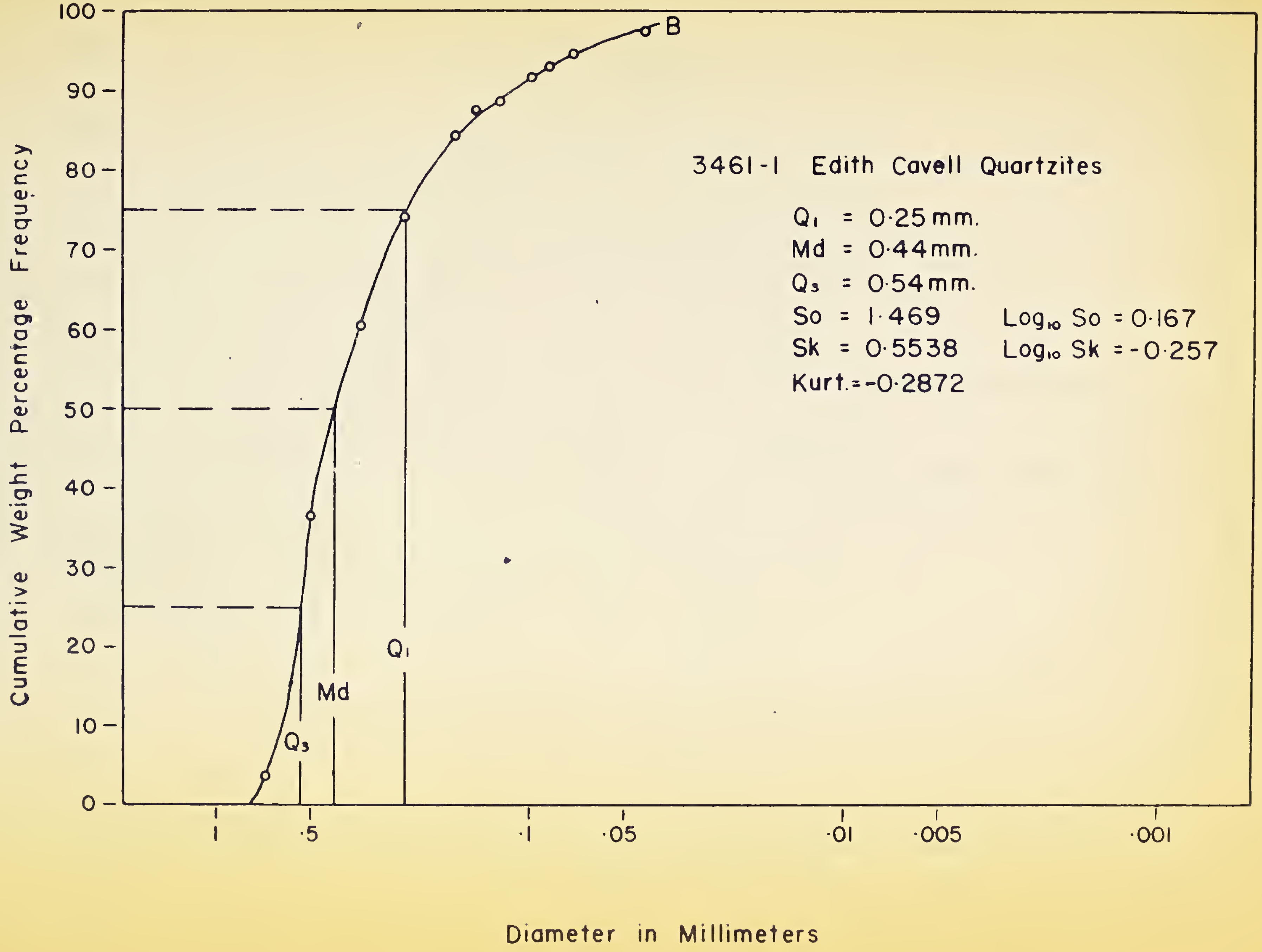
3461-1 Edith Cavell Quartzites
Q_1 = 0·25 mm.
Md = 0·44 mm.
Q_3 = 0·54 mm.
So = 1·469
Sk = 0·5538
Kurt. = -0·2872
Log_{10} So = 0·167
Log_{10} Sk = -0·257
B
Q_1
Md
Q_3
Cumulative Weight Percentage Frequency
100
90
80
70
60
50
40
30
20
10
0
1
·5
·1
·05
·01
·005
·001
Diameter in Millimeters

Figure 9.

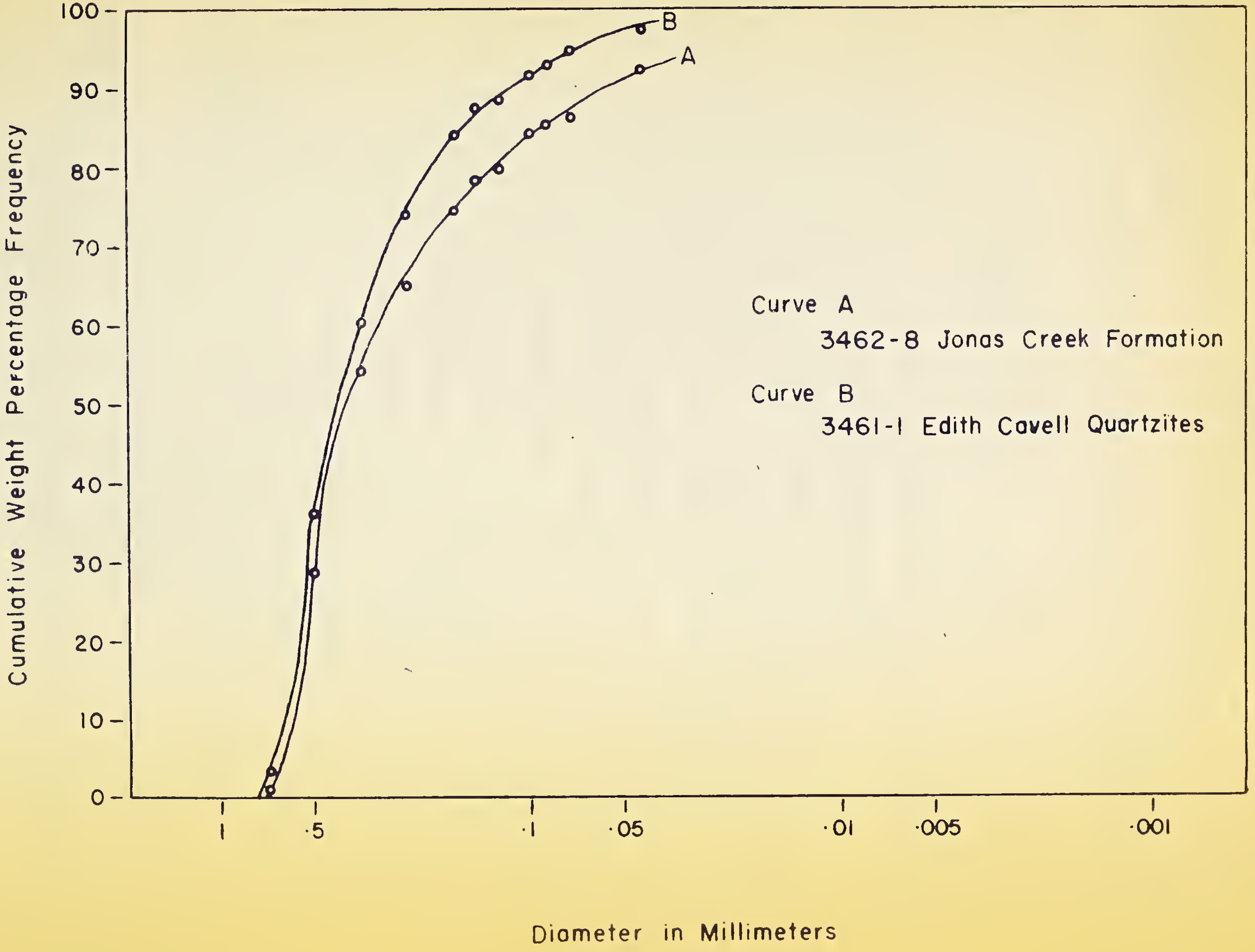
100
90
80
70
60
50
40
30
20
10
0
Cumulative Weight Percentage Frequency
1
·5
·1
·05
·01
·005
·001
Diameter in Millimeters
B
A
Curve A
3462-8 Jonas Creek Formation
Curve B
3461-1 Edith Cavell Quartzites

Figure 10.

CHAPTER FIVE

X-RAY ANALYSIS

GLAUCONITE

General Statement:

X-ray patterns were run on the following three glauconite samples:

3461-5 (AK-55)
KA-113
KA-114

Powder photographs of unoriented material as well as diffractometer readings from orientated powder mounts were employed.

Sample 3461-5 is from the base of the limy series in the Sunset Peak Area (see Appendix A, p. I). Samples KA-113 and KA-114 are from the Franconia formation of Upper Cambrian age, Goodhue County, Minnesota, U. S. A. Sample KA-113 occurs in a sandy glauconitic layer 6½ feet above the base of a roadcut on County Road 34, approximately 3 miles west of Red Wing, SW¼, Sec. 27, Twp. 113 N., Rge. 15 W. Sample KA-114 occurs 22 feet above the base of the same exposure.

Microscopic examination shows glauconite in sample 3461-5 occurs as small dark-green irregular masses, with traces of attached calcite. Sample KA-113 is composed of light-green oval shaped pellets and irregular yellow fragments which may be a result of weathering. Sample KA-114 consists of small light-green smooth oval pellets.

Unorientated Powder Mounts

Procedure:

Each sample was finely crushed in a hand mortar, and shaped

into thin rods by mixing with transparent fingernail polish and rolling between two glass slides. X-ray diffraction photographs were taken in a Phillips powder camera of 114.6 mm. diameter with a slit aperture, using Cu radiation and a Ni filter. Films were exposed one hour. Intensities were estimated visually and are expressed on a one to ten scale.

Results:

Results of the three powder photographs are given in Table 4, and show little variation between line spacings or intensities. Warshaw (1957), quoted by Moore (1958), classified glauconites on the variations in basal spacing in the following manner:

(1) "well-crystallized" glauconite, d (001) = 10.1A°.

(2) "typical" glauconite, d (001) = 10.2 - 10.3A°.

(3) "mixed-layer" glauconite, d (001) = 10.4 - 11.0A°.

(4) "poorly crystallized" glauconite, d (001) $>$ 11.0A°

Basal layer spacings vary from 10.07 to 10.36. On this basis sample 3461-5 would be a "well crystallized" glauconite, and samples KA-113 and KA-114 a "typical" glauconite.

The d spacings compare favourably with the values obtained by Burst (1958, fig. 6) in his randomly orientated powder mounts

Orientated Powder Mounts

Preparation of X-ray diffraction slides:

Two samples were prepared for orientated X-ray diffraction study. One mount was made of the glauconite obtained from sample 3461-5 (KA-55), and one mount was made of the Franconia glauconite

Unorientated Powder Mounts

LINE	3461-5		KA-113		KA-114		Indices hkl Moore(1958)
	d	I(rel)	d	I(rel)	d	I(rel)	
1	10.07	10	10.36	10	10.27	10	001
2	4.48	10	4.54	10	4.54	10	020
3	3.66	6	3.67	5	3.75	5	$11\bar{2}$
4	3.34	5	3.35	5	3.33	5	022
5	3.057	4	3.105	4	3.100	4	112
6	2.587	10	2.593	10	2.596	10	$13\bar{1}$
7	2.406	7	2.421	7	2.421	7	132 or 201
8	1.999	1	1.998	1	1.988	1	005
9	1.666	1	1.675	1	1.679	1	240 $31\bar{2}$ 310 241
10	1.509	10	1.522	10	1.520	10	060 or 330
11	1.302	5	1.316	5	1.318	5	260

Table 4.

(KA-114). The glauconite was hand picked to ensure maximum purity.

A piece of hollow glass tubing one inch in diameter and two inches long was ground flat on one end on a grinding wheel. The flat end was lightly coated with stopcock grease and placed on a clean glass slide.

About 25 milligrams of glauconite was ground to a very fine powder in an agate mortar and transferred to a small beaker containing a few c.c. of water. The mixture was stirred well and poured into the glass cylinder on the glass slide. After the clay-size fractions of glauconite had settled, the liquid was drawn off by means of a fine hollow needle of glass using vacuum suction. After the sediment had dried, the glass cylinder was removed and the stopcock grease wiped from the slide.

Theoretically, the glauconite particles upon settling to the bottom of the sedimentation column should be orientated so that their 001 planes are orientated parallel to the glass slide.

The orientated mounts were run on a Phillips X-ray Diffractometer. The unit consisted of a wide angle goniometer with a geiger tube pick-up, and a Brown recording unit. Settings were as follows:

X-ray Diffractometer: K.V. = 40
M.A. = 15
Cu radiation
Ni filter

Goniometer: Speed 2 degrees/minute

Recorder: Scale factor 16
Multiplier 1
Time constant 4 seconds

Orientated Powder Mounts

LINE	3461-5		KA-114		Indices hkl Moore(1958)
	d	I(rel.)	d	I(rel.)	
1	9.9	9.05s	9.9	9.4	001
2	4.87	6.6B	n.d.		002
3	4.48	7.1s	4.48	6.5	020
4	3.62	6.9s	n.d.		$11\bar{2}$
5	3.31	10s	3.30	10	022
6	3.03	calcite(?) 6.4B	n.d.		112
7	2.866	6.1s	n.d		$11\bar{3}$
8	2.659	5.88	n.d.		023
9	2.564	5.0s	n.d.		$13\bar{1}$
10	2.392	4.9B	n.d.		132 or 201
11	1.989	4.9B	n.d.		005
12	1.65	4.1B	n.d.		240 $31\bar{2}$ 310 241
13	1.501	3.9B	n.d.		330

Table 5.

COMPARISON OF X-RAY DIFFRACTION PATTERNS

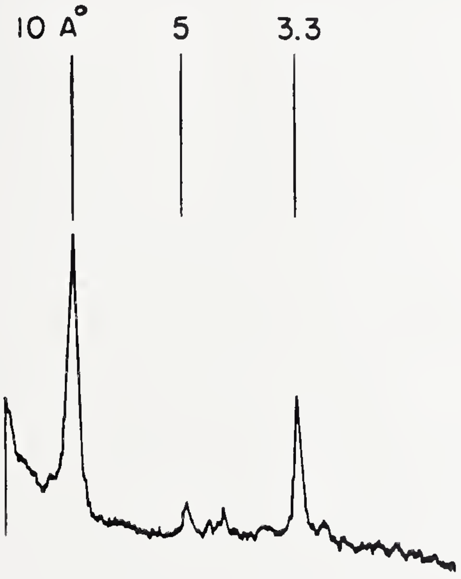

1. Ceratopyge Sandstone, Sweden, Ordovician (after Burst 1958, Fig. 2.).

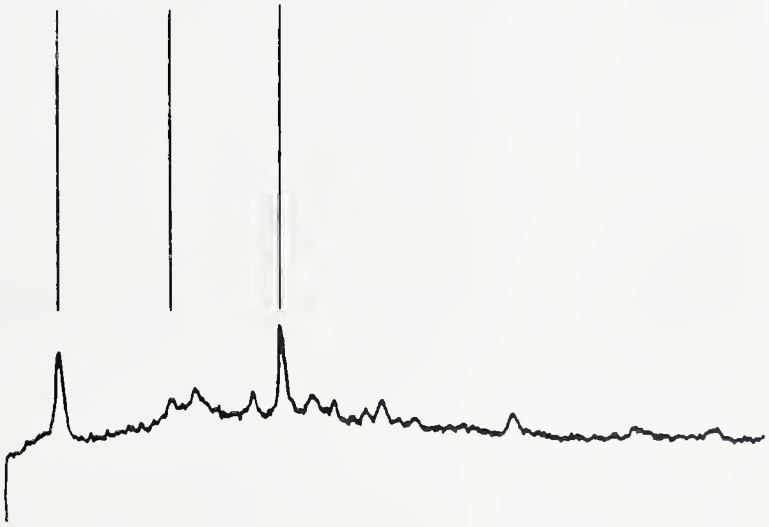

2. Sample 3461-5, Cambrian, Sunset Peak Area, Jasper Park.

PALAEOZOIC GLAUCONITES

Figure 11.

Results:

The results of measurements are given in Table 5. On the whole the basal spacings (d 001) values are a fraction lower on the orientated specimens than values obtained on the random powder mounts. High intensities obtained on spacing of 4.48, 2.58 and 1.51 in the randomly orientated powder mounts have been considerably reduced in the orientated powder mounts.

Comparison of Results:

The results obtained using the orientated X-ray diffraction method compares very well with work done by Burst (1958), and a comparison is shown in Figure 11. The 9.9 and 3.31 basal reflections are high, sharp, and symmetrical, while the 4.48 reflection is moderate and broad. In general the curves correspond very well to his graph of the glauconite from the Ceratopyge Sandstone, Sweden, of Ordovician age (Burst, 1958, Fig. 2, No. 3). Therefore, there is little doubt but that 3461-5 is an ordered glauconite according to Burst's classification.

FELDSPAR

An unoriented powder mount was made of feldspar (A/K 54) obtained from sample 3461-16. The procedure is the same as that used in the preparation of unorientated glauconite powder mounts.

The purpose of running an X-ray diffraction pattern in a Phillips powder camera was to see if the feldspar was a potassium feldspar. Examination of the feldspar with a petrographic microscope showed most of the grains were microcline twinned and partially altered

and coated with a thin film of hematite. Results are tabulated below in Table 6, and show the feldspar to be predominately microcline. A.S.T.M. cards were used to identify the lines.

LINE	I(rel)	d SPACING	IDENTIFICATION
1	8	4.25	orthoclase, quartz
2	1	3.868	microcline
3	1	3.715	microcline
4	2	3.513	orthoclase
5	10	3.27B	orthoclase
6	1	2.973B	microcline
7	1	2.789	microcline, calcite
8	2	2.546B	microcline
9	2	2.454	orthoclase
10	3	2.168	microcline
11	2	1.991	microcline
12	8	1.816	orthoclase, quartz
13	1	1.557	microcline
14	2	1.547	microcline
15	2	1.381	orthoclase

TABLE 6.

CHAPTER SIX

CHEMICAL ANALYSIS AND DEPOSITIONAL ENVIRONMENT OF GLAUCONITE

General Statement

Glauconite occurring in strata of probable Lower (?) Cambrian age was obtained primarily for potassium-argon age dating work. The glauconite is contained in a limy-mud series (suite 3461, samples 4 and 5) 20 feet above the contact of the underlying Edith Cavell quartzite.

Examination of thin sections (Appendix B, page XV and XVI) shows that the glauconite is probably authigenic. The glauconite grains range from fine to medium sand-size. They have an irregular rather than rounded outline, and are associated with organic material, some of which may be trilobite or other arthropod appendage fragments.

Age dating of glauconite by the potassium-argon method is critically dependent upon the percentage of potassium contained in the mineral. The potassium content in glauconites found in beds of similar ages does vary to some degree. This variability may be due more to the structure of glauconite rather than the depositional environment existing at the time the glauconite was formed.

From several chemical analyses of glauconite Burst (1958) constructed chemical formulas which showed a direct relationship to "ordered" and "disordered" glauconites. This ordering and disordering in the layered lattice was confirmed by X-ray studies. X-ray studies of this glauconite show that it is an ordered glauconite. It was felt that making a chemical analysis of this glauconite and constructing the chemical formula would be useful in determining whether or not

this glauconite could be classified as an ordered glauconite on the basis of the chemical formula alone, as Burst (1958) did with his glauconites. It was thought that the analysis might also shed some light on the depositional environment which existed at the time of formation of the glauconite.

Separation of Glauconite

The separation of glauconite from its matrix is a relatively simple but lengthy procedure. Nevertheless it must be done carefully to ensure maximum purity of the sample obtained.

The glauconite was contained in samples 4 and 5, suite 3461. Of the two, sample number 5 contained the most glauconite. To ensure glauconite as pure as possible, weathered surfaces on samples were chipped away. The samples were crushed by hand in an iron mortar to pass through a 45 mesh screen. The disaggregated sample was sized with a series of sieves consisting of the following screen sizes; 45, 60, 80, 120 and 170 mesh (U.S. Sieve Series).

After sieving, a hand magnet was run through the various fractions to remove iron filings derived from crushing in the iron mortar. Each sieve fraction was run through a Frantz Isodynamic Separator. Three current strengths were used; 0.3, 0.5 and 0.6 amperes. The Frantz Separator was kept at a constant slope of 20 degrees and a tilt of 8 degrees. A setting of 0.3 amperes effectively removed minerals more magnetic than glauconite. At 0.5 amperes the main fraction of glauconite was removed, since glauconite is magnetic around 0.35 amperes. At 0.6 amperes remaining glauconite was recovered.

Results of Glauconite Analysis

	Initial %		Corrected % *	
SiO_2	49	14	50	34
TiO_2		11		11
Al_2O_3	20	46	20	95
Fe_2O_3	7	04	7	21
FeO	1	82	1	86
MnO		02		02
MgO	3	28	2	88
CaO	1	09		22
Na_2O		10		10
K_2O	8	95	9	17
P_2O_5		04		04
H_2O^+	6	03	6	18
H_2O^-		88		90
Rb_2O		02		02
CO_2	1	19	-	-
Total	100	17	100	00

* -Corrected for quartz contamination of 0.0004 grams.

-Corrected for MgO and CaO from dolomite matrix impurities.

-Recalculated to 100 %.

-This analysis was used in the calculation of the chemical formula.

Table 7.

[illegible]

[illegible]		[illegible]
[illegible]	....	[illegible]
[illegible]	....	[illegible]
[illegible]	....	[illegible]
[illegible]	....	[illegible]
[illegible]	....	[illegible]
[illegible]	....	[illegible]
[illegible]	....	[illegible]
[illegible]	....	[illegible]
[illegible]	....	[illegible]
[illegible]	....	[illegible]
[illegible]	....	[illegible]
[illegible]	....	[illegible]
[illegible]	....	[illegible]
[illegible]	....	[illegible]
[illegible]	....	[illegible]
[illegible]		[illegible]

[illegible]

The glauconite fractions obtained from the Frantz Separator were separated from impurities by a heavy liquid separation using tetrabromoethane ($C_2H_2Br_4$, S.G. 2.95) mixed with acetone until a Specific Gravity of about 2.65 was obtained. The glauconite fractions were mixed with the liquid and centrifuged for one minute. The quartz, calcite and other impurities sank to the bottom of the tube, while the glauconite floated. The Specific Gravity of the glauconite was judged to be 2.62.

The glauconite was again run through the Frantz Separator using the same current settings. Glauconite separating at 0.6 amperes was centrifuged as before and thoroughly washed with acetone. As a final step the glauconite was run through the Frantz Separator set at a slope of 20 degrees, tilt 12 degrees. The magnetic fraction when examined with a petrographic microscope was found to be pure except for a few calcite grains adhering to some glauconite grains. The sample was now considered pure enough for chemical analysis.

The glauconite was chemically analyzed using the Department of Geology's Rock Analysis Laboratory facilities. Duplicate samples were analyzed. The writer ran one sample while Dr. H. Baadsgaard ran the other as a check.

Flow charts outlining the general procedure are shown in Appendix C, pages XXIV to XXVIII.

Reliability

Results obtained are believed to be reliable, as the total weight percentage on the uncorrected analysis has less than 1% error. Operational errors were checked through duplicate runs made by

H. Baadsgaard and the writer. On the whole, the writer's values ran a little lower than those obtained by H. Baadsgaard. Since this work is new to the writer it is reasonable to assume that if any errors were made, the writer made them. Therefore, values shown in Table 7 are H. Baadsgaard's values. The total Fe_2O_3 is an average of six runs made, and the MgO of four runs with reprecipitation. For some reason, likely operational, the Penfield tube method for determining total H_2O was not satisfactory, and values obtained by this method were much lower than loss of water by total ignition. Original K_2O values obtained were around 7% and were discarded because the writer had trouble with decrepitation of the alkali salts and lost material here on both samples.

The K_2O was rerun, and the values obtained appear reliable.

The 1.19% CO_2 obtained for the glauconite was considered to come from carbonate (matrix) contamination. The glauconite, when dropped in water, produced a white scum on the surface which fizzed with the addition of a few drops of HCl acid. This scum is carbonate material.

The value for CO_2 is reliable. An air blank was first run, followed by decomposing a known amount of pure $CaCO_3$. The results obtained deviated by less than 1/2000 from the theoretical value. Corrections were made for temperature and pressure. Pressure readings of mercury were obtained from the Federal Department of Transport, and the reading used was taken only twenty minutes before the experiment began.

The method of chemical analysis carried out on this glauconite

TABLE 8. GLAUCONITE ANALYSES

									ordered				disordered		
	1	2	3	4	5	6	7	8	9	10	11	12	13	14	15
SiO_2	48.87	49.07	52.64	49.29	43.33	48.54	47.42	47.15	48.0	52.7	48.66	47.1	49.0	51.7	51.5
Al_2O_3	9.53	10.95	5.78	3.17	7.27	7.82	7.19	6.20	10.7	13.7	8.46	11.5	8.4	10.9	23.6
Fe_2O_3	19.26	15.86	17.88	21.72	24.87	17.50	22.64	21.50	18.0	9.5	18.80	16.00	20.0	14.5	10.0
FeO	3.12	1.36	3.85	3.19	2.90	3.07	3.39	3.76	3.9	5.0	3.98	8.00	2.4	4.3	3.7
MgO	3.02	4.49	3.43	3.85	2.95	3.26	2.28	2.80	3.0	3.5	3.56	3.6	4.0	4.5	2.0
CaO	.55	0.07	0.12	0.74	0.10	0.68	0.27	0.46	3.0	0.3	0.62	1.3	0.3	0.00	0.6
K_2O	6.78	7.51	7.42	6.02	6.00	5.87	7.46	6.98	7.8	8.2	8.31	8.2	7.0	6.15	4.8
Na_2O	.69	0.13	0.18	0.12	0.02	0.22	0.05	0.13	0.18	0.1	0.00	0.2	0.18	0.23	0.62
P_2O_5		0.19	0.18	0.32	0.15	0.14	0.22	0.19							
MnO															
TiO_2		0.15	0.16	0.12	0.20	0.10	0.10	0.14							
Rb_2O															
Cr_2O_3		0.07	n.d.	n.d.	n.d.	0.03	0.04	0.05							
S		0.06	n.d.	n.d.	n.d.	0.05	0.05	0.06							
BaO		nt.fd	n.d.	n.d.	n.d.	nt.fd	nt.fd	0.04							
CO_2															
H_2O^+		6.63	5.86	7.21	6.22	6.00	6.07	6.47							
H_2O^-		3.66	2.83	4.60	5.94	6.71	3.01	4.20							
H_2O(1gm)	7.14								7.4	6.8	6.56	6.44	7.5	6.9	4.7
Total	98.96	100.20	100.23	100.35	99.95	99.99	100.19	100.13	101.98	99.80	99.08	102.34	98.78	99.18	100.98

1. Average of 29 analysis from Hendricks, S.B. and Ross, C. S., (1941,pp.619-693).
2-8. Hutton, C.O., and Seelye, F.T., (1941, p. 596).
*9-12. Ordered glauconites, Burst, J.F., (1958, p. 7).
*13-15. Disordered glauconites, Burst, J.F., (1958, p. 7).
16. Illite, Rankama, K. and Sahama, Th. G., (1949, p. 206).
17. 3461-5 Cambrian Glauconite (Uncorrected for impurities).
18. 3461-5 Cambrian Glauconite (Corrected for impurities).

*9. Navesink Fm., N.J. Greensand,
10. Ceratopyge Sandstone, Sweden,
11. Bonneterre Fm., Missouri, Camb Ross, 1941).
12. Franconia Fm., Wisconsin, Camb
13. Bashi Fm., Alabama, Eocene.
14. Pierson Fm., Texas, Eocene.
15. "Subsurface," California, Eoce

YSES

dered		disordered					
11	12	13	14	15	16	17	18
48.66	47.1	49.0	51.7	51.5	50.10	49.14	50.34
8.46	11.5	8.4	10.9	23.6	25.12	20.46	20.95
18.80	16.00	20.0	14.5	10.0	5.12	7.04	7.21
3.98	8.00	2.4	4.3	3.7	1.52	1.82	1.86
3.56	3.6	4.0	4.5	2.0	3.93	3.28	2.88
0.62	1.3	0.3	0.00	0.6	0.35	1.09	.22
8.31	8.2	7.0	6.15	4.8	6.93	8.95	9.17
0.00	0.2	0.18	0.23	0.62	0.05	0.10	.10
						0.04	.04
						0.02	.02
					0.50	0.11	.11
						0.02	.02
						1.19	
					6.82	6.03	6.18
						0.88	.90
6.56	6.44	7.5	6.9	4.7			
99.08	102.34	98.78	99.18	100.98	100.44	100.17	100.00

*9. Navesink Fm., N.J. Greensand, Cretaceous.

10. Ceratopyge Sandstone, Sweden, Ordovician.

11. Bonneterre Fm., Missouri, Cambrian, (Hendricks and Ross, 1941).

12. Franconia Fm., Wisconsin, Cambrian.

13. Bashi Fm., Alabama, Eocene.

14. Pierson Fm., Texas, Eocene.

15. "Subsurface," California, Eocene.

is a time consuming one, which, however, has shown over the years to give the best results compared to more rapid methods.

Glauconite analyses compiled from the literature are listed in Table 8.

Comparison and Discussion of Data

Examination of analyses in the literature show that they differ from the analysis obtained for the Sunset Peak glauconite (#18). This Cambrian glauconite corresponds most closely to #15 on the basis of the Al_2O_3 and SiO_2 content, though not in potassium value, which is higher.

Generally, except for the distinctly higher Al_2O_3 and slightly higher K_2O content, this glauconite is similar to the glauconite obtained from the Ceratopyge sandstone (#10) from Sweden. The X-ray patterns (Figure 11) of both these glauconites are similar. An illite analysis was included to show that, except for a lower K_2O content, the overall values of the oxides of the elements in the illite are strikingly similar to the values obtained for this glauconite.

In general, the Al_2O_3 percentage is approximately two times higher than is found in the more iron-rich glauconites, while the Fe_2O_3 content is two times lower. The K_2O content is higher than average. The other constituents in this glauconite are comparable with the great majority of the listed glauconite analyses.

CALCULATION OF THE CHEMICAL FORMULA OF GLAUCONITE

The formula constructed is based on an idealized unit cell of twenty-four oxygen atoms which can accommodate, after allowances

for hydrogen, forty-four cationic valence units. According to Kelly (1945) these must be distrubuted among the materials contained in the chemical analysis to effect neutrality. The results of calculations are shown in Table 9.

TABLE 9. RESULTS OF CALCULATIONS

Mol.wt.	Constituent	%	Mole-% of Cation	Mole-% of Oxygen	% O	Number of Cations per 11 Oxygen atoms
60.09	SiO_2	50.34	0.8377	1.6754	26.806	3.500
79.90	TiO_2	0.11	0.0014	0.0028	.044	0.0067
101.94	Al_2O_3	20.95	0.4110	0.6165	9.867	1.7170
159.70	Fe_2O_3	7.21	0.0903	0.1355	2.167	0.3774
71.84	FeO	1.86	0.0260	0.0260	.416	0.109
70.93	MnO	0.02	0.003	0.0003	.005	0.001
40.32	MgO	2.88	0.0714	0.0714	1.143	0.298
56.08	CaO	0.22	0.0039	0.0039	.062	0.0163
61.99	Na_2O	0.10	0.0016	0.0016	.026	0.0134
94.19	K_2O	9.17	0.0973	0.0973	1.558	0.8137
141.96	P_2O_5	0.04	0.014	0.0014	0.017	0.0025
18.02	H_2O^+	6.18	-	-	-	-
18.02	H_2O^-	0.90	-	-	-	-
186.96	Rb_2O	0.02	0.0002	0.0001	0.002	0.001
-	CO_2	-	-	-	-	-
		100.00		2.6322	$\frac{42.113}{16} =$	
					2.6321	

The mole-percentage of cations is obtained by dividing the percentage of consistuent by its molecular weight.

e.g. SiO_2: $\frac{50.34}{60.09} = 0.8377$

The mole-percentage of oxygen is obtained by multiplying the number of oxygens/cation by the mole-percentage of cation.

e.g. Si: $2 \times 0.8377 = 1.6754$

In a one-half unit cell, the cations must accommodate eleven oxygen atoms. The total of the mole-percentage of oxygen is 2.6322.

Since eleven oxygen atoms must be distributed among the cations, there are $\frac{11}{2.6322} = 4.179$ oxygen atoms/mole-percentage of cation. The mole-percentage of each cation is multiplied by 4.179, and the value obtained equals the number of cations per eleven oxygen atoms.

e.g. SiO_2: $0.8377 \times 4.179 = 3.500$

The cations must be distributed in the structure. The cations occupy the following positions in the glauconite structure:

Tetrahedral position: Si^{+4}, P^{+5}, Al^{+3}

Octahedral position: Fe^{+3}, Fe^{+2}, Mg^{+2}, Ti^{+4}, Mn^{+2}, Al^{+3}

Interlayer position: K^{+}, Na^{+}, Rb^{+}, Ca^{+2}

The total number of cations which can be accommodated in the tetrahedral position per one-half unit cell is four. The total number of cations provided by the Si^{+4} and P^{+5} atoms is 3.500 + 0.0025 = 3.5025. Since a total number of four cations must be obtained, the remaining value is made up by aluminum. Therefore, the total number of cations in the tetrahedral layer is:

Si^{+4}	3.500
P^{+5}	0.0025
Al^{+3}	0.4975
Total	4.0000

The total number of cations which are accommodated in the octahedral position is two. This value is never less than two, but may be greater than two. The total number of cations which can be accommodated in the octahedral layer is:

Fe^{+3}	0.3774	
Fe^{+2}	0.109	
Mg^{+2}	0.298	
Ti^{+4}	0.0067	
Mn^{+2}	0.001	
Al^{+3}	1.2195	(1.717 - 0.4975)
Total	2.0116	

The number of cations in the interlayer position is:

K^+	0.8137
Na^+	0.0134
Rb^+	0.0010
Ca^{+2}	0.0326
Total	0.8607

The lattice charge must be balanced by the total charge of the interlayer cations, which is 0.861. The total lattice charge is obtained by multiplying the number of cations per eleven oxygen atoms of each element by its valence, and totalling the values. For example, the lattice charge produced by Si^{+4} is 3.500 x 4 = 14.000. The total lattice charge is 21.1385. There are effectively eleven oxygen atoms in a one-half unit cell, with a total valence of 11 x (-2) = -22. Since the total lattice charge of the cations is 21.1385, the difference must be balanced by the interlayer cations.

Total lattice charge from the oxygen atoms = -22.0000
Total lattice charge of the cations = 21.1385
Difference = - 0.8615

This minus charge of 0.862 is balanced by the positive charge of 0.861 supplied by the interlayer cations.

The results are tabulated as follows:

NUMBER OF CATIONS PER ONE-HALF UNIT CELL

Interlayer Adsorbed				Octahedral						Tetrahedral			Total Octrahedral atoms	Charge	
K^+	Ca^{++}	Rb^+	Na^+	Al^{+3}	Fe^{+3}	Fe^{+2}	Mg^{+2}	Ti^{+4}	Mn^{+2}	Si^{+4}	Al^{+3}	P^{+5}		Lattice	Interlayer cations
.814	.016	.001	.013	1.220	.377	.109	.298	.007	.001	3.50	.498	.003	2.012	0.862	0.861

The previous calculations (following the method of Kelly, 1945) result in the distribution of the cations in a one-half unit cell. For the distribution of the cations in a full unit cell, all values must be multiplied by two.

3.g. Si^{+4}: $3.500 \times 2 = 7.00$

Therefore the chemical formula of this glauconite is:

$K_{1.63}(Na, Rb, Ca)_{.06}(Al_{2.44}Fe^{+3}_{.76}Fe^{+2}_{.22}Mg_{.60})(Si_{7.00}Al_{1.00})\ O_{20}(OH)_4$

A schematic presentation of the crystal structure of illite is shown in Figure 12.

Comparison of Glauconite Formulae

Burst (1958) calculated formulas for ordered and disordered glauconites from his chemical analyses. His formulae are tabulated along with the chemical formula obtained for this glauconite in Table 10.

TABLE 10.

Ordered Glauconites	3461-5, Alberta, Cambrian $K_{1.63}(Na,Ca,Rb)_{.06}(Al_{2.44}Fe^{111}_{.76}Fe^{11}_{.22}Mg_{.60})\ (Si_{7.00}Al_{1.00})O_{20}(OH)_4$
	Bonne Terre Fm., Missouri, Cambrian $K_{1.58}(Ca)_{.10}(Al_{.70}Fe^{111}_{2.11}Fe^{11}_{.49}Mg_{.82})\ (Si_{7.22}Al_{.78})\ O_{20}(OH)_4$
	Franconia Fm., Wisconsin, Cambrian $K_{1.52}(Na,Ca)_{0.27}(Al_{.81}Fe^{111}_{1.74}Fe^{11}_{.97}Mg_{.79})\ (Si_{6.85}Al_{1.15})\ O_{20}(OH)_4$
	Ceratopyge Fm., Sweden, Ordovician $K_{1.48}(Na,Ca)_{0.06}(Al_{1.74}Fe^{111}_{1.02}Fe^{11}_{.59}Mg_{.77})\ (Si_{7.47}Al_{.53})\ O_{20}(OH)_4$
	Navesink Fm., New Jersey, Cretaceous $K_{1.43}(Na,Ca)_{.51}(Al_{.81}Fe^{111}_{1.97}Fe^{11}_{.47}Mg_{.66})\ (Si_{6.99}Al_{1.01})\ O_{20}(OH)_4$
Disordered Glauconites	Bashi Fm., Mississippi, Eocene $K_{1.32}(Na,Ca)\ (Al_{.74}Fe^{111}_{2.23}Fe^{11}_{.30}Mg_{.89})\ (Si_{7.28}Al_{0.72})\ O_{20}(OH)_4$
	Burdette Fm., Texas, Upper Cretaceous $K_{1.20}(Na)_{0.09}(Al_{1.66}Fe^{111}_{1.47}Fe^{11}_{0.40}Mg_{0.62})\ (Si_{6.98}Al_{1.02})\ O_{20}(OH)_4$
	Pierson Fm., Texas, Eocene $K_{1.12}(Na)_{0.05}(Al_{1.25}Fe^{111}_{1.58}Fe^{11}_{0.52}Mg_{0.95})\ (Si_{7.41}Al_{0.59})\ O_{20}(OH)_4$
	"Subsurface," California, Eocene $K_{0.81}(Na,Ca)_{0.17}(Al_{2.53}Fe^{111}_{1.05}Fe^{11}_{0.46}Mg_{0.41})\ (Si_{6.84}Al_{1.16})O_{20}(OH)_4$

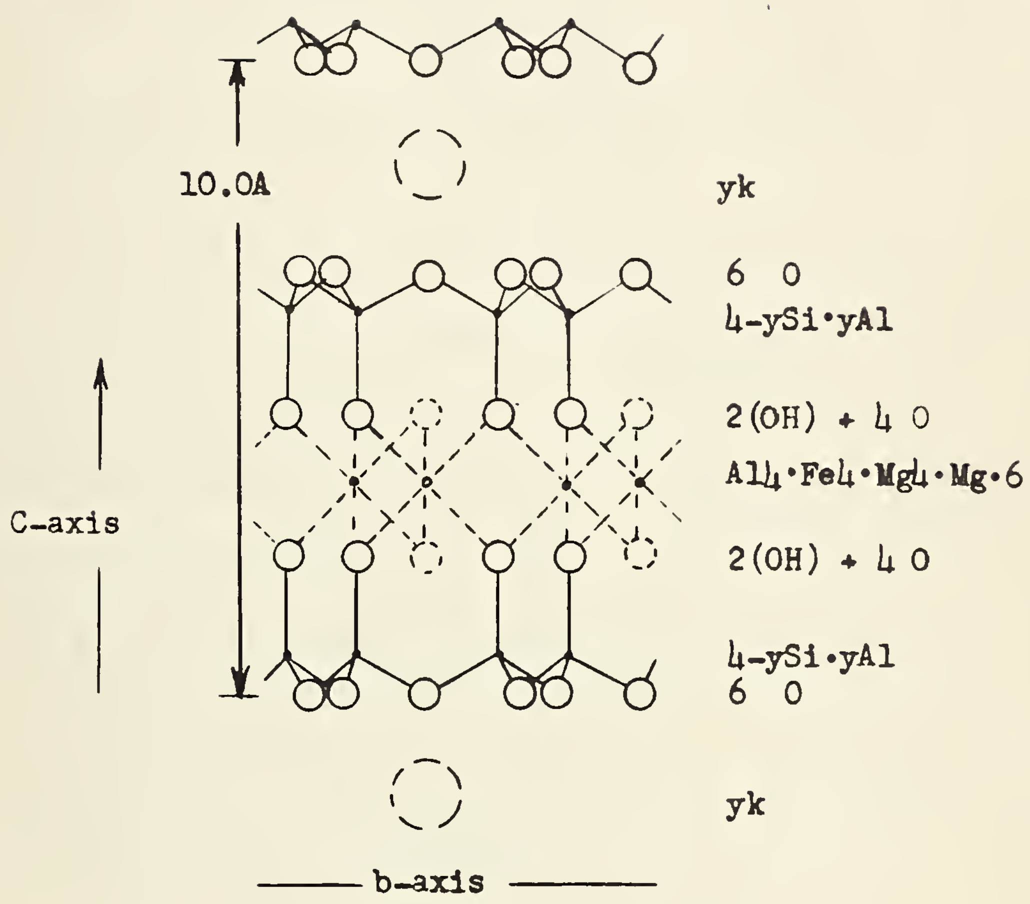
10.0A
yk
6 0
4-ySi·yAl
2(OH) + 4 0
Al4·Fe4·Mg4·Mg·6
C-axis
2(OH) + 4 0
4-ySi·yAl
6 0
yk
b-axis

Illite $(OH)_4Ky(Al_4\cdot Fe_4\cdot Mg_4\cdot Mg_6)(Si_{8-y}\cdot Aly)\ O_{20}$

Fig. 12 Schematic presentation of the crystal structure of the clay mica, illite (from Grim, 1942, p. 244).

It is interesting to note that the ordered glauconites contain more potassium than the disordered glauconites. X-ray work by Burst (1958) substantiates the idea that when the potassium equivalent falls below approximately 1.4 per unit cell, ordered stacking becomes less apparent owing to the decreased binding power normally supplied to the lattice by potassium. From his analyses, Burst (1958) believes that the Bonne Terre glauconite and Franconia glauconite represent an end point mineral composition to which the name glauconite should be applied.

The writer does not entirely agree with Burst. X-ray and chemical analysis data show the glauconite used in this study is ordered. It is entirely possible that the Al^{+3} and Fe^{+3} content of the mineral glauconite may vary considerably. From glauconite analyses examined in the literature it appears that the aluminum-rich glauconite is very rare. The writer considers this glauconite to be representative of aluminum-rich glauconite. It is to be noted that this glauconite corresponds much closer to illite on the basis of chemical analysis than do the iron-rich glauconites.

ORIGIN OF GLAUCONITE

General Statement

Theories regarding the formation of glauconite have been as variable as they are numerous, and only the more important contributions to the literature are considered.

In 1928 Keferstein introduced the term "glauconit", now called glauconite, from the Greek glaucos = bluish green and ite = resembling (Burst, 1958). This term would have undoubtedly included all earthy

green pellets.

In a study of the Monterey Bay Area, California, Galliher (1935) found glauconite directly associated with biotite. He believed that glauconite was formed from biotite as a decomposition product. Hence, the chemical constituents composing glauconite would be derived wholly from biotite. Very little glauconite found on the sea floor today has been associated with biotite.

Takahashi (1939) discarded the idea of a mica parent for glauconite. He proposed that the mother materials of glauconite were substances that were gelatinized before being transformed into glauconite. He found glauconite filling cavities of fossils, such as foraminifera, the canal of sponge spicules or fissures in minerals.

According to Burst (1958) the theory of lattice closure by potassium fixation is a more likely generalization to explain glauconite formation than the decomposition of biotite or the formation from colloidal gels. The theory in general is that potassium reacts with colloidal silicates by entering between silicate layers, forming such strong bonds as to prevent re-expansion of the crystal lattice and thus re-entrance of water and opening up of the crystal lattice. The potassium is trapped in nonexchangeable form. Kunze and Jeffries (1953) have confirmed this theory with X-ray work on soils.

Burst (1958) postulated three requirements for glauconite formation: (1) a layered silicate lattice, (2) plentiful supplies of iron and potassium, and (3) a favourable environmental oxidation potential. Galliher (1935), and others believed glauconite to have formed under anaerobic or reducing conditions. Takahashi (1939)

thought glauconite formation to have taken place in the sea having a temperature of not less than normal sea water. Krumbein and Garrels (1952) believed glauconite to form in weakly oxidizing to weakly reducing conditions, or with an oxidation potential from +.1 to -.1, and also in weakly alkaline (pH 7-8) conditions. On the other hand, Teodorovich, G.I. (see Chilingar, G.V., 1955) thought that glauconite formed in a weakly oxidizing zone, in which the oxidation-reduction dividing line was markedly below the surface of sediment. The pH values range from 7.2 to 6.6 (neutral) in his "glauconite facies."

Cloud (1955) believes that glauconite is mainly found in marine waters 10 to 400 fathoms in depth and is probably rare above 5 and below 1000 fathoms.

The writer found no mention in the literature of glauconite being found in fresh water sediments.

DISCUSSION OF MAJOR THEORIES OF GLAUCONITE FORMATION

Biotite mica: $K(Mg, Fe, Mn)_3 (OH, F)_2 AlSi_3O_{10}$

TABLE 11. CHEMICAL ANALYSIS OF BIOTITE

	1	2
SiO_2	35.67	36.46
Al_2O_3	14.56	17.15
Fe_2O_3	3.03	8.17
FeO	23.23	14.46
MgO	9.24	8.70
CaO	1.13	0.98
K_2O	8.06	8.23
Na_2O	.49	0.91
TiO_2	-	0.56
MnO	-	1.25
F	-	0.18

1. Gruner (1935)
2. Rankama and Sakama (1950, p. 156)

Compared to most glauconites, biotite has an excess of FeO, MgO, Al_2O_3 and a deficiency in SiO_2 and Fe_2O_3. To form glauconite, biotite would have to undergo a change from a trioctahedral to a dioctahedral lattice. This would involve a partial breakdown of the biotite lattice, and the substitution of Fe^{+3} ions for Al^{+3} in the octahedral layer. Furthermore, this process would have to take place in semi-oxidizing conditions to permit some of the Fe^{+2} to be oxidized to Fe^{+3}.

Although the direct association of glauconite with biotite is known, it is not often found. It seems to the writer that this is perhaps only one process for the formation of glauconite, and takes place only under special environmental conditions.

Gelatinized Substances:

According to Rice (1955, p. 149) a gel is defined as a form of matter in colloidal state that does not dissolve but nevertheless remains suspended in a solvent from which it fails to precipitate without the intervention of heat or of an electrolyte; also, gelatinization is defined as solubility with the formation of jelly-like silica. Takahashi (1939) proposed that the mother materials of glauconite were substances that were gelatinized before being transformed into glauconites. This statement, is a very broad one, and covers almost every type of silicate structure, from clays and micas to relict Al-O-Si chains which may be present in colloidal suspension as a result of weathering of silicate rocks (feldspars etc.). The fact that he found glauconite associated with decaying organisms, coprolites (excretions of mudeaters), and iron sulphide may be due partly to environmental conditions produced by the presence of these organisms.

Colloidal Silicate Lattices

It seems reasonable that glauconite would more likely form from material having a similar crystal lattice structure, such as clays, particularly illite. Clay minerals are phyllosilicates and have a sheet structure somewhat like that of the micas. They consist of two types of layers. One is a silica tetrahedral layer consisting of SiO_4 groups linked together to form a hexagonal network of the compositions Si_4O_{10} repeated indefinitely. The second type of layer is the alumina or aluminum hydroxyls between which aluminum atoms with octahedral coordination are situated in such a position that they are equidistant from six oxygens or hydroxyls. Yoder and Eugster (1955) have shown that illite is essentially clay-size muscovite, sometimes with clay-size quartz. They indicate that muscovite is an authigenic clay mineral in many sediments.

Thus silicate lattices from partially formed and degraded illite may well provide the structural foundations for the formation of of glauconite (Burst, 1958). All that is needed is an abundant supply of iron or aluminum and potassium. Supplies of Fe^{+2} and Fe^{+3} ions could be supplied by decaying organic material by bacteria under mildly oxidizing and reducing conditions. Enough potassium could be obtained from normal hydrolyzate sediments on the sea floor, and normal marine water by processes of base exchange and potassium fixation.

DEPOSITIONAL ENVIRONMENT

According to Burst (1958) the distinguishing chemical features of glauconite are a K_2O content of 7-8 per cent, and 20-25 per cent of total iron in which the ferric iron has been reported to exceed the

ferrous iron by a multiple 3 to 9.

The chemical analysis of this glauconite shows the total iron content to be 9.07 per cent, with a ferric to ferrous iron ratio of approximately 3 to 1. Moreover, the K_2O content exceeds 8 per cent (9.17), which is high compared to most glauconites. Burst (1958) suggests that potassium fixation is limited by the capacity of the depositional medium to supply potassium to the structure, and not so much the nature of the structure itself. Most of the K_2O percentages shown in Table 8, except for Burst's (1958) analyses, are of glauconites developing on the sea floor at the present time. These K_2O values range from 5.87 to 7.51 per cent. In general it seems that the older the glauconite the higher the K_2O content. The general concensus of opinion is that once glauconites are formed they do not absorb potassium from the surrounding depositional medium. The only way the writer can account for the higher percentage of K_2O in this glauconite is that a fairly high concentration of potassium was present in the environmental medium during the formation of the glauconite.

The Al_2O_3 content of this glauconite is 20.95 per cent, while the values in Burst's (1958) ordered glauconites vary from 8.46 to 13.7 per cent. It is to be noted that the percentage values of Al_2O_3 and total iron in Burst's (1958) glauconites are practically the reverse of the values obtained for this glauconite. Usually glauconites form in a semi-reducing to semi-oxidizing environment. Although the amount of iron in the sea is very low, numerous organisms absorb iron from sea water and bottom sediments to aid them in their physiological

processes. Death of these organisms result in decomposition by bacteria which could create local reducing environments sufficient to counteract the overall normal oxidizing environment, producing a mildly semi-oxidizing to semi-reducing environment that seems necessary for the formation of glauconite. Thus a liberal supply of Fe^{+2} and Fe^{+3} ions would be available for glauconite formation, both ions substituting in the octahedral position in the structure.

One might ask the question; is an abundant supply of iron always necessary for the formation of glauconite? The writer thinks not. If there is a deficiency of iron in a sedimentary basin, all that is required is an available ion having a similar ionic radius and coordination number as the Fe^{+2} and Fe^{+3} ions. Such an ion is Al^{+3}, which can substitute in the octahedral position of the glauconite structure in the same manner as the Fe^{+2} and Fe^{+3} ions. This is what appears to have happened in this glauconite. The alteration of various silicates to glauconite not in close association with decaying organisms would be accomplished in a depositional area of semi-oxidizing conditions such as restricted basins, lagoons, or a shallow shelf.

The formation of this glauconite took place in slightly alkaline, warm, shallow marine water on a stable shelf area relatively free from clastic deposition, where mildly semi-oxidizing to semi-reducing conditions prevailed. The basin was fairly high in potassium, low in iron, and relatively enriched in aluminum; a reasonable supposition for a basin bordered by the exposed granitic Canadian Shield.

CHAPTER SEVEN

GEOCHRONOLOGY

Introduction

Age dating was undertaken with a dual purpose; firstly, to establish an age for the glauconite contained in samples four and five, suite 3461, from the Sunset Peak Area of Jasper Park; secondly, to establish an age for a microcline feldspar contained in an arkosic bed (sample 3462-16) of the basal Jonas Creek formation in the Nigel Pass Area of Jasper Park.

The presence of glauconite and feldspar from Cambrian strata in Jasper Park furnishes an opportunity to obtain an age by the potassium-argon method.

Separation of Material

The glauconite (AK-55) used for age-dating was an aliquot of the sample used in the chemical analysis.

The feldspar was concentrated using the heavy liquid centrifuge separation technique described in the discussion of the separation of glauconite.

Examination of the feldspar mounted in Canada Balsam shows the grains to be partially covered with sericite and a thin film of hematite. As a further check, both as to the identification and purity of the feldspar, an X-ray powder photograph was taken in a Phillips powder camera of 114.6 mm. diameter. Results are tabulated in Table 6. Quartz, which appears to the only impurity present, has no effect on the potassium-argon age.

Argon extractions and mass spectrometric measurements were carried out at the University of Alberta by H. Baadsgaard.

Results

Calculations of the potassium-argon ages gave the following results:

Sample	Location	%K	A^{40}/K^{40}	Age
Glauconite AK-55	Sunset Peak Area	7.43	0.02701	413 m.y.
Glauconite AK-55	Sunset Peak Area	7.43	0.0231	359 m.y.
Glauconite AK-9	Sunset Peak Area	7.26	0.02842	432 m.y.
Feldspar AK-54	Nigel Pass Area	8.04	0.02207	344 m.y.

All dates for the above samples were calculated using:

$$\lambda_e = 0.583 \times 10^{-10} \text{ yrs.}$$

$$\lambda_\beta = 4.89 \times 10^{-10} \text{ yrs.}$$

The AK-9 sample of glauconite was collected by C.W. Hunt in 1957 from the same glauconite-bearing beds and locality as the AK-55 sample.

Interpretations

A rubidium-strontium age of 465±65 million years was obtained by Cormier et al (1957) on glauconite collected from the Mount Whyte formation along the Brazeau River in the Rocky Mountains of Alberta.

In 1958, H. Baadsgaard of the University of Alberta, obtained an age of 432 million years for the glauconite collected by C.W. Hunt in 1957. It is believed that up to eighteen per cent argon-leakage may have occurred while running the specimen in the argon train or earlier in its history, and the age should be 470-500 million years.

The ages of 359 and 413 million years obtained for this glauconite are definitely low. The 413 million year age may be attributed to argon-leakage and errors in analytical procedure, as an air correction of almost fifty per cent was involved. The 359 million year age is a direct result of argon lost when heating the sample in the argon extraction train. The age of this glauconite is probably closer to 470-500 million years. Lipson's work on Cretaceous and Tertiary glauconites gives age dates that suggest argon-leakage (Lipson, 1956).

Reports on age dating of glauconite by the rubidium-strontium method by Cormier (1957) and the potassium-argon method by Hurley (1958) show the ages suggested by the spread of both methods are:

Upper Cambrian (several formations) 410-454 m.y.

Middle and Lower Cambrian (two formations) 465-584 m.y.

There is some doubt as to whether the formation containing the glauconite dated 584 million years is Lowermost Cambrian or Uppermost Precambrian. Except for this discrepancy, the age of the glauconites conform reasonably with Holmes B Time Scale.

The age obtained for the feldspar is 344 million years. The feldspar is definitely detrital. The presence of colored zircons associated with the feldspar point to a Precambrian age but an explanation other than normal argon leakage from the feldspar must account for the young age obtained. Feldspars have been known to lose up to thirty-five per cent radiogenic argon. A correction for thirty-five per cent argon loss gives a maximum age of only 460 million years. It may be that the age of 344 million years reflects some type of orogenic event, during which time the feldspar was subjected to increased

temperature and stress resulting in a subsequent loss of radiogenic argon. In this case the radiogenic argon measured in the feldspar may be in part that which accumulated since the orogeny. It is possible that radiogenic argon was lost during subsequent disturbances, such as the uplifting of the Rocky Mountains in Upper Eocene and Lower Oligocene time. There is also the possibility that the feldspar has lost little argon, and the 344 million year age obtained represents the time of formation of the feldspar.

R.E. Folinsbee and H. Baadsgaard obtained an age of 360 million years for biotite contained in the Ice River Complex, B.C., and a similar age for the Mt. Fitton granite, Yukon. These ages may represent the time of emplacement of the alkalic complexes.

Other age dates recently obtained at the University of Alberta by Folinsbee and Baadsgaard are:

(1) Lower Devonian bentonite from volcanic glass, Gaspé, Quebec, dated at 335 million years.

(2) Kinnekulle biotite from Upper Ordovician bentonite, Sweden, dated at 410 million years.

The above dates are plotted on the Holmes B Time Scale (see Figure 13).

Hurley et al (1959) obtained an age of 375-410 million years for glauconites from Lower Ordovician beds (Fulkoping, Sweden) by the rubidium-strontium and potassium-argon age-dating methods. All the above dates conform with the Holmes B Time Scale.

Hunt (1958) obtained ages of 600 and 620 million years for biotite from the contact of the Purcell intrusion at Kingsgate,

British Columbia. Hunt (1958) believes the minimum age of the Purcell sills to be approximately 600 million years. It is postulated with reservations, that the Lower Cambrian quartzites in the area studied were deposited between 600 and 470 million years ago. The evidence at hand indicates about 360± million years ago an orogeny bordering the craton took place. The ages obtained for the biotite from the Kingsgate sill and Ice River Complex and the feldspar from the Jonas Creek formation may reflect this orogeny.

It is interesting to note that White (1959) postulates the Cariboo orogeny, which folded Cariboo strata (early Cambrian) in south-central B. C., took place from Upper Ordovician through Devonian time.

Figures 14 and 15 are after White (1959). Figure 14 outlines the palaeogeographic extent of Palaeozoic Orogenies. Figure 15 shows the time and intensities of orogenies in the Canadian Western Cordillera.

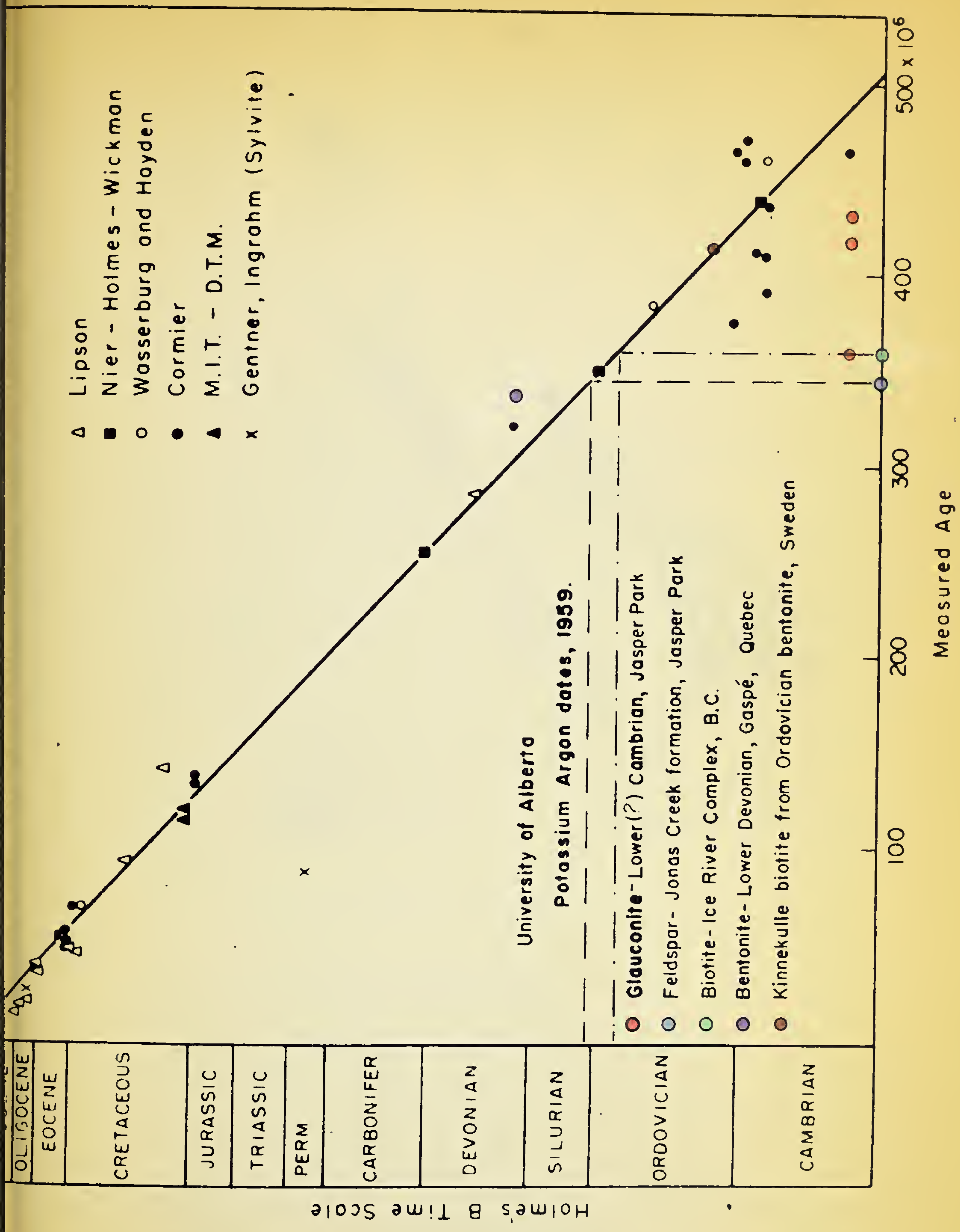
△ Lipson
■ Nier - Holmes - Wickman
○ Wasserburg and Hayden
● Cormier
▲ M.I.T. - D.T.M.
x Gentner, Ingrahm (Sylvite)
University of Alberta
Potassium Argon dates, 1959.
Glauconite-Lower(?) Cambrian, Jasper Park
Feldspar- Jonas Creek formation, Jasper Park
Biotite-Ice River Complex, B.C.
Bentonite-Lower Devonian, Gaspé, Quebec
Kinnekulle biotite from Ordovician bentonite, Sweden
100
200
300
400
500 x 10⁶
Measured Age
OLIGOCENE
EOCENE
CRETACEOUS
JURASSIC
TRIASSIC
PERM
CARBONIFER
DEVONIAN
SILURIAN
ORDOVICIAN
CAMBRIAN
Holme's B Time Scale

Figure 13.

PALAEOGEOGRAPHIC EXTENT OF PALAEOZOIC OROGENIES

IN THE CANADIAN WESTERN CORDILLERA

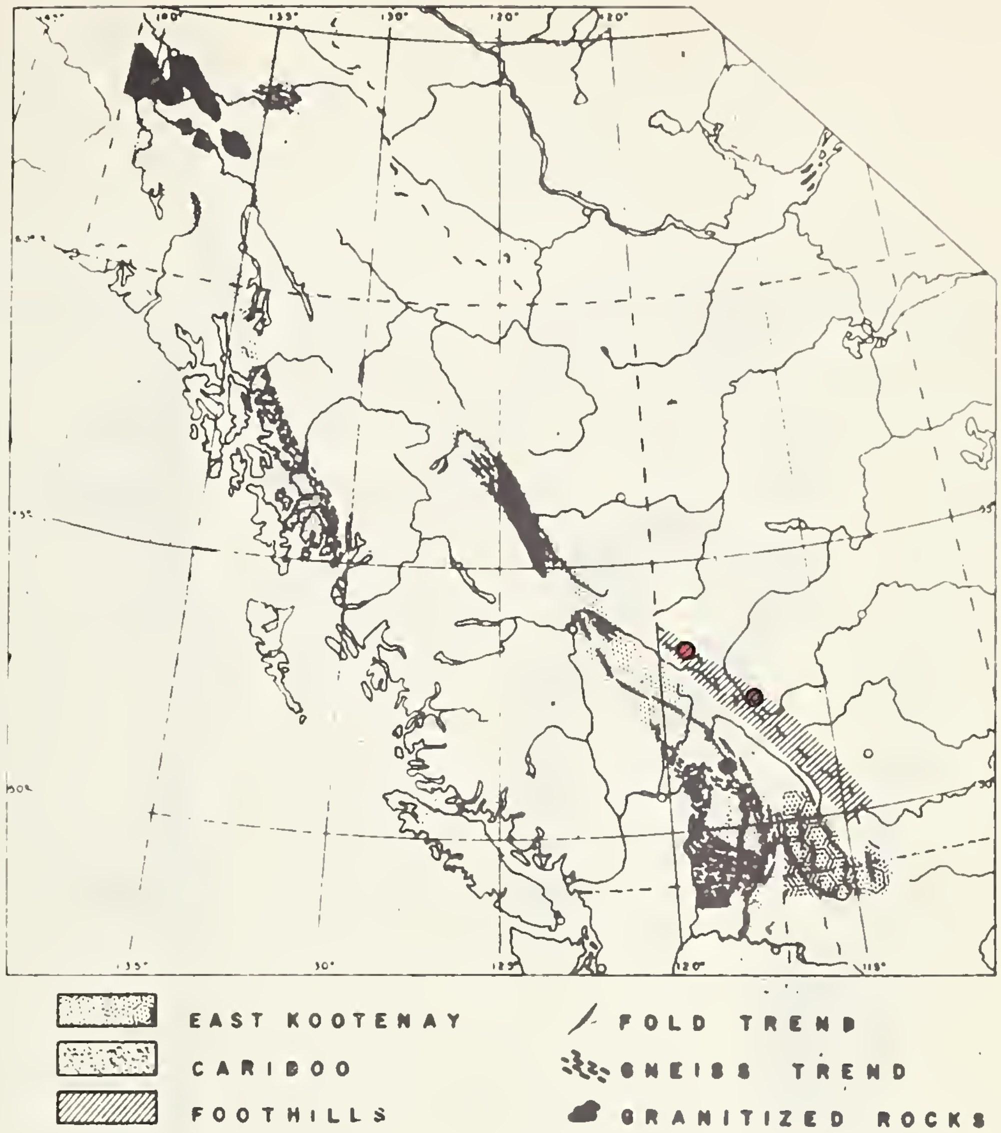
EAST KOOTENAY
CARIBOO
FOOTHILLS
FOLD TREND
GNEISS TREND
GRANITIZED ROCKS

● Sunset Peak Area

● Nigel Pass Area

(After White, 1959, Fig. 2, p. 67)

Figure 14.

TIME AND INTENSITY OF OROGENIES IN THE

CANADIAN WESTERN CORDILLERA

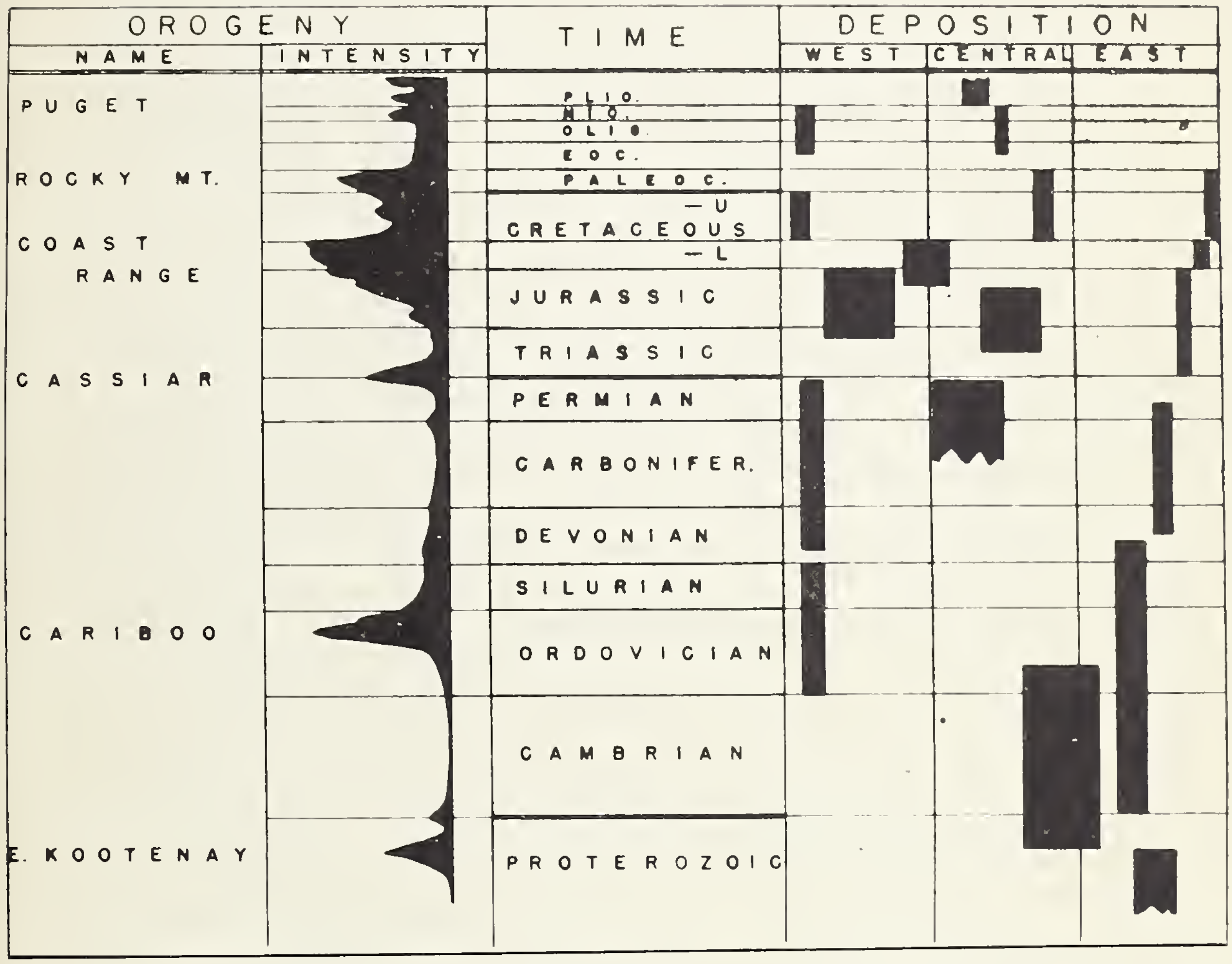

(After White, 1959, Fig. 14, p. 98)

Figure 15.

CHAPTER EIGHT

SUMMARY AND CONCLUSIONS

Cambrian formations in Jasper Park, Alberta represent marine deposition on a slowly subsiding shelf area bordering the craton. Lower Cambrian formations in both the Nigel Pass and Sunset Peak Areas consist, with the exception of upper limy beds, almost wholly of massive quartzites composed of well rounded and sorted, fine to coarse sand-size quartz grains and siliceous rock fragments cemented with authigenic silica. These quartzites may represent a beach or littoral deposit. Middle and Upper (?) Cambrian formations consist of interbedded thick dolomitic limestones and thin shales. The dolomitic limestones, for the most part, are composed of cryptocrystalline to medium-crystalline calcite, dolomite and bioclastic material, some associated with glauconite. It is thought that most of these carbonate deposits were originally deposited as limy muds which recrystallized to calcite and were later dolomitized. Thin-section studies alone are insufficient evidence on which to draw a definite conclusion as to whether or not dolomitization was penecontemporaneous with deposition or a post-lithification feature.

Glauconite contained in limy beds in the Sunset Peak Area, point to mildly oxidizing to reducing conditions and a slow rate of deposition.

With the exception of Archaeocyathidae and fossil fragments contained in limy beds in the Sunset Peak Area, both sections are unfossiliferous.

The Edith Cavell quartzites have been assigned a Lower

Cambrian age, and correlated with the Lower Cambrian Jonas Creek formation in the Nigel Pass Area.

Since the glauconite-bearing beds in the Sunset Peak Area underlie Archaeocyathidae-bearing beds, the glauconite is considered to be Lower (?) Cambrian in age.

The age of the glauconite as determined by potassium-argon dating methods is 359-432 million years. This age is believed low due to argon leakage.

Chemical analysis and X-ray studies indicate the glauconite is ordered. The glauconite has the chemical formula $K_{1.63}(Na,Rb,Ca)_{.06}(Al_{2.44}Fe^{+3}_{.76}Fe^{+2}_{.22}Mg_{.60})(Si_{7.00}Al_{1.00})O_{20}(OH)_4$. It is considered that this glauconite is a representative of aluminum-rich glauconites, which are rare.

The Lower Cambrian quartzites are believed to have been derived from the craton and Precambrian Beltian sediments.

BIBLIOGRAPHY

Allan, J. A., Warren, P. S., and Rutherford, R. L., (1932), A Preliminary Study of the Eastern Ranges of the Rocky Mountains in Jasper Park, Alberta; Royal Soc. Canada, Trans. 3rd Series, vol. 26, sec. IV, pp. 225-248.

Allan, J. A., (1938), Cambrian in the Vicinity of Sunwapta Pass, Jasper Park, Alberta; Trans. Royal Soc. Canada, vol. 32, pp. 131-121.

Beveridge, A. J., (1956), Relation of Some British Columbia Intrusives to the Alberta Sedimentary Basin; M.Sc. Thesis, University of Alberta, Edmonton.

Bragg, W. L., (1937), Atomic Structures of Minerals; Cornell University Press, Ithaca, N. Y., 292 pp.

Burst, J. F., (1958), Mineral Heterogeneity in "Glauconite" Pellets; Publication No. 146, Shell Development Company, Exploration and Production Research Division, Houston, Texas, 12 pp.

Burling, L. D., (1914), Early Cambrian Stratigraphy in the North American Cordillera, with Discussion of Albertella and Related Faunas; Geol. Survey Canada, Mus. Bull. No. 2, pp. 93-129.

______ (1915), Shallow Water Deposition in the Cambrian of the Canadian Cordillera; Ottawa Naturalist, vol. 29, pp. 87-88.

______ (1922), A Cambro-Ordovician Section in Beaverfoot Range, near Golden, British Columbia; Geol. Mag., vol. 59, pp. 452-461.

______ (1923), A Cambro-Ordovician Section near Mount Robson, British Columbia; Bull. Geol. Soc. Amer., vol. 34, pp. 721-748.

______ (1955), Annotated Index to the Cambro-Ordovician of the Jasper Park and Mount Robson Region; Guide Book, 5th Annual Field Conference, Alberta Soc. Petroleum Geol., pp. 15-51.

Burwash, R. A., (1957), Reconnaissance of Subsurface Precambrian of Alberta; Bull. Am. Assoc. Petroleum Geol., vol. 41, pp. 70-103.

Chilingar, G. V., (1955), Review of Soviet Literature on Petroleum Source-Rocks; Bull. Am. Assoc. Petroleum Geol., vol. 39, pp. 764-767.

______ (1956), Joint Occurrence of Glauconite and Chlorite in Sedimentary Rocks; Am. Assoc. Petroleum Geol., vol. 40, No. 2, pp. 394-398.

[illegible]

[illegible]

[illegible]

[illegible]

[illegible]

[illegible]

[illegible]

[illegible]

[illegible]

[illegible]

[illegible]

[illegible]

[illegible]

[illegible]

Cloud, P. E. Jr., (1955), Physical Limits of Glauconite Formation; Bull. Am. Assoc. Petroleum Geol., vol. 39, pp. 484-492.

Cormier, R. F., (1957), Variations in Isotopic abundance of Strontium, Calcium, and Argon and Related Topics; NYO - 3937. Fourth Annual Progress Report, U. S. Atomic Energy Commission, Contract AT(30-1)-1381 (M.I.T.), pp. 2-23.

Curtis, G. H., and Reynolds, J. H., (1958), Notes on the Potassium-Argon Dating of Sedimentary Rocks; Bull. Geol. Soc. Amer., vol. 69, No. 2, pp. 151-159.

Deiss, C., (1939), Cambrian Formations of Southwestern Alberta and Southeastern British Columbia; Bull. Geol. Soc. Amer., vol. 50, pp. 951-1026.

______ (1940), Lower and Middle Cambrian Stratigraphy of Southwestern Alberta and Southeastern British Columbia; Bull. Geol. Soc. Amer., vol. 51, pp. 731-794.

______ (1941), Cambrian Geography and Sedimentation in the Central Cordilleran Region; Bull. Geol. Soc. Amer., vol. 52, pp. 1085-1116.

Doeglas, D. J., (1946), Interpretation of Mechanical Analysis; J. Sedim. Petrol., vol. 16, pp. 19-40.

Dowling, D. B., (1912), Geology of Roche Miette Map Area, Jasper Park, Alberta; Geol. Survey Canada Summ. Rep't., pp. 201-219.

Evans, C. S., (1933), Brisco-Dogtooth Map Area, British Columbia; Geol. Survey Canada Summ. Rep't., 1932, pt. A 11, pp. 106-176.

Folinsbee, R. E., Lipson, J., and Reynolds, J. H., (1956), Potassium-Argon Dating; Geochemica et Cosmochimica Acta 10, pp. 60-68.

Galliher, E. W., (1935a); Glauconite Genesis; Bull. Geol. Soc. Amer., vol. 46, pp. 1351-1356.

______ (1935), Geology of Glauconite; Bull. Am. Assoc. Petroleum Geol., vol. 19, pp. 1569-1601.

______ (1939), Biotite-Glauconite Transformation and Associated Minerals; Recent Marine Sediments, Tulsa, Am. Assoc. Petroleum Geol., pp. 513-515.

Grim, R. E., (1942), Modern Concepts of Clay Materials; J. Geol., vol. 50, pp. 225-275.

Gruner, J. W., (1935), The Structural Relationship of Glauconite and Mica, Am. Mineralogist, vol. 20, pp. 699-714.

Harker, P., and Hutchinson, R. D., (1953), A New Occurrence and Redescription of Gogia prolifica Walcott; J. Paleontology, vol. 27, No. 2, pp. 285-287.

Hendricks, S. B. and Ross, C. S., (1941), Chemical Composition and Genesis of Glauconite and Celadonite; Am. Mineralogist, vol. 26, pp. 683-691.

Hough, J. L., (1940), Sediments of Buzzards Bay, Massachusetts; J. Sedim. Petrol., vol. 10, pp. 19-32.

______ (1942), Sediments of Cape Cod Bay, Massachusetts; J. Sedim. Petrol., vol. 12, pp. 10-30.

Hughes, R.D., (1953), Geology of Portions of Sunwapta and Southest Map Areas, Jasper National Park, Alberta; unpublished Ph.D. Thesis, University of Oklahoma.

Hunt, G. H., (1958), Petrology of the Purcell Sills in the St. Mary Lake Area, B. C.; M.Sc. thesis, University of Alberta, Edmonton.

Hurley, P. M., Pinson, W. H., Cormier, R. F., and Fairbairn, (1958), Age Study of Lower Paleozoic Glauconites; NYO-3939, Sixth Annual Progress Report, U. S. Atomic Energy Commission, Contract AT(30-1)-1381 (M.I.T.), pp. 53-62.

______ ______ ______ ______ (1959), Age Study of Lower Paleozoic Glauconites; Am. Geophysical Union, Program Abstracts, 40th Annual Meeting, p. 41.

Hutton, C. O., and Seelye, F. T., (1941), Composition and Properties of Some New Zealand Glauconite; Am. Mineralogist, vol. 26, pp. 595-604.

Hutton, C. O., (1950), Studies of Heavy Detrital Minerals; Bull. Geol. Soc. Amer., vol. 61, pp. 635-716.

Kawase, Y., and Okulitch, V. J., (1957), Archaeocyatha from the Lower Cambrian of the Yukon Territory; J. Paleontology, vol. 31, No. 5, pp. 913-930.

Kelly, W. P., (1945), Calculating Formulas for Fine-Grained Minerals on the Basis of Chemical Analysis; Am. Mineralogist, vol. 30, pp. 1-26.

Kindle, E. M., (1929), The Succession of Fossil Faunas in the Eastern Part of Jasper Park; Am. Jour. Science, vol. 18, pp. 177-192.

Krumbein, W. C., and Pettijohn, F. J., (1938), Manual of Sedimentary Petrography; New York, Appleton-Century, 549 pp.

Krumbein, W. C., and Tisdel, F. W., (1940), Size Distribution of Source Rocks of Sediments; Am. Jour. Science, vol. 238, pp. 296-305.

Krumbein, W. C., and Garrels, R. M., (1952), Origin and Classification of Chemical Sediments in Terms of pH and Oxidation-Reduction Potentials; J. Geology, vol. 60, No. 1, pp. 1-33.

Krynine, P. D., (1946), The Tourmaline Group in Sediments, J. Geology, vol. 54, pp. 65-87.

Kuenen, P. H. H., and Migliorini, C. I., (1950), Turbidity Currents as a Cause of Graded Bedding; J. Geology, vol. 58, pp. 91-127.

Kunze, G. W., and Jeffries, C. D., (1953), X-Ray Characteristics of Clay Minerals as Related to Potassium Fixation; Proc. Soil Sci. Soc., vol. 17, pp. 242-244.

Levinson, A. A., (1955), Studies in the Mica Group; Am. Mineralogist, vol. 40, pp. 41-50.

Light, M. A., (1952), Evidence of Authigenic and Detrital Glauconite; Science, vol. 115, pp. 73-75.

Lipson, J., (1956), Potassium-Argon Dating of Sediments; Geochemica et Cosmochimica Acta 10, pp. 149-151.

______ (1958), Potassium-Argon Dating of Sedimentary Rocks; Bull. Geol. Soc. Amer., vol. 69, No. 2, pp. 137-150.

Martens, J. H. C., (1939), Beaches; Recent Marine Sediments, Tulsa; Am. Assoc. Petroleum Geol., pp. 207-218.

Mayne, K. I., Lambert, R. St. J., and York, D., (1959), The Geologic Time-Scale; Nature, vol. 38, No. 4656, pp. 212-214.

McEvoy, J., (1900), Report on the Geology and Natural Resources of the country Traversed by the Yellowhead Pass Route; Geol. Survey Canada, Ann. Rep't. 11, Sec. D.

Moore, J. M., (1958), X-Ray Diffraction Study of Glauconite; NYO-3938. Fifth Annual Progress Report for 1957-58, U. S. Atomic Energy Commission, Contract AT(30-1)-1381 (M.I.T.), pp. 108-120.

North, F. K., and Henderson, G. G. L., (1954), Summary of the Geology of the Southern Rocky Mountains of Canada, 4th Annual Field Conference, Alberta Soc. Petroleum Geol., pp. 15-81.

Okulitch, V. J., (1955), Archaeocyatha; Treatise on Invertebrate Paleontology, Part E, Geol. Soc. Amer., University of Kansas Press, 122 pp.

______ (1956), The Lower Cambrian of Western Canada and Alaska; 20th International Geologic Congress, Mexico, vol. 2, part 2, pp. 701-734.

Plumley, W. J., (1948), Black Hills Terrace Gravels: A Study in Sediment Transport; J. Geology, vol. 55, pp. 526-577.

Rankama, K. and Sahama, Th. G., (1950), Geochemistry; University of Chicago Press, 911 pp.

Rasetti, F., (1951), Middle Cambrian Stratigraphy and Faunas of the Canadian Rocky Mountains; Smith. Misc. Coll., vol. 116, No. 5, pp. 1-270.

______ (1956), The Middle and Upper Cambrian of Western Canada; 20th International Geologic Congress, Mexico, vol. 2, part 2, pp. 735-750.

Raymond, P. E., (1930), The Paleozoic Formations of Jasper Park; Am. Jour. Science, vol. 20, pp. 289-311.

______ (1939), Prehistoric Life; Harvard University Press, 312 pp.

Rice, C. M., (1955), Dictionary of Geological Terms; Edwards Brothers, Inc., 465pp.

Ross, C. S., (1926), The Optical and Chemical Composition of Glauconite; Proc. U. S. Nat. Museum, vol. 69, Art. 2.

Schneider, H., (1927), A Study of Glauconite; J. Geology, vol. 35, pp. 289-310.

Shimer, H. W., and Schrock, R. R.,(1944), Index Fossils of North America; John Wiley and Sons, Inc., 837 pp.

Takahashi, J., and Yagi, T., (1929), Peculiar Mud-Grains and Their Relation to the Origin of Glauconite; Econ. Geology, vol. 24, pp. 838-852.

Takahashi, J., (1939), Synopsis of Glauconitization; Recent Marine Sediments, Tulsa; Am. Assoc. Petroleum Geol., pp. 503-512.

Trask, P. D., (1932), Origin and Environment of Source Sediments of Petroleum, Houston, Gulf Publ. Co., 323 pp.

Twenhofel, W. H., (1941), The Frontiers of Sedimentary Mineralogy and Petrology; J. Sedim. Petrol., vol. 11, pp. 53-63.

Udden, J. A., (1914), Mechanical Composition of Clastic Sediments; Bull. Geol. Soc. Amer., vol. 25, pp. 655-744.

Warren, P. S., (1951), Rocky Mountain Geosyncline in Canada; Royal Soc. Canada, Trans., vol. XVL, sec. 4, pp. 1-10.

Warren, P. S., and Stelck, C. R., (1958), Continental Margins of Western Canada; Alberta Soc. Petroleum Geol., vol. 6, No. 2, pp. 29-42.

Wasserburg, G. J., and Hayden, R. J., (1955), A^{40}-K^{40} Dating; Geochimica et Cosmochimica Acta 7, pp. 51-60.

Wentworth, C. K., (1922), A Scale of Grade and Class Terms for Clastic Sediments; J. Geology, vol. 30, pp. 377-392.

Williams, G. D., (1958), Sedimentary and Metamorphic Petrography of Some Proterozoic Formations of the Eastern Cordillera, Alberta and British Columbia; unpublished Report, University of Alberta, Edmonton.

Williams, H., Turner, F. J., and Gilbert, M. C., (1958), Petrography: An Introduction to the Study of Rocks in thin Sections; W. H. Freeman and Company, San Francisco, 406 pp.

White, Wm. H., (1959), Cordilleran Tectonics in British Columbia; Bull. Am. Assoc. Petroleum Geol., vol. 43, No. 1, pp. 60-100.

Walcott, C. D., (1908), Nomenclature of Some Cambrian Cordilleran Formations; Smith. Misc. Coll., vol. 53, No. 1, pp. 1-12.

______ (1913), Cambrian Formations of the Robson Peak District, British Columbia and Alberta, Canada; Smith. Misc. Coll., vol. 57, No. 12, pp. 55-59.

______ (1917), Fauna of the Mount Whyte Formation; Cambrian Geology and Paleontology; Smith. Misc. Coll., vol. 67, No. 3, pp. 61-114.

______ (1928), Pre-Devonian Paleozoic Formations of the Cordilleran Provinces of Canada; Smith. Misc. Coll., vol. 75, No. 5, pp. 175-368.

Yoder, H. S., and Eugster, H. P. (1955), Synthetic and Natural Muscovites; Geochemica et Cosmochimica Acta 8, pp. 225-280.

APPENDIX A

LOCATION OF OUTCROP SAMPLES

SUNSET PEAK AREA (Sample suite 3461)

Suite of samples collected by Dr. R.E. Folinsbee through the courtesy of Imperial Oil Company Limited from Cambrian formations above the Castle Mountain fault, headwaters of Hardscrabble Creek and west fork of Sulphur Creek, 53° 30' north latitude 119° 00' west longitude.

Bottom
(1) Worm tubules. *Scolithus*. From massive Edith Cavell quartzite.
(2) Massive Edith Cavell 100' below buff muddy series contact.
(3) Grit, tubules and phosphatic pebbles from 52' below Edith Cavell/muddy series contact.
(4) From glauconite rich zone in muddy series 20' above contact.
(5) From base of limy zone rich in glauconite 35' above contact.
(6) Limy beds with fossils. *Archaeocyathidae* and gastropods?
(7) Below massive bed-poorly consolidated sandstone.
(8) Bentonitic(?) shale.
(9) Iron nodules in ironstone.
(10) Glauconite in quartzite - 48' above #9.
(11) Oolitic limestone (Bosche formation ?) about 1250' above the Edith Cavell quartzite.
(12) Bosche(?) formation above contact.
(13) Calcareous siltstone 200' above algal zone.
Top

For detailed hand specimen descriptions see Appendix B, Megascopic Descriptions.

NIGEL PASS AREA (Sample suite 3462)

Suite of samples collected by the writer and Mr. N.G. Koch from Cambrian formations on the west and east side of Nigel Pass summit, headwaters Nigel Creek and the Brazeau River, Twp. 38, Rge. 22 W5 (52° 15' north latitude 117° 6' west longitude).

Top
(1) Upper Cambrian(?) - limestone, black, fine to coarse-crystalline, with scattered black chert(?) nodules. Thin bedded and laminated. Junction of Nigel Creek and upper right fork on west side of Nigel Pass.
(2) Upper Cambrian(?) - limestone, black, massive bedded. Strike N. 60° W, dip 28° SW. Headwaters of Brazeau River on the east side of the pass summit along the falls.

(3&4) Massive limestone weathering light grey.
(5) Sandy dolomite and quartzite weathering buff, 2' below #3.
(6) Sandstone, light-grey, 8' below #3, with _Scolithus_ borings.
(7) Algal limestone, dark-grey, fine-crystalline, thin bedded, immediately overlying the Jonas Creek formation contact.
(8) Jonas Creek formation. Pink weathering massive quartzites and grit beds, 35' below contact, with _Scolithus_ borings.
(9) Quartzite, 100' below contact, with _Scolithus_ borings.
(10) _Scolithus_ in quartzite, 150' below contact.
(11) Quartzite, 300' below contact.
(12) Quartzite, 500' below contact.
(13) Grit beds and fine conglomerate about 1000' below contact.
(14) Coarse conglomerate about 1100' below contact.
(15) Boulder conglomerate. Some boulders up to 1' in diameter, about 2000' + below contact.
(16) Fine conglomerate about 2500' below contact.
Bottom

For detailed hand specimen descriptions see Appendix B, Megascopic Descriptions.

APPENDIX B

THIN SECTION DESCRIPTIONS

3462-2 UPPER CAMBRIAN(?), NIGEL PASS AREA

Megascopic description

LIMESTONE, dark-blue-grey, weathering grey-buff, cryptocrystalline, dense.

Microscopic description

TEXTURE: Very fine to medium-crystalline calcite in irregular patches and stringers and ovoid porphyroblasts up to three mm. long, surrounded by cryptocrystalline to microcrystalline calcite.

STRUCTURE: Microconvolute bedding and slumping evident.

MINERALOGY: Calcite 70%; as a cryptocrystalline to microcrystalline groundmass.
Calcite 29%; as fine to medium-crystalline grains in porphyroblasts, patches and stringers.
Limonite, Hematite and Rutile less than 1%; surrounding porphyroblasts.
Pyrite less than 1%; as minute cubes dispersed throughout the groundmass.

REMARKS: The sediment was probably originally deposited as a lime mud which has since been recrystallized and replaced by calcite. The porphyroblasts may have been mud pellets or oolites originally. Recrystallization appears to have taken place shortly after deposition.

CLASSIFICATION: Calcilutite.

3462-3 MOUNT WHYTE FORMATION, NIGEL PASS AREA

Megascopic description

LIMESTONE, medium-grey, weathering buff, cryptocrystalline, dense.

Microscopic description

TEXTURE: Very fine to medium-crystalline calcite in irregular patches and stringers surrounded by cryptocrystalline calcite.

STRUCTURE: None apparent.

MINERALOGY: Calcite 60%; as a cryptocrystalline groundmass.
Calcite 39%; as very fine to medium-crystalline calcite infilling veins and patches.
Quartz less than 1%; as silt-size fragments enclosed in the cryptocrystalline groundmass.

CEMENT: None apparent, although some may have been present in the carbonate groundmass.

REMARKS: The sediment was probably initially deposited as a lime mud, which has since been recrystallized and replaced by calcite. The irregular patches and stringers may represent pre-existing shrinkage cracks before recrystallization.

CLASSIFICATION: Calcilutite.

3462-4 MOUNT WHYTE FORMATION, NIGEL PASS AREA

Megascopic description

LIMESTONE, light-grey-blue, weathering buff, cryptocrystalline to microcrystalline, with a few "floating" fine to medium quartz grains aligned parallel to the bedding. A few buff organic fragments appear to be dispersed randomly throughout. A well developed stylolite runs normal to the bedding. Traces of pyrite occur in minute specks.

Microscopic description

TEXTURE: Cryptocrystalline to microcrystalline calcite envelopes porphyroblasts composed of medium to coarse calcite grains with well developed mosaic texture.

STRUCTURE: Fine to coarse quartz grains, well rounded, "float" in the cryptocrystalline groundmass. Minute veins of calcite transect the bedding.

FRAMEWORK: Calcite 20%; as porphyroblasts composed of fine to medium calcite.
Quartz 9%; as rounded silt to coarse sand grains "floating" in the groundmass.
Pyrite less than 1%; as minute subhedral crystals.

MATRIX: Approximately 70% of the slide is composed of microcrystalline calcite, part of which has partially replaced the porphyroblasts and the rare shell(?) fragment.

REMARKS: The sediment was probably initially deposited as a lutite, which has since been recrystallized and replaced by calcite. The porphyroblasts may have originally been pore spaces, oolites, mud pellets, or small spherical organisms. Calcite veins may represent shrinkage cracks.

CLASSIFICATION: Calcilutite.

3462-6 MOUNT WHYTE FORMATION, NIGEL PASS AREA

Megascopic description

SANDSTONE, light-grey, weathering buff, fine-to medium-grained, fairly well sorted, silica cemented.

Microscopic description

TEXTURE: Very fine to medium grained quartz, subrounded to rounded, loosely packed, well sorted, original porosity 20-25%.

STRUCTURE: Quartz grains partially orientated with their long axis parallel to the bedding.

FRAMEWORK: Quartz 77%; highly strained in part with some suturing. Orientated dusty inclusions common, and apatite needles less common.

Siliceous rock fragments (microquartzite) less than 1%.

Accessory minerals less than 1%; as fine silt-size euhedral zircon crystals, and apatite needles in quartz.

Secondary less than 1%; limonite, pyrite, hematite.

CEMENT: Dolomite 8%; as porosity infillings.
Barite 1%; as porosity infillings.
Quartz 12%; as authigenic quartz overgrowths having optical continuity with the original quartz grains.

REMARKS: Silt-size quartz grains are more angular than fine to medium quartz grains. Dolomite, calcite and barite have partially replaced the silica cement. The highly strained extinction exhibited by some of the quartz grains indicate their source may be metamorphic. Cementation appears to have occurred shortly after deposition.

CLASSIFICATION: Quartz arenite (Williams et al, 1958, p. 293).

3462-7 MOUNT WHYTE FORMATION, NIGEL PASS AREA (Pl. 11, fig. 3).

Megascopic description

LIMESTONE, dark-bluish-grey, weathering buff, very fine crystalline,

with algal structures up to one-half inch diameter, rounded, composed of fine-crystalline dolomite. Algae weather out as knobs. Fine veins of calcite transect matrix and algal structures.

Microscopic description

FRAMEWORK: Algae composed of fine-to medium-grained dolomite. Little relic structure is preserved, and in many cases has been partially deformed and impregnated with fine grains of quartz and feldspar along the margins.

MINERALOGY: Dolomite 58%.
Quartz less than 1%.
Potassium feldspar less than 1%.
Limonite 1%.

MATRIX: Very fine to fine-crystalline dolomite, and rare very fine-grained angular quartz grains.

CEMENT: Dolomite 39%.
Quartz less than 1%.
Limonite less than 1%; as grain coatings.
Barite less than 1%.

REMARKS: The original algal structures were buried in a limy mud which had recrystallized to calcite. Cementation of barite, quartz and limonite followed. Dolomitization probably took place shortly after burial as the algal structures are little deformed.

CLASSIFICATION: Algal limestone.

3462-8 JONAS CREEK FORMATION, NIGEL PASS AREA (Pl. 8, fig. 1)

Megascopic description

SANDSTONE, light-grey-brown, weathering reddish-brown, coarse-grained quartz, silica cemented. Iron content gives rise to light and dark bands on weathered surface.

Microscopic description

TEXTURE: Medium-to coarse-grained quartz, subrounded to rounded, well sorted. Mosaic texture moderately developed due to pressure-welding along grain contacts, and authigenic overgrowths in optical continuity with original quartz grains. Milled, finely divided quartz, calcite, chlorite and sericite along grain boundaries; some intersticies filled with fine crystalline calcite. Opaque material concentrated along grain boundaries.

STRUCTURE: Slight elongation of quartz grains.

FRAMEWORK: Quartz 82%; in the main, moderately strained, slightly fractured, with slight clouded appearance due to alteration products (sericite?). Orientated dusty inclusions common, as are minute transparent rutilated(?) crystals and rare apatite euhedra.

Opaque Material less than 1%.

Accessory minerals less than 1%; rounded zircon, apatite needles.

Secondary minerals 1%; limonite, chlorite, sericite.

CEMENT: Quartz, calcite and barite 15%; approximately 10% of entire slide is composed of authigenic quartz overgrowths, and 5% of the slide is crystallized and recrystallized calcite and barite.

REMARKS: The quartz grains are well rounded as shown by the "ghost" quartz grains surrounded by dusty rims of iron oxide. Complete mosaic texture has not been attained as is indicated by thin streaks of calcite and milled quartz separating some of the grains.

CLASSIFICATION: Quartz arenite.

3462-9 JONAS CREEK FORMATION, NIGEL PASS AREA

Megascopic description

SANDSTONE, buff, weathering yellow to reddish-brown. Medium-to coarse-grained quartz, silica cemented.

Microscopic description

TEXTURE: Medium-to coarse-grained quartz in equal proportions, subrounded, moderately to fairly well sorted. Mosaic texture moderately developed with authigenic quartz overgrowths in optical continuity with original subrounded quartz grains. Sericite, chlorite and calcite (less) along grain boundaries. Rare interstice filled with finely divided calcite. Opaque, brown iron oxide partly borders grain boundaries.

STRUCTURE: Slight elongation of medium quartz grains.

FRAMEWORK: Quartz 97%; moderately strained, medium-size grains show slight fracturing; some grains partially clouded due to alteration products. Orientated dusty inclusion uncommon, as are small transparent needle-like crystals.

Opaque material less than 1%.

Accessory minerals less than 1%; ilmenite, dark-brown tabular crystals with altered leucoxene. Zircon, clear to purple hyacinth, rounded. Apatite, transparent needles.

Secondary minerals less than 1%; limonite, yellow-brown bordering quartz grains. Chlorite and sericite bordering quartz grains and infilling fractures.

CEMENT: Silica 10-12%; composed of authigenic quartz overgrowths with traces of intermixed sericite and chlorite.

REMARKS: "Ghost" quartz grains with dusty rims show the original quartz grains were subrounded. Where suturing is developed between quartz grains and quartz cement re-entrants and interpenetrations are common.

CLASSIFICATION: Quartz arenite.

3462-11 JONAS CREEK FORMATION, NIGEL PASS AREA (Pl. 10, fig. 3).

Megascopic description

SANDSTONE, mauve, weathering purple, fine-to medium-grained quartz, silica cementated. Colour due to iron oxides.

Microscopic description

TEXTURE: Fine to medium-grained quartz, well sorted, rounded and packed. Mosaic texture well developed due to authigenic quartz overgrowths in optical continuity with the quartz grains.

STRUCTURE: None apparent.

FRAMEWORK: Quartz 71%; partly strained. Orientated dusty inclusions and colourless apatite needles uncommon.

Opaque material less than 1%.

Accessory minerals less than 1%; zircon and apatite.

Secondary minerals 3%; pennine, as disseminated masses and radiating fibres.

CEMENT: Quartz 20%; as authigenic overgrowths.

Hematite 5% as subhedral crystals to disseminated masses partially surrounding the quartz grains.

REMARKS: Hematite rims partially surrounding the "ghost" quartz grains show the original grains were rounded to subrounded. Hematite crystals with partially developed crystal faces suggest the silica may have been deposited before the hematite. Little suturing is developed between quartz grains.

CLASSIFICATION: Quartz arenite.

3462-12 JONAS CREEK FORMATION, NIGEL PASS AREA

Megascopic description

SANDSTONE, light-pink, weathering pink. Fine to coarse quartz grains, massive bedded.

Microscopic description

TEXTURE: Fine to coarse grained quartz, subrounded, moderately sorted, moderately developed mosaic texture. Milled, finely divided quartz with sericite along some grain boundaries.

STRUCTURE: None apparent.

FRAMEWORK: Quartz 79%; mostly strained, with most grains coated with dusty alteration products.

Siliceous rock fragments less than 1%; a few well rounded fine to medium sand-size grains composed of microgranular quartz are dispersed throughout the slide.

Accessory minerals less than 1%; zircon, as tabular to squat crystals with rounded ends. Pitted surfaces and fine inclusions common. Ilmenite, as disseminated needles. Apatite, as squat to tabular crystals.

Secondary 1%; leucoxene from ilmenite. Hematite, as fine subhedral crystals.

CEMENT: Silica 20%; as authigenic quartz overgrowths in optical continuity with the subrounded quartz grains. Very minor amounts of microgranular siliceous (quartz?) rock fragments plus traces of sericite and chlorite compose the rest of the cement.

REMARKS: Microquartzite grains, although few, are subrounded. Mosaic texture moderately developed, as shown by sericite and siliceous rock fragments between some of the quartz grains.

CLASSIFICATION: Quartz arenite.

3462-13 JONAS CREEK FORMATION, NIGEL PASS AREA

Megascopic description

SANDSTONE, light-pink-buff, weathering pink. Coarse grained quartz with quartz phenoclasts up to four mm. in diameter. Silica cemented with kaolin alteration.

Microscopic description

TEXTURE: Fine to coarse grained quartz, subrounded to rounded, moderate to well sorted, well packed. Mosaic texture moderately

developed. Quartz grains are partially surrounded by iron oxide rims, which are surrounded by authigenic quartz having optical continuity with the quartz grains; or milled, finely divided siliceous rock fragments (quartz) with kaolinite and possibly chlorite.

STRUCTURE: None apparent.

FRAMEWORK: Quartz 85%; mostly strained. Dusty inclusions common, some grains covered with dusty alteration products.

Siliceous rock fragments (microcrystalline quartz) less than 1%.

Opaque material less than 1%.

Accessory minerals less than 1%; zircon, as minute squat crystals. Ilmenite, as fine aggregates.

Secondary minerals less than 1%; leucoxene, altering from ilmenite.

CEMENT: Quartz 15% as microgranular quartz intermixed with kaolinite dispersed in patches and thin stringers.

REMARKS: Grinding the slide too thin has plucked out some of the quartz grains. Quartz grains that are well packed are more elongated than rounded.

CLASSIFICATION: Quartz arenite.

3462-15 JONAS CREEK FORMATION, NIGEL PASS AREA (Pl. 10, fig. 4) (Pl. 11, fig. 4)

Megascopic description

BOULDER CONGLOMERATE, pebbles and boulders quartzite, white to pink, subrounded to rounded, flattened parallel to the bedding planes and "float" in matrix. Largest boulder measures seventy mm. in diameter, but in outcrop boulders measured were over one foot in diameter. Matrix pink, weathering dark-pink, composed mostly of coarse sand to granule-size quartz and feldspar grains, subrounded.

Microscopic description

FRAMEWORK: Rounded pebble twenty-five mm.+ diameter composed of medium to coarse quartz grains, well sorted well rounded, moderately packed, with authigenic quartz growths in optical continuity with the quartz grains. Mosaic texture moderately developed. The pebble makes up approximately 50% of the slide.

MINERALOGY: Quartz 35%.

Feldspar 5%; as orthoclase.

Siliceous rock fragments less than 1%.

Accessory minerals less than 1%; zircon, as minute euhedral crystals.

CEMENT: Quartz 20%; as overgrowths bordered with sericite.

MATRIX: 50% of slide.

TEXTURE: Medium to mostly very coarse grained quartz and feldspar, poorly sorted, moderately packed, subrounded to angular. Mosaic texture moderately developed. Numerous fine quartz fragments and sericite surround the quartzite pebbles.

STRUCTURE: None observed.

MINERALOGY: Quartz 29%; highly strained, with suturing. Numerous grains have tight crenulated boundaries. Inclusions are uncommon although some grains are covered with dusty alteration products.

Feldspar 8%; microcline twins, highly strained, subrounded, partially altered to sericite and kaolinite. The feldspar are divided as follows:

Microcline 5%.
Orthoclase 2%.
Plagioclase (Ab_3An_7) 1%.

Opaque material less than 1%.

Accessory minerals less than 1%; zircon, as squat, tabular well developed crystals. Ilminite, as fine aggregates.

Secondary minerals less than 1%; leucoxene, from ilmenite.

Hematite less than 1%; covering grain surfaces.

CEMENT: Quartz 5%; as authigenic quartz overgrowths.
7%; as sericite rolled with quartz.

REMARKS: The quartzite pebble makes up approximately one-half the slide. The quartz and feldspar grains in the matrix are much less rounded, sorted and packed than are the quartz and feldspar grains composing the pebble.

CLASSIFICATION: Subarkosic (Ortho) conglomerate.

3462-16 JONAS CREEK FORMATION, NIGEL PASS AREA (Pl. 6, fig. 4).

Megascopic description

ARKOSIC SANDSTONE, pink, weathering dull-pink, composed of coarse sand to granule-sized grains of quartz and pink feldspar, poorly sorted, well cementated.

Microscopic description

TEXTURE: Medium to mostly coarse-sand to granule-size quartz and

feldspar grains, subangular to subrounded, poorly sorted, moderately to well packed.

STRUCTURE: None apparent.

FRAMEWORK: Quartz 53%; fractured and highly strained. Dusty inclusions common as are small needle-like crystals. Apatite euhedral crystals rare.

Feldspar 25%; as orthoclase and microcline with poorly developed grid twinning, fresh to completely sericitized (used for feldspar K/A age dating).

Rock Fragments 2%; as microquartzites and very fine grained siliceous metamorphic(?) rocks.

Accessory minerals less than 1%; as zircon and apatite.

MATRIX: 8% as finely divided recrystallized quartz, feldspar, and irregularly distributed sericite.

CEMENT: Quartz 12%; authigenic overgrowths having optical continuity with the original quartz grains fill the original pore spaces and attack feldspar cleavage planes. Hematite less than 1%, as rims partially surrounding the original quartz grains.

REMARKS: Quartz and feldspar grains are highly strained and exhibit irregular extinction under x-nicols. Authigenic quartz overgrowths are also strained indicating that stress occurred after deposition. The milled sericite and quartz matrix is suggestive of an original clay matrix which has since been recrystallized. The original porosity of the rock was about 12%.

CLASSIFICATION: Metamorphosed arkosic arenite, "Arkose".

3461-1 EDITH CAVELL QUARTZITE, SUNSET PEAK AREA

Microscopic description

TEXTURE: Fine to mostly coarse-grained quartz, well rounded, well packed, well sorted. Mosaic texture well developed. Some grains are partially surrounded by rims of iron oxide, which in turn is surrounded by authigenic quartz having optical continuity with the rounded quartz grains. Some of the quartz grains are fractured and exhibit highly strained extinction under crossed nicols.

STRUCTURE: None apparent.

FRAMEWORK: Quartz 69%; in the main slightly to highly strained. Dusty inclusions common, small apatite needle inclusions uncommon.

Siliceous rock fragments (microquartzite) 3%.

Accessories: Zircon less than 1%; as subhedral to well rounded hyacinths.

Apatite less than 1%; as needle inclusions in quartz.

Tourmaline less than 1%; green, fine-grained, well rounded, slightly pleochroic. Strained uniaxial negative figure. One grain exhibits a feathered overgrowth.

Glauconite less than 1%; occurring as very fine well rounded grains, pale green, very slightly to nonpleochroic.

Hematite less than 1%; partially bordering quartz grains.

Leucoxene less than 1%; as clusters of needles.

Illite 2%; in matrix.

MATRIX: 10%; as fine rolled or milled illite, sericite(?) with siliceous argillaceous paste. Glauconite associated only with matrix.

CEMENT: Quartz 15%; as authigenic highly strained overgrowths.

REMARKS: The original porosity of the rock was about 15%, and has been filled with authigenic silica. The strained quartz overgrowths suggest that some stress has taken place after burial. The authigenic overgrowth on one of the rounded tourmaline grains indicates that the tourmaline had been transported a considerable distance before being deposited, after which the overgrowth began to form. The well rounded glauconite grains and their association with the matrix shows that the glauconite may be detrital. The matrix seems to be associated with a concentric arrangement of quartz grains which may represent a relict structure of a Scolithus worm tube. If so, the glauconite may be authigenic, having formed after the death of the organism.

CLASSIFICATION: Quartz arenite.

3461-2 EDITH CAVELL FORMATION, SUNSET PEAK AREA

Megascopic description

SANDSTONE, dull-white, weathering buff-orange, fine-to medium-quartz grains, well rounded, silica cemented.

Microscopic description

TEXTURE: Mostly fine to some medium grained quartz, well rounded, fairly well packed. Mosaic texture only moderately developed. Authigenic quartz is in optical continuity with the original rounded quartz grains. Suturing of grain boundaries common.

FRAMEWORK: Quartz 79%; moderately to highly strained. Dusty inclusions common, as are minute needle-like crystals and apatite crystals.

Siliceous rock fragments (microquartzite) less than 1%.

Apatite less than 1%.

Zircon less than 1%; as small tabular, rounded to subhedral hyacinths.

Leucoxene less than 1%; as needle aggregates.

CEMENT: Quartz 20%; as strained authigenic overgrowths on quartz grains.

REMARKS: Well rounded quartz grains indicate the grains have a long abrasive history. The strained cement shows stress has occurred after burial.

CLASSIFICATION: Quartz arenite.

3461-3 EDITH CAVELL FORMATION, SUNSET PEAK AREA (Pl. 9, fig. 4) (Pl. 11, fig. 1)

Megascopic description

SANDSTONE, light-grey, weathering mottled-buff, fine-to coarse-grained quartz, rounded, silica cemented. Porphyroblasts of black phosphate, weathering black to blue-black, up to one-half inch in diameter, rounded. The phosphate porphyroblasts are associated with, and appear to partially replace Scolithus borings in some cases.

Microscopic description

TEXTURE: Fine to coarse-grained quartz, well rounded moderately to well packed in patches, surrounded by authigenic quartz overgrowths in optical continuity with the original quartz grains, and milled, finely divided sericite and illite with siliceous material in patches. Mosaic texture moderately developed. A well rounded porphyroblast (nodule) composed of phosphate measures eleven mm. in length.

FRAMEWORK: Quartz 69%; moderately to highly strained. Dusty opaque inclusions common; less common are apatite needles and randomly orientated opaque needle-like crystals.

Collophane 10%; as a rounded porphyroblast or nodule, impregnated with angular to rounded silt to fine sand-size quartz grains and fine chlorite and hematite.

Tourmaline, less than 1%; greenish-blue, moderately pleochroic, coarse-grained, well rounded but broken and fractured. An excellent uniaxial negative optic axis figure was obtained.

Zircon less than 1%; as subhedral to rounded grains. One crystal with knee-twinning was observed.

Leucoxene less than 1%; as small clusters of needle shaped crystals.

Hematite less than 1%; partially surrounding quartz grains and patches in the collophane. One crystal with a hexagonal shape was observed.

Pyrite less than 1%; replacing hematite.

CEMENT: About 20% of the slide is composed of strained authigenic quartz. Some interstices are filled with finely divided quartz, sericite and limonite. Interstices near the collophane porphyroblast are also impregnated with collophane.

REMARKS: Strained authigenic quartz overgrowths indicate stress has been applied after burial. The tourmaline by nature of its colour would be according to Krynine (1946) of the granitic or pegmatite variety. The well rounded quartz grains are indicative of a long transportation history.

CLASSIFICATION: Quartz arenite with phosphate porphyroblast (nodule).

3461-4 LOWER(?) CAMBRIAN MUDDY SERIES, SUNSET PEAK AREA

Used for glauconite K/A age dating and chemical analysis.

Megascopic description

GLAUCONITIC DOLOMITIC LIMESTONE, buff with green fine-grained glauconite, weathering orange flecked with green. Hand specimen too small to determine the nature of any bedding.

Microscopic description

TEXTURE: Calcite and dolomite, anhedral, fine-to medium-grained enveloping fine-to medium-grained glauconite, silt to fine sand-size quartz grains and silt-size anhedral zircons. Mosaic texture well developed.

STRUCTURE: Glauconite grains show some parallel alignment of their long axis throughout the slide.

MINERALOGY: Calcite and dolomite 94%; as fine-to medium-grained anhedral crystals, which have attacked and replaced some of the glauconite and quartz grains.

Glauconite 5%; fine-to medium-grained in the main, with some irregular patches up to 1 mm. in length. Colour light-to medium-green, nonpleochroic, subrounded, occurring as irregular patches and stringers as a result of calcite replacement.

Quartz 1%; as silt to fine sand-size grains, angular to well rounded with some authigenic quartz overgrowths in optical continuity with the rounded grains.

Accessory minerals: Zircon less than 1%; as anhedral, rounded very fine silt-size grains.
Hematite less than 1%; as irregular minute patches.

REMARKS: The original sediment may have been deposited as a limy mud. "Floating" quartz grains, some with authigenic overgrowths attached show partial replacement by calcite and dolomite. The somewhat parallel alignment of the glauconite grains indicate the sediment was originally bedded. The calcite and dolomite have completely replaced the original lime mud, as well as destroyed and replaced in part quartz and glauconite grains.

CLASSIFICATION: Glauconitic arenaceous calcarenite.

3461-5 LOWER(?) CAMBRIAN MUDDY SERIES, SUNSET PEAK AREA (Pl. 7, fig. 3) (Pl. 8, fig. 2)
Used for glauconite K/A age dating and chemical analysis.

Megascopic description

GLAUCONITIC DOLOMITIC LIMESTONE, buff with fine-green glauconite, weathering mottled and orange, fine-to medium-crystalline calcite with irregular contorted bedding. Oval shaped pellets up to 7 mm. in length are composed of calcite and glauconite, with the latter rimming some of the pellets.

Microscopic description

TEXTURE: Fine to mostly medium to coarse anhedral calcite and dolomite enveloping fine-to medium-grained glauconite, silt to very fine sand-size quartz grains and collophane fossil fragments.

STRUCTURE: Glauconite grains show elongation and parallel alignment to the bedding.

MINERALOGY: Calcite and dolomite 76%; as fine-to coarse-grained anhedral crystals which have partially destroyed and replaced glauconite and quartz grains.
Collophane 5%; as rounded, oval, wedge-shaped organic remains up to 1 mm., with quartz and glauconite inclusions in some cases. The organic remains are probably trilobite fragments and faecal pellets.
Glauconite 6%; as light-green, slightly pleochroic medium-size grains, partially rounded but in most cases occurring as irregular patches. Glauconite included in the collophane organic structures is generally well rounded.
Quartz 3%; as mostly angular to some subrounded fine-to medium-size grains, which show considerable replacement by calcite.

Muscovite less than 1%; as thin irregular slightly bent fibres.

Pyrite less than 1%; as tiny grains.

REMARKS: The glauconite and quartz grains inside some of the organic structures must have been deposited in the structures shortly after their deposition on the sea floor. The glauconite grains are considered to have formed in situ, having been rolled, rounded and deposited in the organic structures by gentle wave action. Calcite and dolomite have completely replaced what was originally a limy mud, and attacked and partially replaced glauconite and quartz grains not incorporated in organic remains.

CLASSIFICATION: Glauconitic fossiliferous calcarenite.

3461-6 LOWER CAMBRIAN, SUNSET PEAK AREA (Pl. 4, fig. 1-10)
(Pl. 7, fig. 1,2)
(Pl. 9, fig. 1,3)

Megascopic description

LIMESTONE, light-brown, weathering orange, very fine to fine crystalline, with numerous fragments of poorly preserved Archaeocyathidae, trilobite spines, and Helenia(?) or similar pteropod.

Microscopic description

TEXTURE: Fine to very coarse anhedral calcite grains possessing a well developed mosaic texture, with quartz, fine-to medium-grained, well rounded. Numerous oolites, fossil fragments of trilobite spines(?) and Archaeocyathidae scattered throughout the slide.

STRUCTURE: None apparent.

MINERALOGY: Bioclastic material 40%; not exceeding three mm. in diameter.

Quartz 20%; "floating" in calcite.

Calcite 29%; as very coarse anhedral grains.

Calcite 10%; as fine anhedral grains.

Glauconite less than 1%; very fine grained, sub-rounded, scattered throughout the slide.

Collophane 1%; in some fossil fragments.

REMARKS: The coarse anhedral grains of calcite may represent cement, whereas the fine calcite grains may represent matrix. Quartz grains are moderately strained.

CLASSIFICATION: Bioclastic arenaceous calcarenite.

3461-7 SUNSET PEAK AREA

Megascopic description

SANDSTONE, light-grey, weathering mottled-buff-yellow and orange, fine-to medium-grained quartz, rounded. Scolithus borings up to one-half inch in diameter weather out as knobs.

Microscopic description

TEXTURE: Very fine to coarse-grained quartz, rounded, moderately sorted, poorly packed, cemented with rolled, milled, finely divided quartz and sericite. A cross section of a Scolithus tube in the center of the slide is composed of mostly medium to coarse quartz grains, rounded, well packed, silica cemented with authigenic quartz overgrowths having optical continuity with the original rounded quartz grains. The Scolithus tube measures about one-half inch in diameter.

STRUCTURE: None apparent.

FRAMEWORK: Quartz 87%; highly strained, partly fractured; some grains partly clouded due to alteration products. Orientated dusty inclusions uncommon.

Siliceous rock fragment 1%; as rounded quartzite grains, medium to coarse grained.

Accessory minerals less than 1%; leucoxene altered from ilmenite. Zircon, clear to hyacinth, very fine grained, rounded to tabular outline.

MATRIX: 12%; as rolled, milled, finely divided quartz, sericite and illite(?) in small patches and stringers.

3461-9 LOWER(?) OR MIDDLE(?) CAMBRIAN, SUNSET PEAK AREA (Pl. 6, fig. 1) (Pl. 10, fig. 1)

Megascopic description

IRONSTONE, massive to thin-bedded, reddish-brown, weathering reddish-brown to deep-red, with iron nodules up to three-eighths inches in diameter. Quartz in matrix medium-grained, well rounded.

Microscopic description

FRAMEWORK: Pisoliths, well rounded, up to four mm. diameter. Most pisoliths possess a detrital quartz nucleus, coarse-grained, well rounded, which is surrounded by rims of cryptocrystalline to very fine crystalline calcite, hematite and in some cases small patches of pyrite.

MINERALOGY: Quartz 25%.
Calcite 50%; as cryptocrystalline to fine-crystalline grains.
Hematite 25%.

MATRIX: Quartz 55%; fine-to coarse-grained, well rounded, with rare apatite needle inclusions; dusty inclusions fairly common. On the whole, the grains are well strained.
Hyperthene less than 1%; green, slightly pleochroic, fine-grained, well rounded.
Calcite 10%; as cryptocrystalline to fine-crystalline anhedral grains.
Hematite 10%; as dark-brown amorphous material disseminated throughout the matrix.
Pyrite less than 1%; as disseminated masses.

REMARKS: The matrix composes 75% of the slide, the calcite has in many instances strongly attacked quartz grains along fractures.

CLASSIFICATION: Pisolitic hematite sandstone.

3461-10 MIDDLE(?) CAMBRIAN, SUNSET PEAK AREA (Pl. 6, fig. 2).

Megascopic description

LIMESTONE, dark-tan, weathering buff-yellow, fine-to medium-crystalline, with glauconite, very dark-green, fine-grained, evenly distributed throughout the rock.

Microscopic description

TEXTURE: Irregularly shaped elongate bodies up to one-half mm. in diameter filled with fine-to medium-crystalline calcite.

STRUCTURE: None apparent.

FRAMEWORK: Calcite 35%; as very fine to fine grains composing the irregularly shaped bodies.
Quartz 8%; as silt to fine sand-size grains, angular to subrounded.
Glauconite 1%; as light-green fine to coarse grains, some well rounded, some irregular in outline to rod-shape.
Hematite less than 1%; in small patches and stringers scattered throughout the slide, but noticeably associated with glauconite.

MATRIX: Calcite 25%; as very fine anhedral grains.

CEMENT: 30%; as medium to coarse anhedral calcite forming a

mosaic pattern around some of the glauconite and organic(?) bodies. Some of the grains contain rounded "ghost" outlines.

REMARKS: The organic(?) bodies have been completely recrystallized to calcite. The calcite cement has attacked some of the glauconite grains. Hematite seems to be preferentially associated with glauconite.

CLASSIFICATION: Calcarenite.

3461-11A BOSCHE(?) FORMATION OR EQUIVALENT, SUNSET PEAK AREA (Pl. 8, fig.3) (Pl. 11, fig.2)

Megascopic description

OOLITIC LIMESTONE, dark-grey-brown, weathering buff-yellow, cryptocrystalline groundmass, with oolites up to one mm. diameter. Oolites weather out as dark pin-heads.

Microscopic description

FRAMEWORK: Ooliths having an average diameter of one mm. make up 65% of the slide, and are composed mostly of very fine-crystalline calcite in the nucleus grading to microcrystalline calcite near the outer rims. Rims of calcite in concentric bands surround the nucleus.

MINERALOGY: Calcite 64%.
Limonite less than 1%; as brown rims surrounding calcite crystals.

MATRIX: Calcite 33%; as silt to very fine sand-size grains.
Quartz less than 1%; as subangular silt-size grains.
Limonite less than 1%; surrounding calcite grains and lining minute stylolytic partings.
Glauconite less than 1%; in oolite core.

CEMENT: Calcite 2%; as fine sand-size anhedral calcite grains.

REMARKS: The ooliths are well rounded, but a few are flattened. Rims of fibrous calcite indicate that the original ooliths may have been composed of aragonite which has since been recrystallized. The matrix may have originally been a lime mud, and the calcite cement may represent infilling of pore spaces.

CLASSIFICATION: Oolitic calcarenite.

3461-11B BOSCHE(?) FORMATION OR EQUIVALENT, SUNSET PEAK AREA

Megascopic description

LIMESTONE, dark-grey, weathering buff-yellow, cryptocrystalline,

dense.

Microscopic description

TEXTURE: Very fine to medium crystalline calcite occurring in irregular patches and stringers, in small ovoid porphyroblasts up to two mm. long, and as the nucleus in one oolith; all enclosed in a microcrystalline to very fine crystalline calcite groundmass.

STRUCTURE: None apparent.

MINERALOGY: Calcite 39%; in irregular patches and stringers.
60%; as a microcrystalline to very fine crystalline groundmass.
Quartz less than 1%; as coarse silt-size grains.
Limonite less than 1%; as opaque material bordering calcite.

REMARKS: The sediment may have been originally deposited as a limy mud which has since recrystallized to calcite. The irregular patches and stringers may represent original porosity or shrinkage cracks. All the porphyroblasts except one do not appear to be oolitic in origin.

CLASSIFICATION: Calcilutite.

3461-12A BOSCHE(?) FORMATION OR EQUIVALENT, SUNSET PEAK AREA (Pl. 7, fig.4)

Megascopic description

PISOLITIC (ALGAL) LIMESTONE, grey-buff, weathering yellow-buff, cryptocrystalline, very silty with grey algal pisolites up to ten mm. in diameter, weathering out as knobs.

Microscopic description

FRAMEWORK: Algae up to ten mm. in diameter, rounded. Most of the algae have grown around a "U" shaped core up to five mm. in length, composed of what may have originally been a small shell fragment which has since been recrystallized to calcite. Surrounding the core are concentric rings composed of fine silt-size quartz grains and cryptocrystalline calcite. In some of the algae the core is absent.

MINERALOGY: Quartz 17%; as very fine silt-size angular quartz grains.
Calcite 32%; as cryptocrystalline grains comprising the core (when present) and the algal structure.
The algae make up approximately 50% of the slide.

MATRIX: Quartz 32%; as coarse silt-size grains, mostly subangular, poorly packed, partly strained.

Calcite 17%; as a fine cryptocrystalline groundmass.

Echinoderm fragments less than 1%; as small circular shaped disks up to 0.025 mm. in diameter with radiating septa(?).

Glauconite less than 1%; as silt-size subrounded to rounded grains.

Limonite less than 1%; bordering quartz grains and algae.

Hematite less than 1%; as irregular patches distributed throughout the matrix, and replacing glauconite where the glauconite has fractured.

Illite(?) less than 1%; as small minute shreds and patches.

The matrix comprises 50% of the slide.

REMARKS: The algae, in most cases, has grown around a "U" shaped shell fragment. Silt-size quartz grains, glauconite, echinoderm fragments and other shell debris have filled the shell shortly after deposition. The echinoderm fragments are better preserved in the core of the algae than in the matrix. The round shape of the glauconite grains may be due to rolling on the sea floor by aqueous currents. The calcite in the matrix may represent what was originally a limy mud. The algae is similar to the form genus Penostroma, while the echinoderm fragments may be a form associated with Gogia (see text, page 17).

CLASSIFICATION: Pisolitic (algal) calcilutaceous siltstone.

3461-12B BOSCHE(?) FORMATION OR EQUIVALENT, SUNSET PEAK AREA

Megascopic description

LIMESTONE, dark-grey, weathering buff-yellow, microcrystalline, dense.

Microscopic description

TEXTURE: Microcrystalline to minor very fine crystalline calcite with coarse silt-sized quartz grains, subangular to subrounded.

STRUCTURE: Minute stylolitic partings lined with limonite transects the slide.

MINERALOGY: Calcite 97%; as microcrystalline to very fine crystalline calcite.

Quartz less than 1%; as coarse silt-sized grains "floating" in the carbonate.

Limonite less than 1%; in irregular patches and lining stylolitic partings.

CEMENT: Quartz and calcite 2%; surrounding some of the fine crystalline calcite.

Organic material less than 1%; trilobite(?) fragments.

REMARKS: The sediment may have been initially deposited as a silty lutite, which has since been replaced and recrystallized by calcite. Some of the fine-grained calcite may have originally been silt-size quartz grains. Irregular edges on some of the quartz grains "floating" in the carbonate show the effect of calcite replacement.

CLASSIFICATION: Calcilutite.

3461-13 BOSCHE(?) FORMATION OR EQUIVALENT, SUNSET PEAK AREA (Pl. 10, fig.2)

Megascopic description

SILTSTONE, dark-grey, weathering buff-yellow, calcareous, micaceous, thin bedded and laminated.

Microscopic description

TEXTURE: Very fine sand to silt-sized quartz grains, subangular to subrounded, circular to elongate, well sorted, poorly packed.

STRUCTURE: Quartz grains and mica flakes are preferentially orientated with their long axis parallel to the bedding planes.

FRAMEWORK: Quartz 45%; partly strained, edges in part serrated by calcite cement.

Phlogopite mica 10%; pale-brown to colourless, pleochroic dark-brown to green, occurring as fibres up to one-half mm. in length.

Glauconite less than 1%; light-green, very slightly pleochroic, grading from coarse-silt to very fine sand-size grains, subrounded.

Feldspar less than 1%; Ab_6An_4 (Andesine).

Accessories less than 1%; zircon, as minute euhedral crystals.

Secondary less than 1%; hematite, as small subhedral crystals and irregular patches.

CEMENT: Calcite 45%; as a cryptocrystalline to microcrystalline groundmass.

REMARKS: The glauconite grains are the same size as the quartz grains and in the main do not appear to be rolled or flattened. The glauconite appears to be authigenic. What is now calcite cement was probably originally a lime mud, which has since recrystallized into calcite.

CLASSIFICATION: Micaceous calcilutaceous siltstone.

APPENDIX C

ANALYTICAL METHODS

Duplicate samples of glauconite were analyzed. The writer ran one sample while Dr. H. Baadsgaard ran the other as a check.

Main Portion

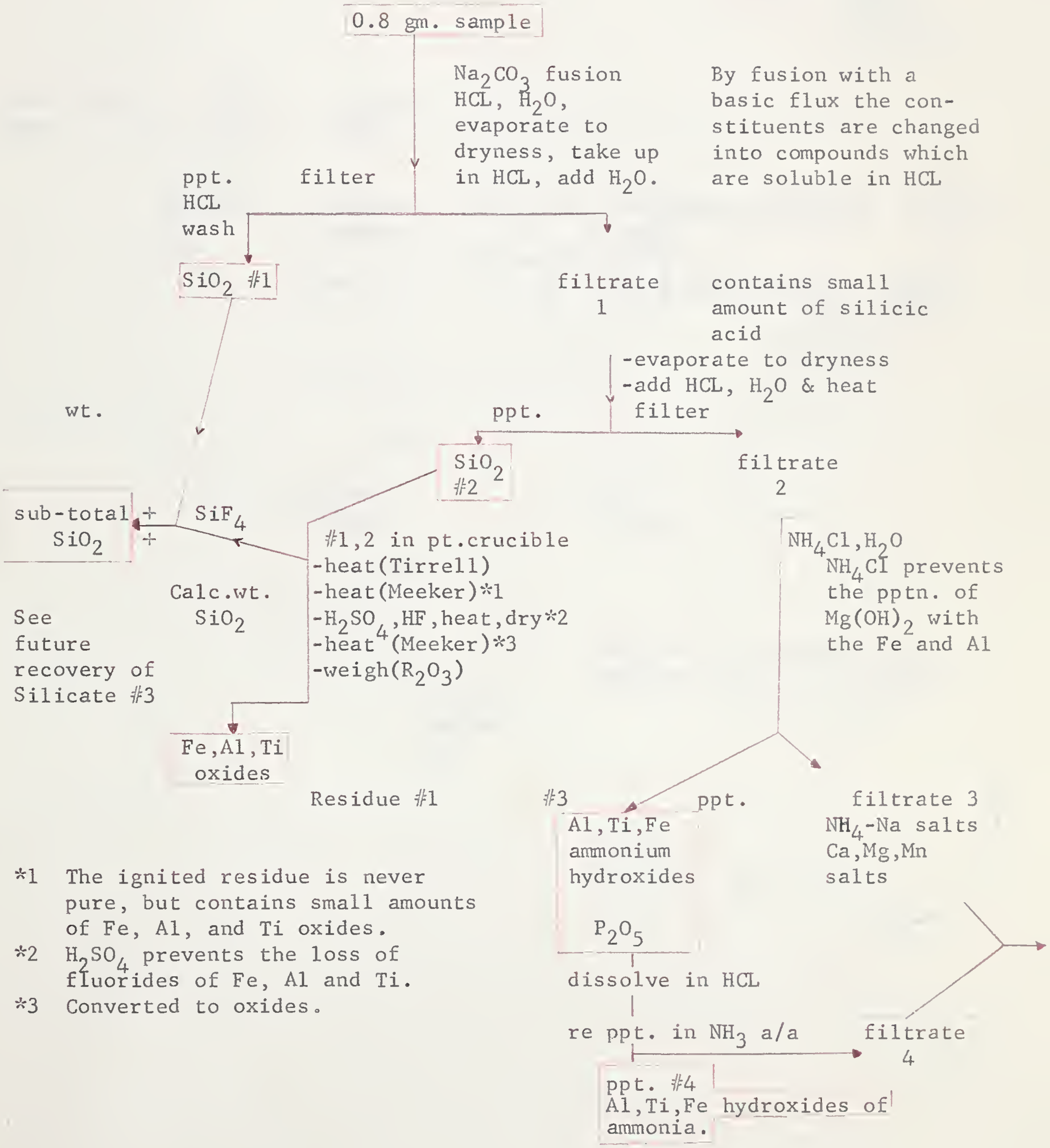
0.8 gm. sample
Na_2CO_3 fusion
HCL, H_2O,
evaporate to dryness, take up in HCL, add H_2O.
By fusion with a basic flux the constituents are changed into compounds which are soluble in HCL
ppt.
HCL wash
filter
SiO_2 #1
filtrate 1
contains small amount of silicic acid
-evaporate to dryness
-add HCL, H_2O & heat
filter
wt.
ppt.
SiO_2 #2
filtrate 2
sub-total SiO_2
+ SiF_4
+
#1,2 in pt.crucible
-heat(Tirrell)
-heat(Meeker)*1
-H_2SO_4,HF,heat,dry*2
-heat (Meeker)*3
-weigh(R_2O_3)
Calc.wt. SiO_2
See future recovery of Silicate #3
NH_4Cl, H_2O
NH_4Cl prevents the pptn. of $Mg(OH)_2$ with the Fe and Al
Fe,Al,Ti oxides
Residue #1
#3
ppt.
Al,Ti,Fe ammonium hydroxides
P_2O_5
filtrate 3
NH_4-Na salts
Ca,Mg,Mn salts
dissolve in HCL
re ppt. in NH_3 a/a
filtrate 4
ppt. #4
Al,Ti,Fe hydroxides of ammonia.

*1 The ignited residue is never pure, but contains small amounts of Fe, Al, and Ti oxides.

*2 H_2SO_4 prevents the loss of fluorides of Fe, Al and Ti.

*3 Converted to oxides.

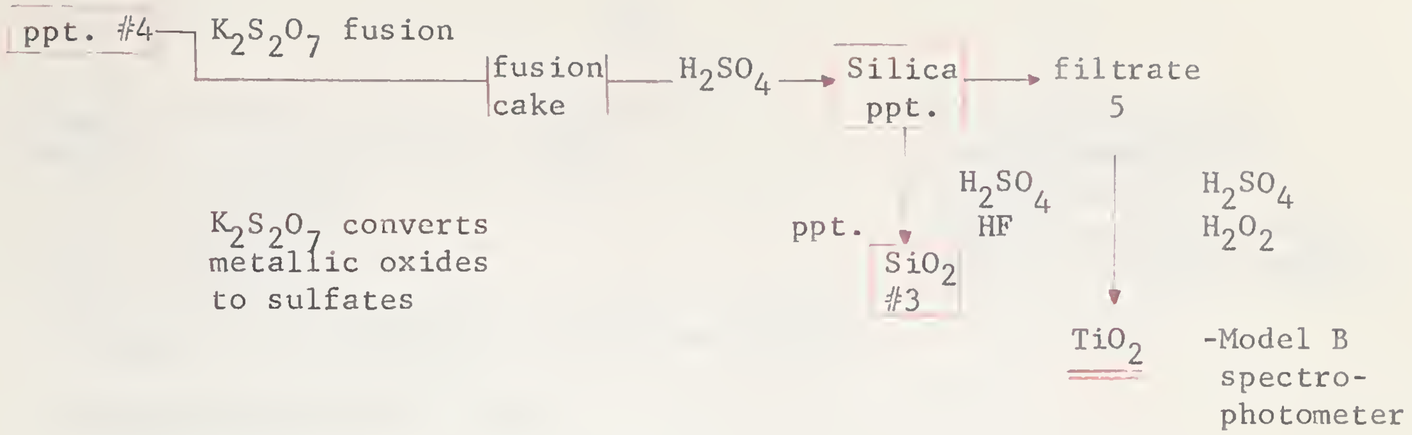
ppt. #4
$K_2S_2O_7$ fusion
fusion cake
H_2SO_4
Silica ppt.
filtrate 5
$K_2S_2O_7$ converts metallic oxides to sulfates
ppt.
H_2SO_4
HF
SiO_2 #3
H_2SO_4
H_2O_2
TiO_2
-Model B spectro-photometer

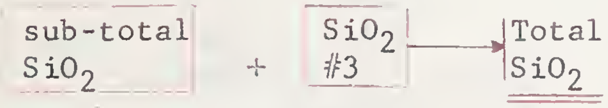
sub-total SiO_2
+
SiO_2 #3
Total SiO_2

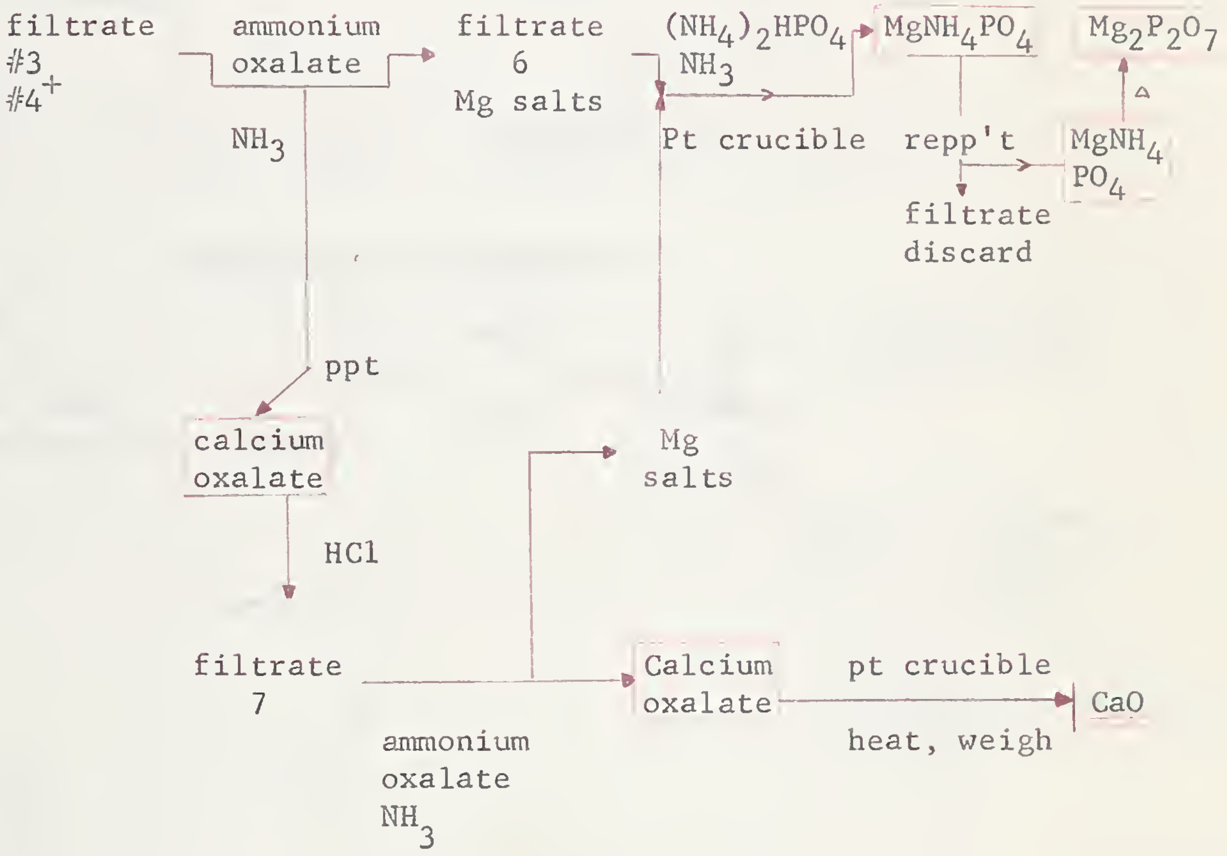
filtrate #3 #4+
ammonium oxalate
filtrate 6
Mg salts
$(NH_4)_2HPO_4$
NH_3
$MgNH_4PO_4$
$Mg_2P_2O_7$
Δ
Pt crucible
repp't
$MgNH_4PO_4$
filtrate discard
NH_3
ppt
calcium oxalate
HCl
Mg salts
filtrate 7
ammonium oxalate
NH_3
Calcium oxalate
pt crucible
heat, weigh
CaO

Total H_2O

$$\boxed{\text{1 gm sample}} \xrightarrow[\text{O_2 flame, Pb flux, weigh}]{\text{Penfield tube}} \boxed{\text{total } H_2O}$$

Also, heated 1 gm sample 100-1000° C total ignition Loss of weight = total water + CO_2-(Fe $\rightarrow Fe_2O_3$)

Weight of Penfield tube + water-wt of dry Penfield tube = wt. of H_2O

H_2O^-

$$\boxed{\text{1 gm sample}} \xrightarrow[\text{cool, weigh}]{\text{heat } 110^\circ\text{C}} \boxed{H_2O^-}$$

-(hydroscopic or adsorbed water)

H_2O^+

$$\boxed{H_2O \text{ total}} - \boxed{H_2O^-} = \boxed{H_2O^+}$$

-(combined water in mineral)

Manganese and Phosphorous

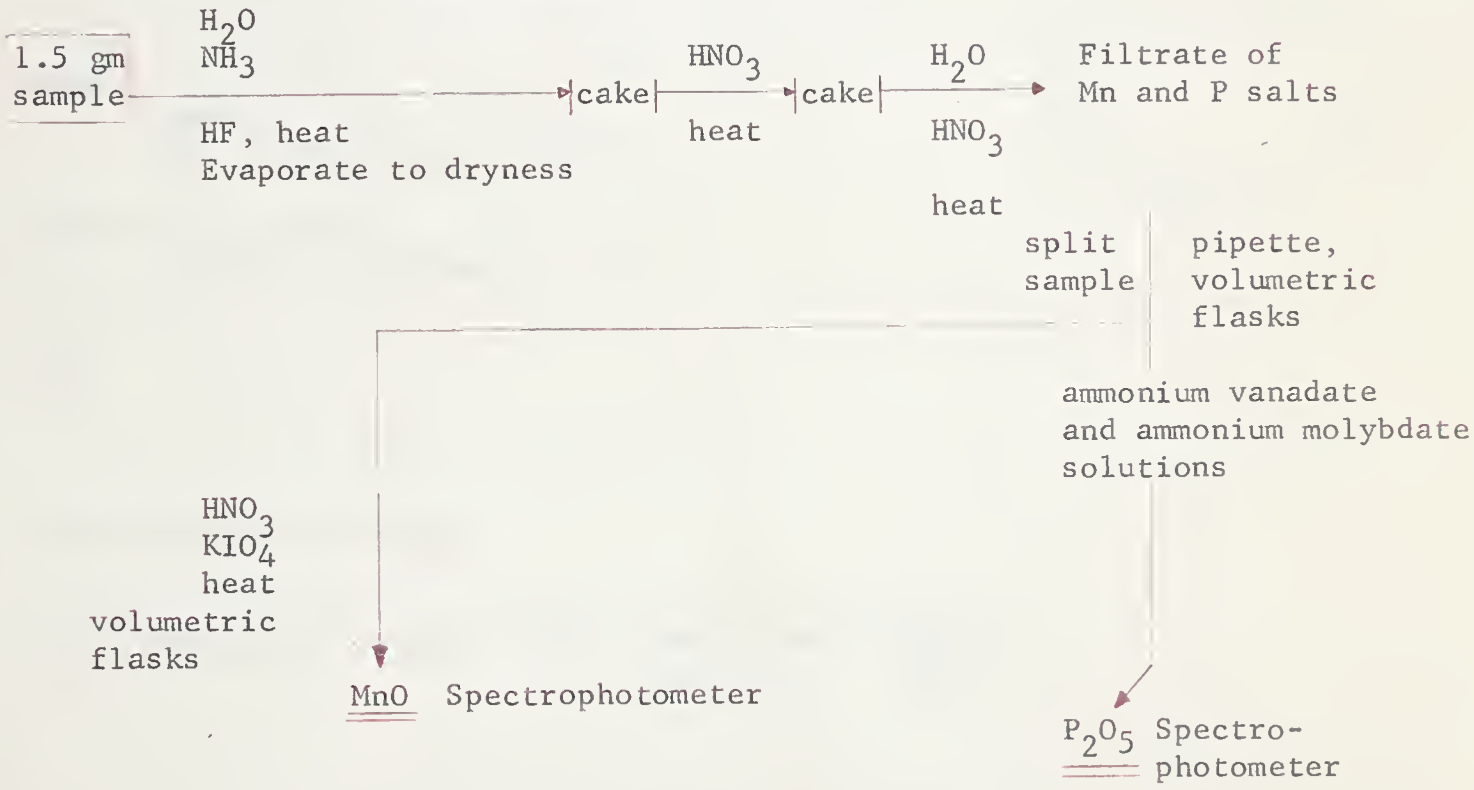

1.5 gm sample

H_2O, NH_3, HF, heat, Evaporate to dryness → cake

HNO_3, heat → cake

H_2O, HNO_3, heat → Filtrate of Mn and P salts

split sample

pipette, volumetric flasks

HNO_3, KIO_4, heat, volumetric flasks → MnO Spectrophotometer

ammonium vanadate and ammonium molybdate solutions → P_2O_5 Spectrophotometer

Iron

Total Iron

1 gm
sample

(Iron reduced to ferrous form with stannous chloride)

HCl
HF
$SnCl_2$
potentiometric titration
with $Ce(SO_4)_2$

Total
iron

Ferrous Iron

0.5 gm
sample

H_2SO_4
HF in absence of air

Boric acid solution
titrate with $KMnO_4$

FeO

-

Total iron - FeO = Fe_2O_3

Al_2O_3 = Total R_2O_3-(P_2O_5 + TiO_2 + Total Iron + SiO_2)
as Fe_2O_3 #3

Alkali Determination

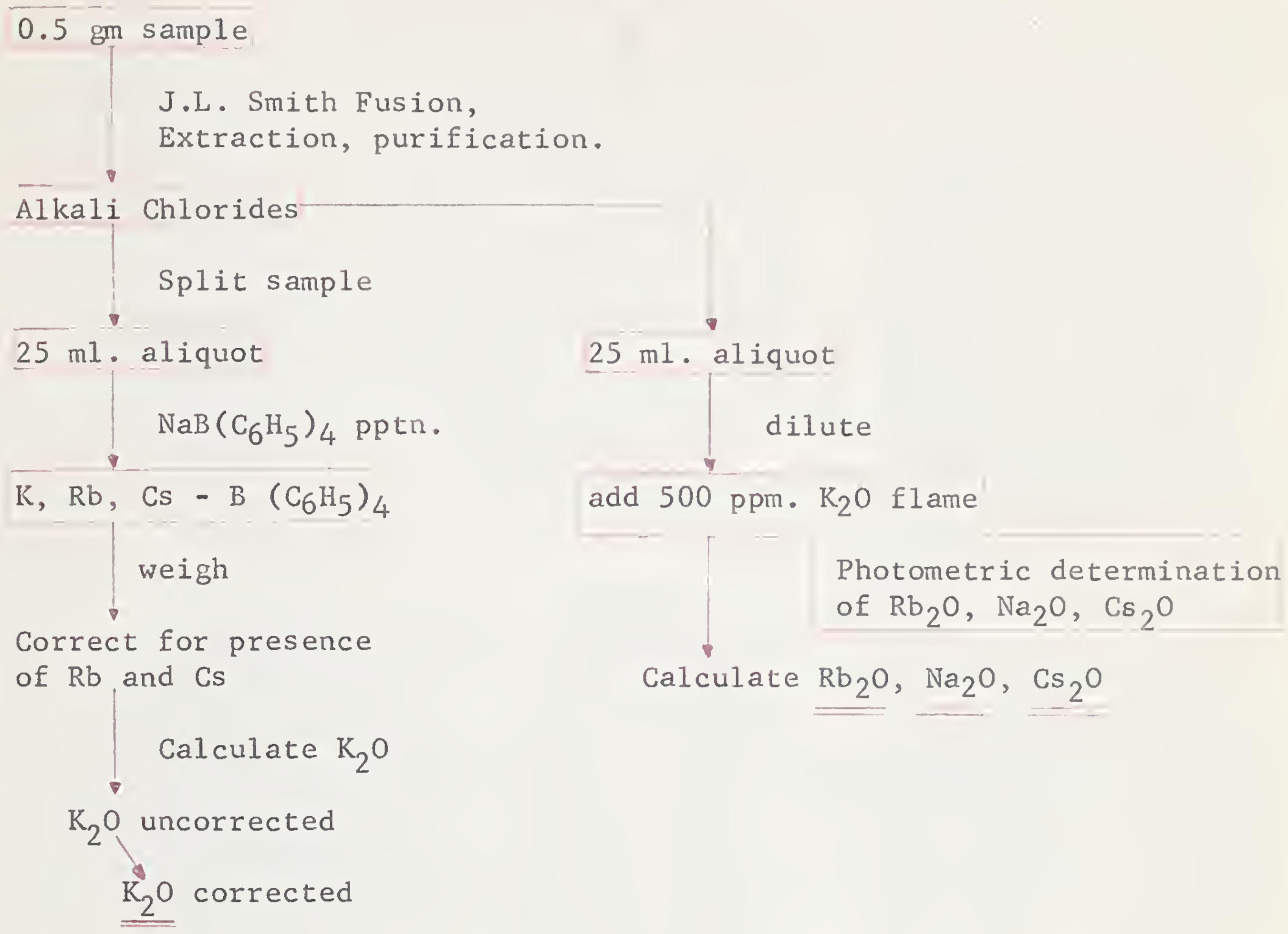
0.5 gm sample
J.L. Smith Fusion, Extraction, purification.
Alkali Chlorides
Split sample
25 ml. aliquot
$NaB(C_6H_5)_4$ pptn.
K, Rb, Cs - $B(C_6H_5)_4$
weigh
Correct for presence of Rb and Cs
Calculate K_2O
K_2O uncorrected
K_2O corrected
25 ml. aliquot
dilute
add 500 ppm. K_2O flame
Photometric determination of Rb_2O, Na_2O, Cs_2O
Calculate Rb_2O, Na_2O, Cs_2O

CO_2

.5 gm sample + $H_2O \xrightarrow{\Delta}$ boiling + dilute HCL acid to free carbonate

$\longrightarrow CO_2$

Volume of CO_2 from sample determined with a Fisher gas absorption train.

(CO_2 absorbed by KOH).

Corrected for temperature and barometric pressure.

EXPLANATION OF PLATE I

Photomicrographs of Heavy Minerals

Figure 1: Zircon, pale hyacinth, rounded with round dark inclusions; x 180; Sunset Peak Area, sample 3461-1.

Figure 2: Zircon, pale hyacinth, well rounded with dark inclusions; x 180; Sunset Peak Area, sample 3461-1.

Figure 3: Zircon, dark hyacinth, well rounded; x 180; Sunset Peak Area, sample 3461-1.

Figure 4: Zircon, pale hyacinth, well rounded with bipyramid overgrowth; x 180; Sunset Peak Area, sample 3461-1.

Figure 5: Zircon, pale hyacinth, rounded, fractured normal to C axis, dark inclusions, zoned; x 180; Sunset Peak Area, sample 3461-1.

Figure 6: Zircon, dark hyacinth, well rounded, dark inclusions, fissured; x 180; Sunset Peak Area, sample 3461-1.

Figure 7: Zircon, pale hyacinth, subrounded, dark inclusions, bipyramidal overgrowth on one end; 0.6 mm. long; Sunset Peak Area, sample 3461-5.

Figure 8: Zircon, hyacinth, well rounded, pitted surface; x 180; Sunset Peak Area, sample 3461-8.

Figure 9: Zircon, deep purple hyacinth, rounded; x 180; Sunset Peak Area, sample 3461-10.

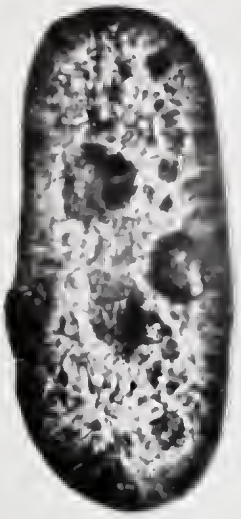

1

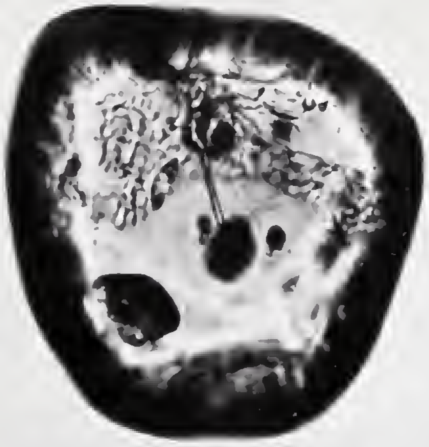

2

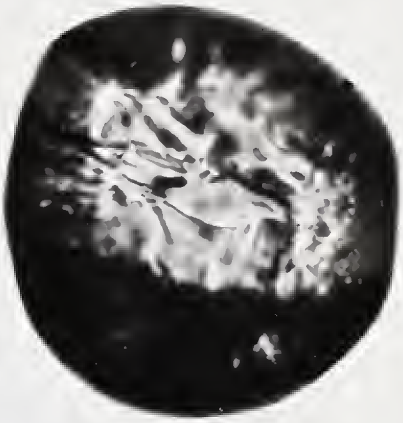

3

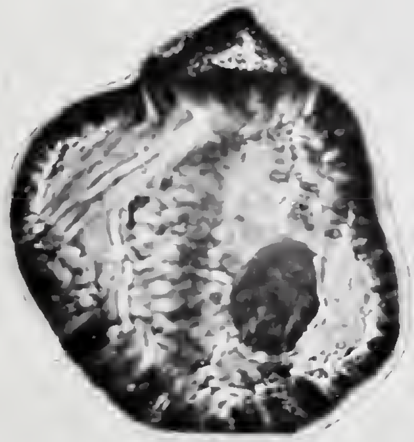

4

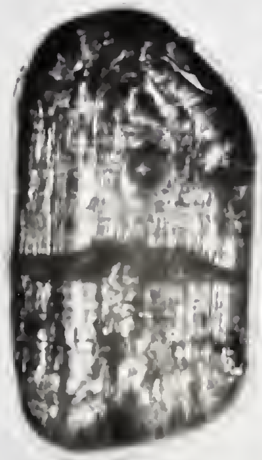

5

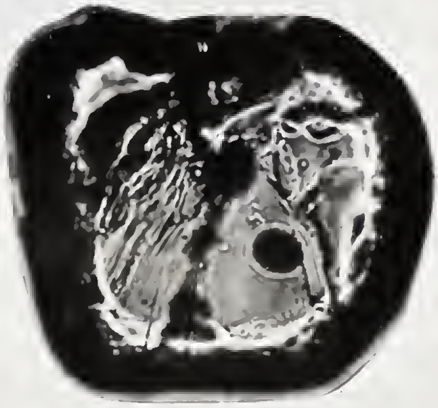

6

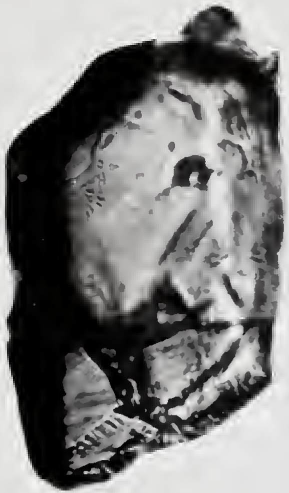

7

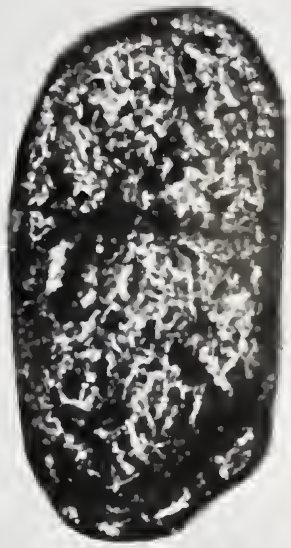

8

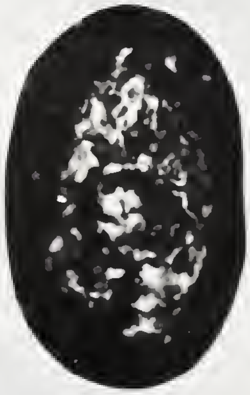

9

PLATE I

EXPLANATION OF PLATE II

Photomicrographs of Heavy Minerals

Figure 1: Zircon, pale-brown, rounded with brown inclusion or core; 0.4 mm. long, Nigel Pass Area, sample 3462-8.

Figure 2: Zircon, hyacinth, tabular, rounded, faintly zoned, colourless overgrowth on right side; x 180; Nigel Pass Area, sample 3462-8.

Figure 3: Zircon, pale hyacinth, well rounded, partly pitted surface; 0.3 mm. diameter; Nigel Pass Area, sample 3462-16.

Figure 4: Zircon, dark reddish-brown, subhedral, dark core with radiating fissures; 0.3 mm. long; Nigel Pass Area, sample 3462-16.

Figure 5: Zircon, deep-purple hyacinth, subhedral with dark core; 0.3 mm. long; Nigel Pass Area, sample 3462-16.

Figure 6: Zircon, dark reddish-brown, subhedral, dark core; 0.3 mm. long; Nigel Pass Area, sample 3462-16.

Figure 7: Zircon, deep-purple hyacinth, subrounded, fissured parallel to C axis; 0.25 mm. long; Nigel Pass Area, sample 3462-16.

Figure 8: Zircon, dark-reddish-brown, tabular, subrounded; 0.25 mm. long; Nigel Pass Area, sample 3462-16.

Figure 9: Zircon, deep-purple hyacinth, subhedral, dark core with zoning; 0.3 mm. long; Nigel Pass Area, sample 3462-16.

Figure 10: Zircon, hyacinth, subhedral, dark inclusions; 0.25 mm. long; Nigel Pass Area, sample 3462-16.

Figure 11: Zircon, dark-brown, euhedral with partially developed colourless overgrowth on right side; 0.3 mm. long; Nigel Pass Area, sample 3462-16.

Figure 12: Zircon, dark-brown, euhedral, fractured; 0.3 mm. long; Nigel Pass Area, sample 3462-16.

Figure 13: Zircon, dark-reddish-brown, euhedral, dark core with radiating microfissures, poorly zoned; 0.3 mm. long; Nigel Pass Area, sample 3462-16.

Figure 14: Zircon, dark-reddish-brown, euhedral, dark core, zoned; 0.4 mm. long; Nigel Pass Area; sample 3462-16.

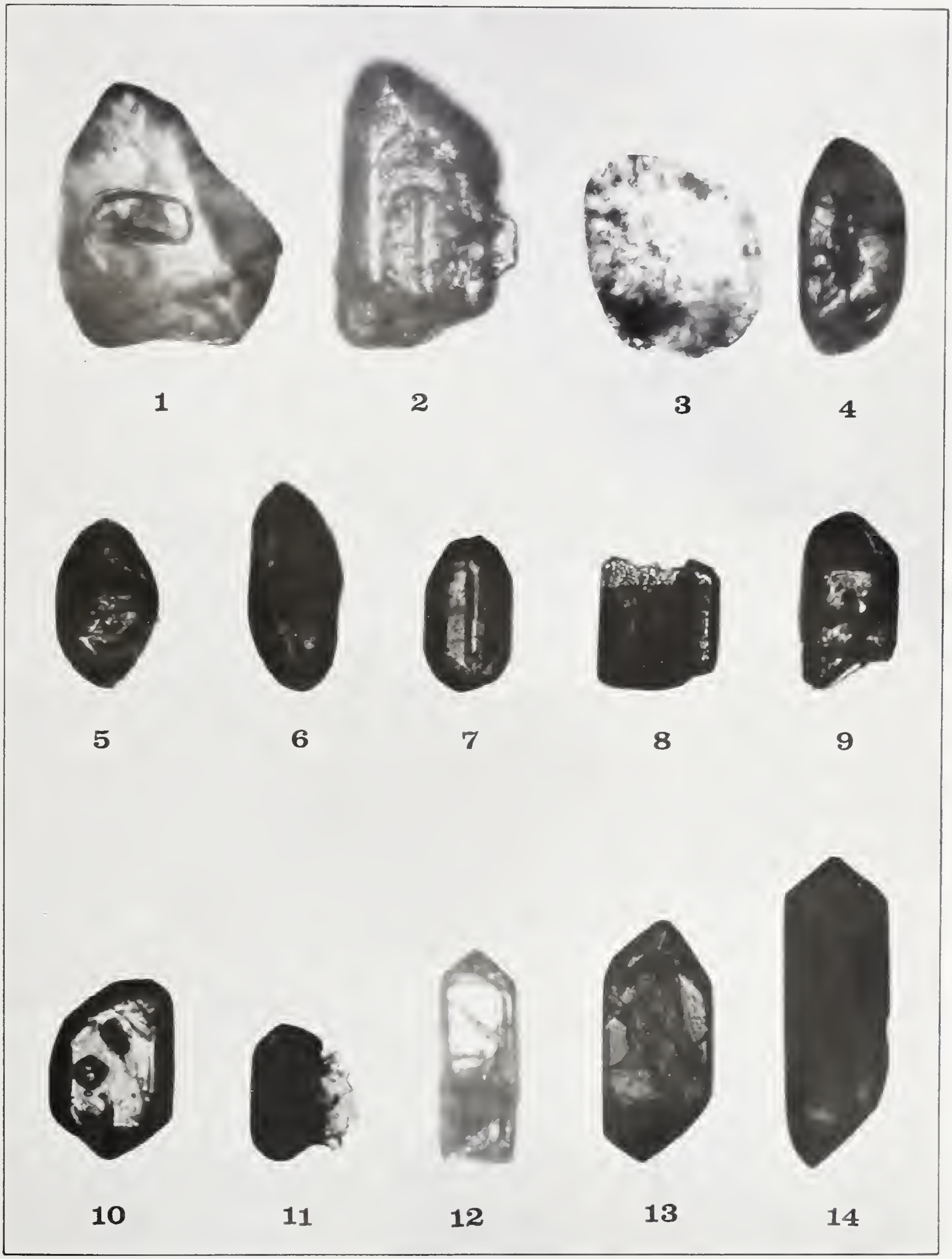
1
2
3
4
5
6
7
8
9
10
11
12
13
14

PLATE 2

EXPLANATION OF PLATE III

Photomicrographs of Heavy Minerals

1. Tourmaline, deep-blue, angular, with bubble inclusions, 0.4 mm. long, sample 3462-8.

2. Tourmaline, green, corners rounded, bubble inclusions, 0.4 mm. long, sample 3462-16.

3. Tourmaline, brown, rounded, bubble inclusions, 0.4 mm. diameter, sample 3462-16.

4. Tourmaline, brown, subhedral, bubble inclusions, faint colourless overgrowth at top end, length of grain 0.4 mm, sample 3462-16.

5. Apatite, pale-yellow, subhedral, few bubble inclusions, 0.4 mm. long, sample 3462-16.

6. Apatite, pale-yellow, subhedral, rounded, pitted surface, bubble inclusions, 0.3 mm. long, sample 3462-16.

7. Apatite, pale-yellow, well rounded, smooth surface, rare bubble inclusion, 0.3 mm. long, sample 3462-8.

8. Barite, tabular, colourless, dark with iron staining, bubble inclusions numerous, 0.3 mm. long, sample 3462-8.

9. Barite, colourless, irregularly fractured, dark rims and inclusions hematite, numerous bubble inclusions, 0.4 mm. long, sample 3462-8.

10. Barite, colourless, euhedral, numerous bubble and opaque (hematite?) inclusions; x 180; sample 3462-8.

1

2

3

4

5

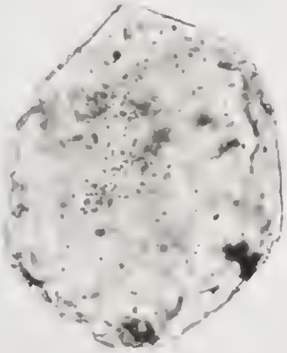
6

7

8

9

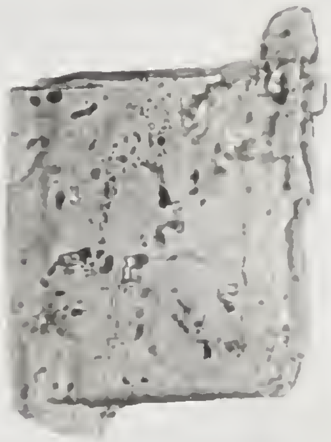
10

PLATE 3

EXPLANATION OF PLATE IV

Photomicrographs of Glauconite

Specimens 1 to 10 after HCL acid treatment.

1. Glauconite; lobate grain with nodular surface, 0.7 mm. long; sample 3461-6.

2. Glauconite; rounded grain with nodular surface, 0.6 mm. long; sample 3461-6.

3. Glauconite; well developed lobate grain, 0.7 mm. long; sample 3461-6.

4. Glauconite, nodular, 0.6 mm. long; sample 3461-6.

5. Glauconite; external mould with smooth surface, calcite originally in center; 0.6 mm. long; sample 3461-6.

6. Glauconite, nodular and pitted surface, 0.6 mm. long; sample 3461-6.

7. Glauconite; nodular grain, 0.6 mm. long; sample 3461-6.

8. Glauconite pellet, interior originally composed of calcite, 0.6 mm. long; sample 3461-6.

9. Glauconite, knobby surface, 0.3 mm. long; sample 3461-6.

10. Rounded coarse sand grain cemented to glauconite pellet of similar size, 0.6 mm. long, sample 3461-6.

11,12. Glauconite, mounted in Canada balsam, rounded outline, lobate; x-nicols x 120; sample 3461-5.

13. Glauconite, mounted in Canada balsam, subrounded; light-grey tinge on edges due to thinness of grain; x-nicols x 120; sample 3461-4.

1

2

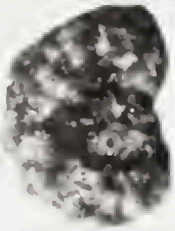

3

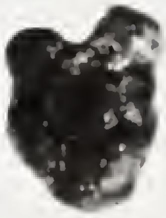

4

5

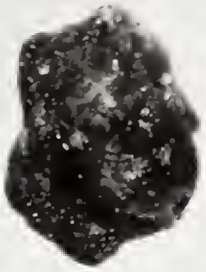

6

7

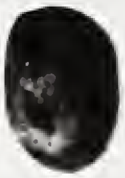

8

9

10

11

12

13

PLATE 4

EXPLANATION OF PLATE V

Photomicrographs of Thin Sections

Figure 1: Specimen 3462-2; Calcilutite; dark-grey and white grains cryptocrystalline calcite, cut by horizontal veins of fine-grained calcite; x 32; Nigel Pass Area; described on page III.

Figure 2: Specimen 3462-3; Calcilutite; dark-grey cryptocrystalline calcite, light-grey grains coarse crystalline calcite infilling patches and stringers; x 32; Nigel Pass Area; described on page III.

Figure 3: Specimen 3462-4; Calcilutite; white grains quartz, grey grains medium crystalline calcite, black grains cryptocrystalline calcite; quartz grains "float" in calcite groundmass; x 31; Nigel Pass Area;

Figure 4: Specimen 3462-6; Quartz arenite; rounded light-grey to white grains quartz, light-grey grains with cleavage calcite, dark-grey grains with cleavage dolomite; x 32; Nigel Pass Area; described on page V.

1

2

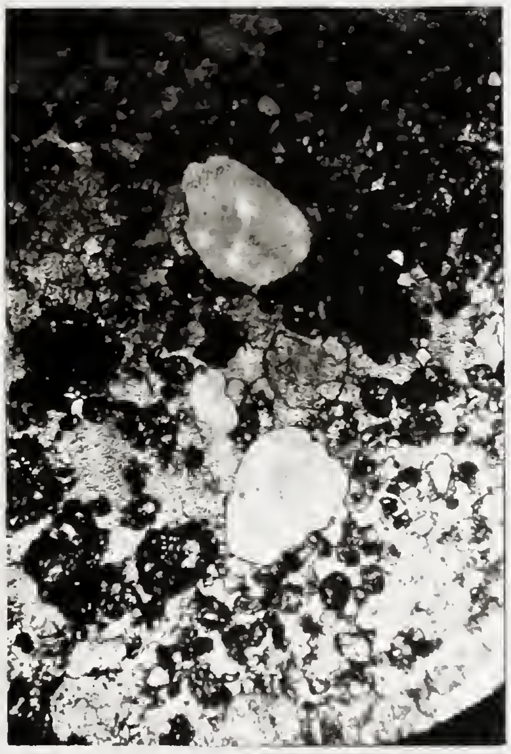

3

4

PLATE 5

EXPLANATION OF PLATE VI

Photomicrographs of Thin Sections

Figure 1: Specimen 3461-9; Pisolitic hematitic sandstone; rounded white fragments are quartz, dark-grey to black material hematite. Note rounded quartz nucleus surrounded by rims of light-grey cryptocrystalline to fine-crystalline calcite; x 120; Sunset Peak Area; described on page XVIII.

Figure 2: Specimen 3461-10; Calcarenite; light-grey grains with cleavage calcite, subrounded medium-grey grain in center is glauconite impregnated with irregular black grains of hematite; x 60; Sunset Peak area; described on page XIX.

Figure 3: Specimen 3462-10; Quartz arenite; light-grey grains are quartz, dark material infilling grain boundaries is hematite; x 36; Nigel Pass Area.

Figure 4: Specimen 3462-16; Metamorphosed arkosic arenite; white grains are quartz, light-grey grains with cleavage are potash feldspars, rounded patchy white and grey grain at bottom is quartzite; x 120; Nigel Pass Area; described on page XI.

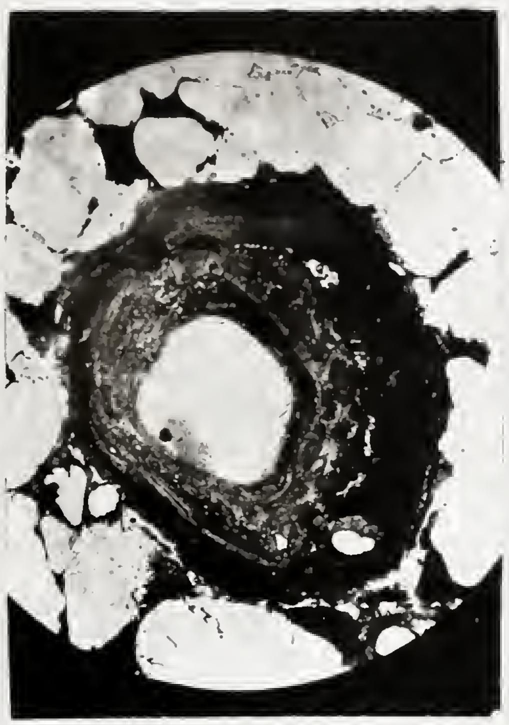

1

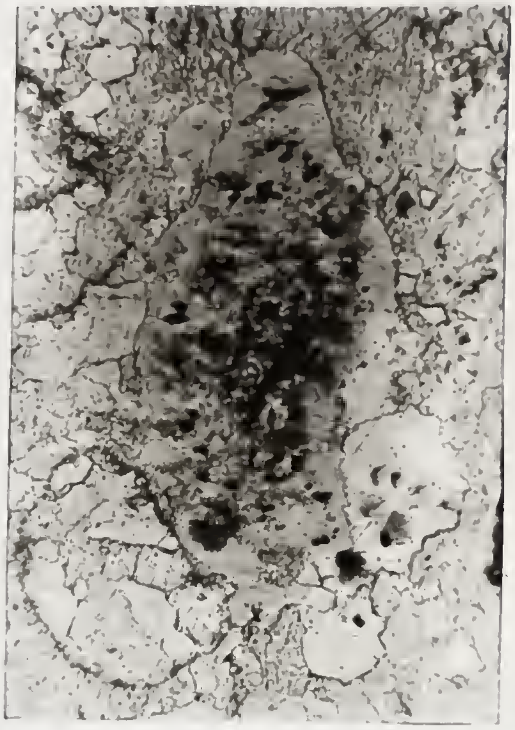

2

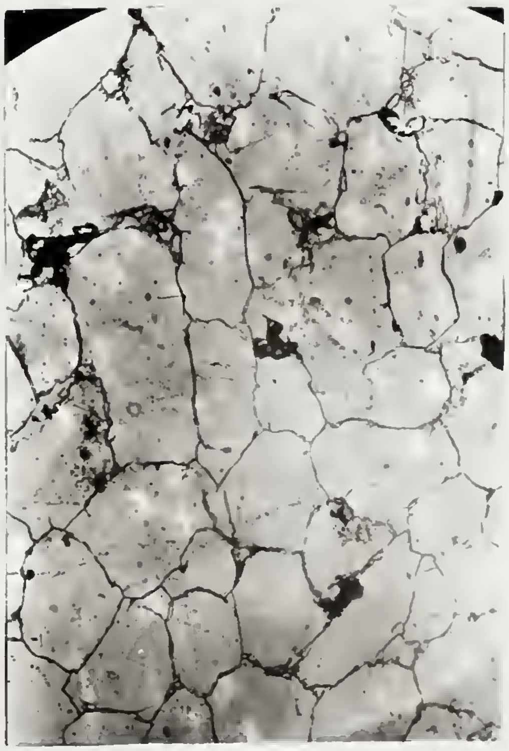

3

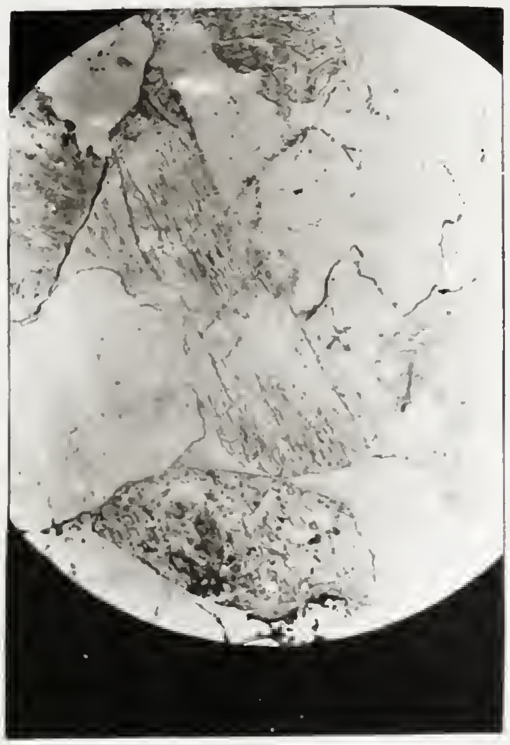

4

PLATE 6

EXPLANATION OF PLATE VII

Photomicrographs of Thin Sections

Figure 1: Specimen 3461-6; Bioclastic arenaceous calcarenite; white fragments are quartz, light-grey fragments calcite, black fossil fragment trilobite(?) appendage composed of collophane; x 20; Sunset Peak Area; described on page XVII.

Figure 2: Specimen 3461-6; Bioclastic arenaceous calcarenite; white fragments quartz, grey fragments calcite, dark-grey fossil fragment Archaeocyathidae composed of collophane; x 15; Sunset Peak Area; described on page XVII.

Figure 3: Specimen 3461-5; Glauconitic fossiliferous arenaceous calcarenite; white and grey fragments calcite, inked outline of arthropod(?) fragment showing internal segmentation; x 15; Sunset Peak Area; described on page XVI.

Figure 4: Specimen 3461-12A; Pisolitic (algal) calcilutaceous siltstone; dark-grey and white mass outside algae composed of cryptocrystalline calcite with quartz, horseshoe-shaped light-grey fragment organic shell, rounded grey fragments on inside of horseshoe-shaped shell echinoderm fragments which may be a form associated with Gogia; x 5; Sunset Peak Area; described on page XXI.

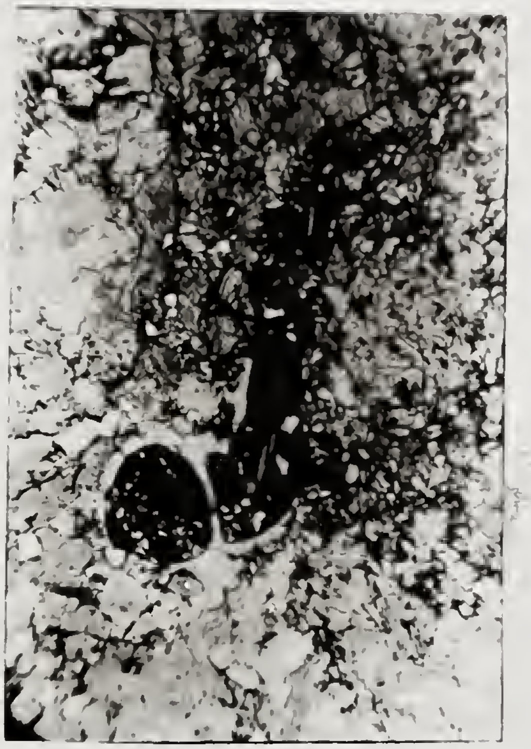

1

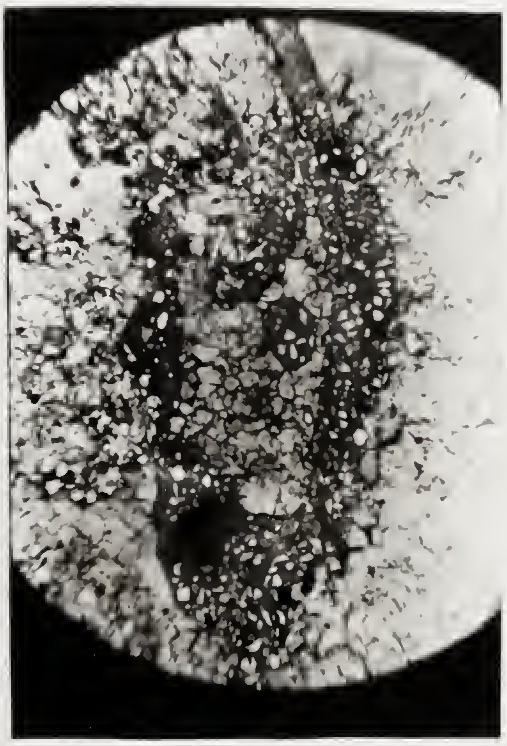

2

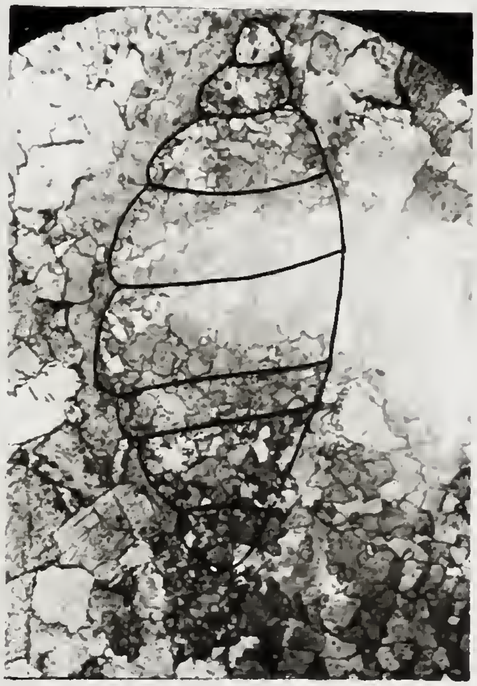

3

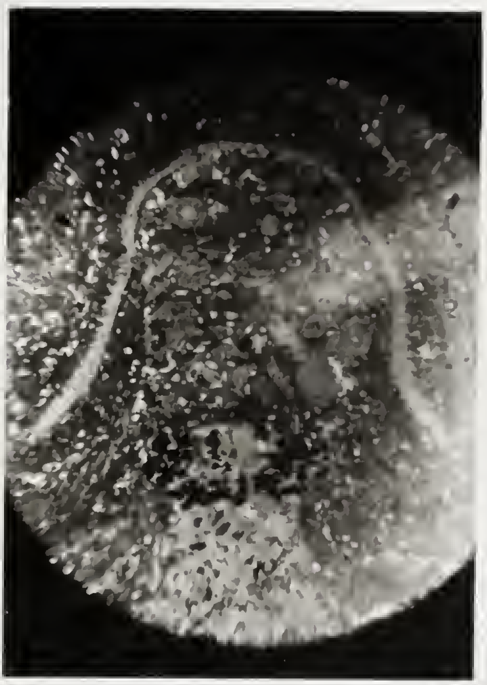

4

PLATE 7

EXPLANATION OF PLATE VIII

Photomicrographs of Thin Sections

Figure 1: Specimen 3462-8; Quartz arenite; rounded light-grey grains are quartz, rimmed with iron oxides and authigenic silica cement. Dark grains in center are calcite and/or dolomite contaminated with limonite; x 52; Nigel Pass Area; described on page VI.

Figure 2: Specimen 3461-5; Glauconitic fossiliferous arenaceous calcarenite; grains surrounding pellet are dolomite, pellet composed of collophane, with glauconite, medium-grey, dolomite, dark-grey, and hematite, black, inside of pellet; x 50; Sunset Peak Area; described on page XVI.

Figure 3: Specimen 3461-11A; Oolitic calcarenite; organic pellet infilled with rounded glauconite grains, white, irregularly shaped organic fragments, white and dark, dark-grey material calcite. Pellet surrounded by dark calcite and quartz, white; x 120; Sunset Peak Area; described on page XIX.

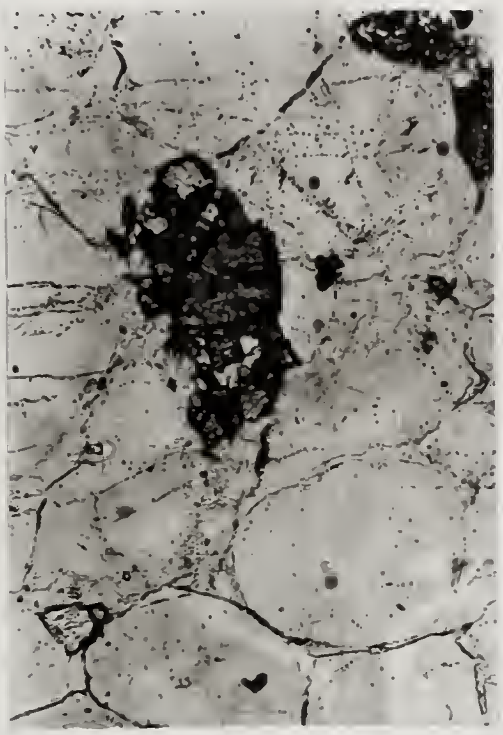

1

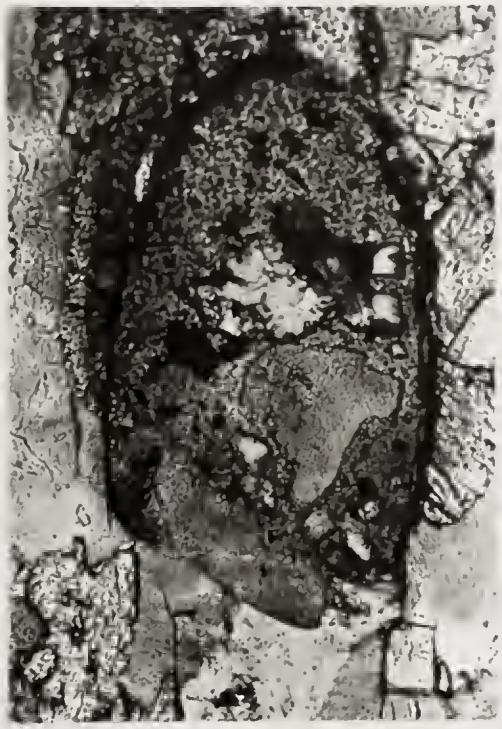

2

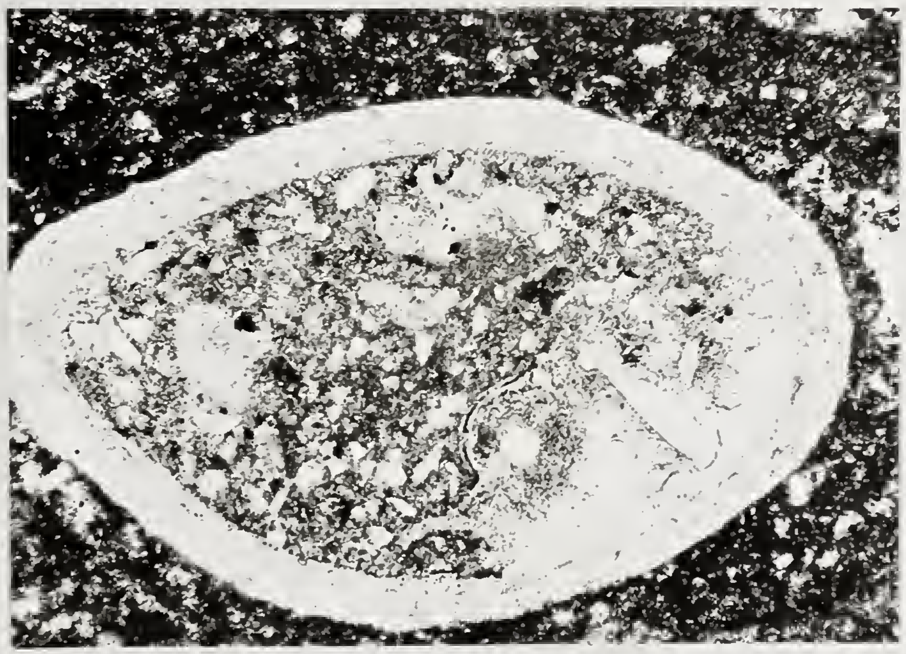

3

PLATE 8

EXPLANATION OF PLATE IX

Photomicrographs of Thin Sections

Figure 1: Specimen 3461-6; Bioclastic arenaceous calcarenite; cross-section of trilobite(?) spine. Dark material collophane and glauconite. Vacuole on right, white. Rim of spine calcite or dolomite. Spine surrounded by dolomite. White grains in matrix are quartz; x 120; Sunset Peak Area; described on page XVII.

Figure 2: Specimen 3461-5; Glauconitic fossiliferous arenaceous calcarenite; glauconite grain in center surrounded by a mosaic of dolomite; x 130; Sunset Peak Area; described on page XVI.

Figure 3: Specimen 3461-6; Bioclastic arenaceous calcarenite; organic fragment on right largely replaced by dolomite, with collophane, glauconite and quartz inside fragment. Matrix is anhedral dolomite, grey, and rounded quartz grains, white; x 52; Sunset Peak Area; described on page XVII.

Figure 4: Specimen 3461-3; Quartz arenite; collophane on right, rounded, fractured and broken tourmaline grain in center, surrounded by quartz, white; x-nicols; x 130; Sunset Peak Area; described on page XIV.

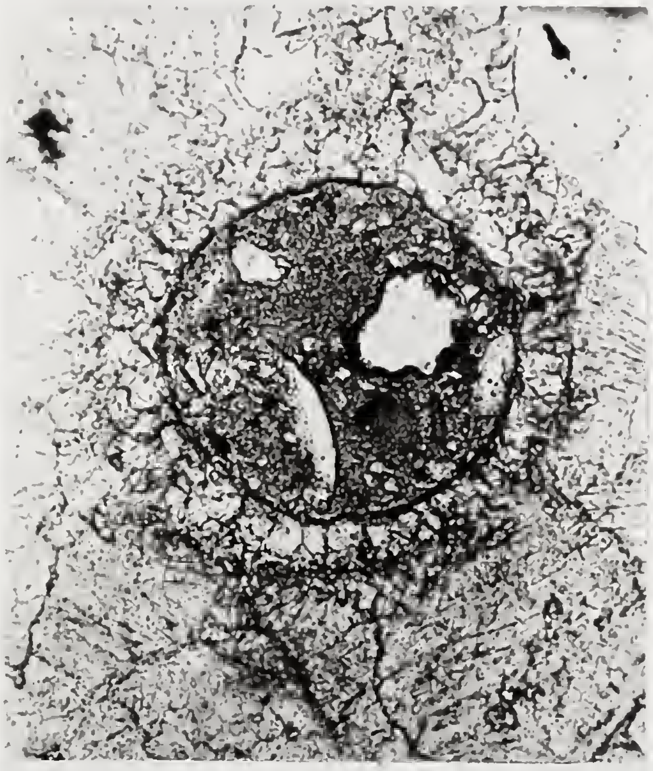

1

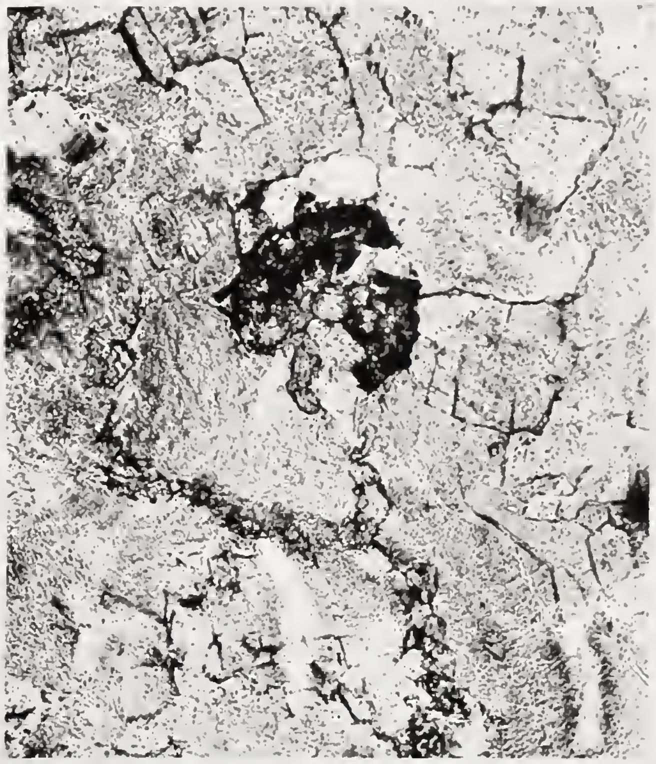

2

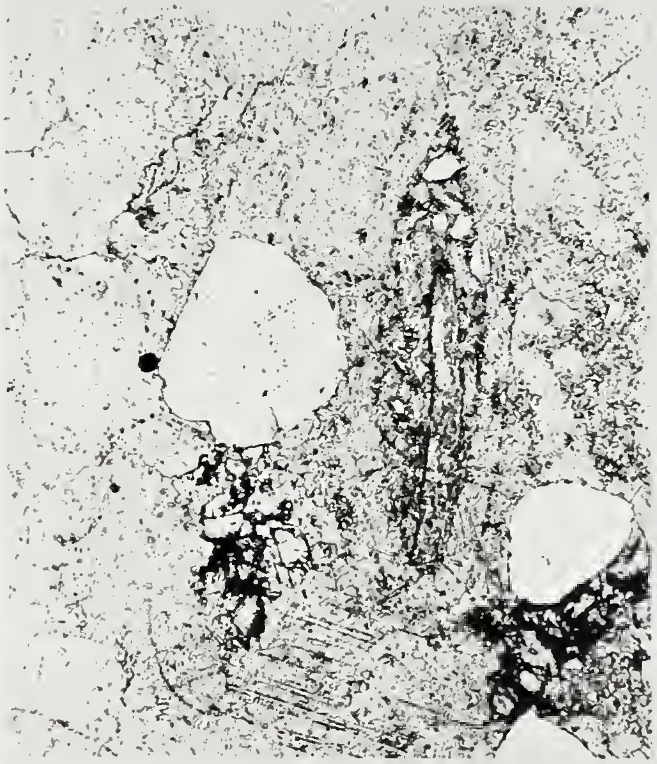

3

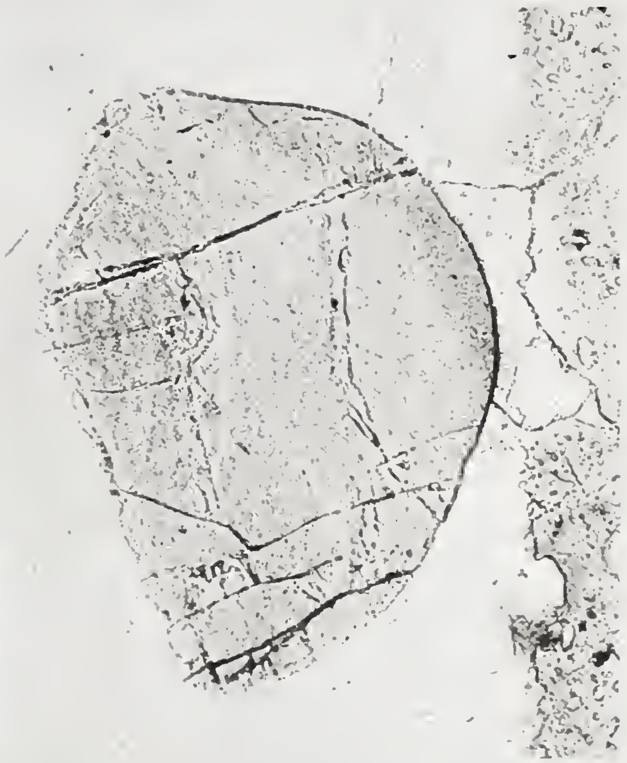

4

PLATE 9

EXPLANATION OF PLATE X

Photomicrographs of Thin Sections

Figure 1: Specimen 3461-9; Pisolitic hematite sandstone; hematite black, rolled with quartz and calcite in center. Pisolith surrounded by quartz grains, white; x 120; Sunset Peak Area; described on page XVIII.

Figure 2: Specimen 3461-13; Micaceous calcilutaceous siltstone; phlogopite mica orientated parallel to the bedding, black. Lighter grey material cryptocrystalline calcite. White grains quartz; x 120; Sunset Peak Area; described on page XXII.

Figure 3: Specimen 3462-11; Quartz arenite; rounded quartz grains surrounded by cement of authigenic quartz and hematite; x 180; Nigel Pass Area; described on page VIII.

Figure 4: Specimen 3462-15: Subarkosic (ortho) conglomerate; rounded quartz grains composing quartzite pebble in upper left. Matrix marked by subrounded to angular feldspar (microcline) and white quartz grains, cemented by authigenic quartz and sericite; x-nicols; x 50; Nigel Pass Area; described on page X. For photograph of hand specimen see Plate II fig. 4.

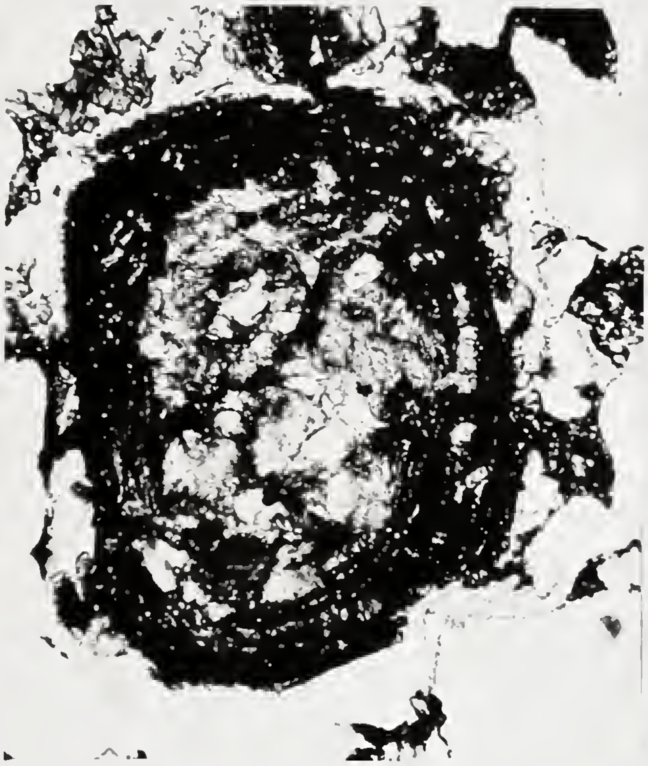

1

2

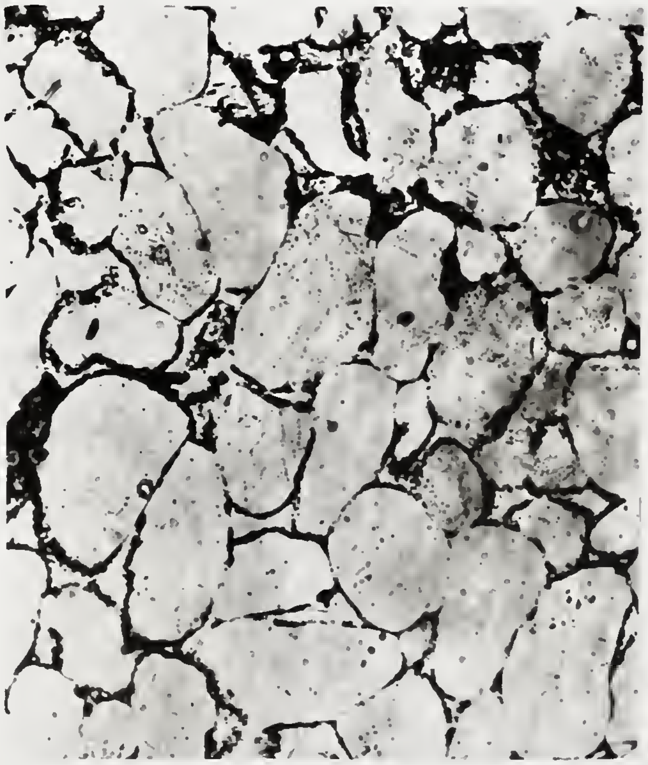

3

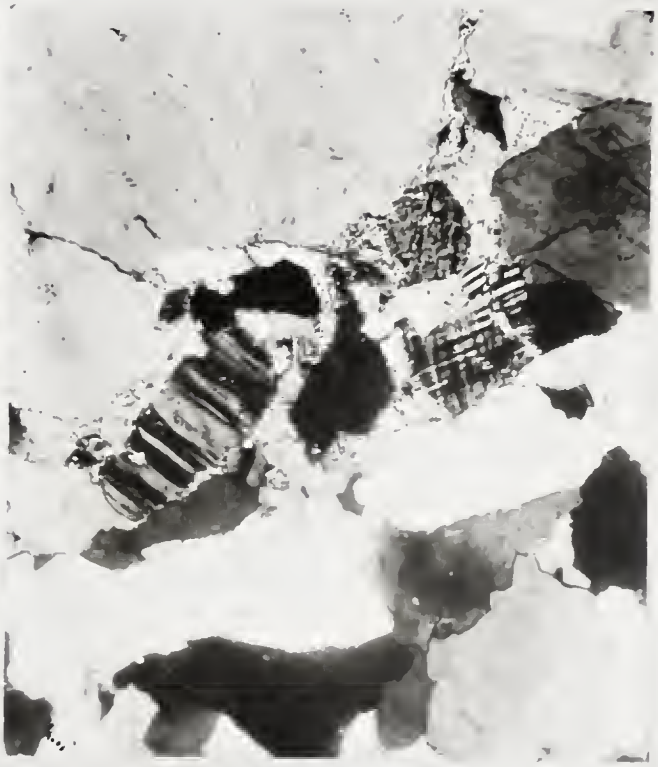

4

PLATE 10

EXPLANATION OF PLATE XI

Figure 1: Photomicrograph of thin section, specimen 3461-3; Quartz arenite; needle aggregates of sphene(?) or rutile(?) embedded in quartz matrix; x 180; Sunset Peak Area; described on page XIV.

Figure 2: Photomicrograph of thin section, specimen 3461-11A; Oolitic calcarenite; well rounded calcite oolites surrounded by cryptocrystalline calcite; x 50; Sunset Peak Area; described on page XIX.

Figure 3: Photograph of hand specimen 3462-7; Algal limestone; Nigel Pass Area; thin section described on page V.

Figure 4: Photograph of hand specimen 3462-15; Subarkosic (Ortho) conglomerate; Nigel Pass Area; thin section described on page X, microphotograph of thin section on Plate 10, fig. 4.

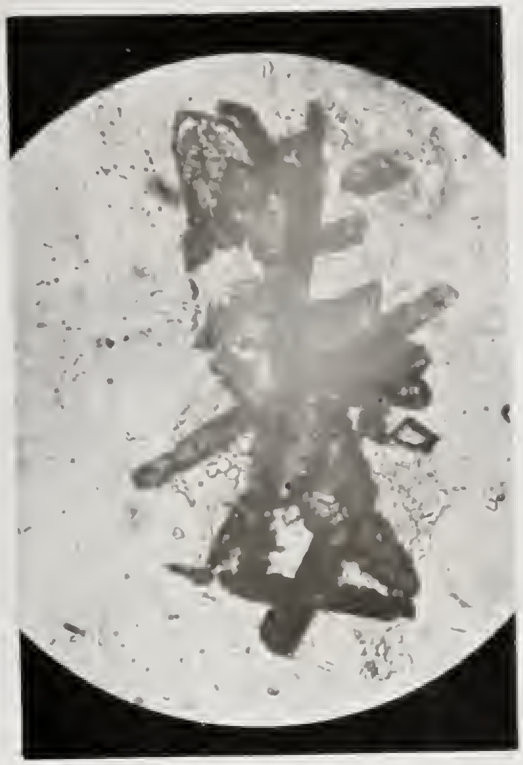

1

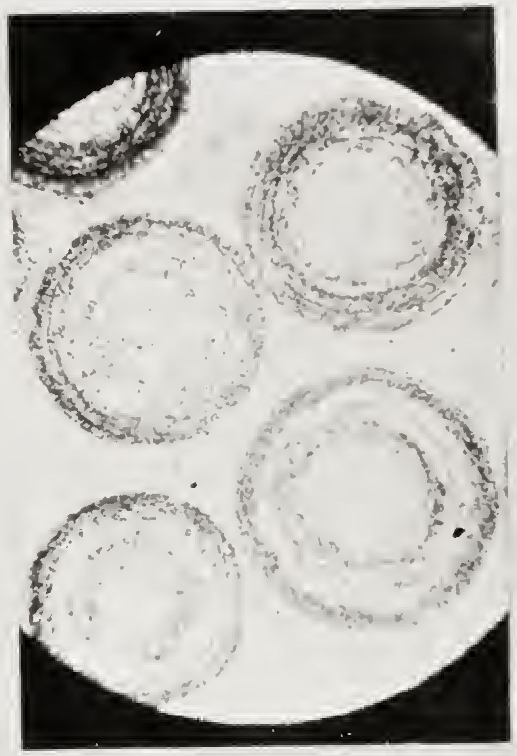

2

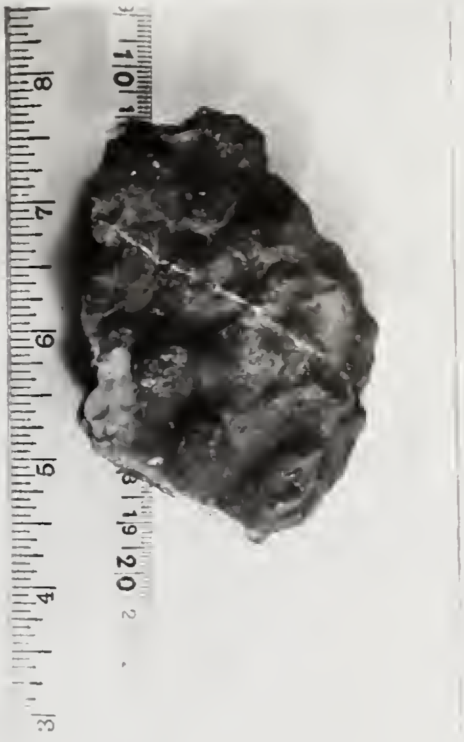

3

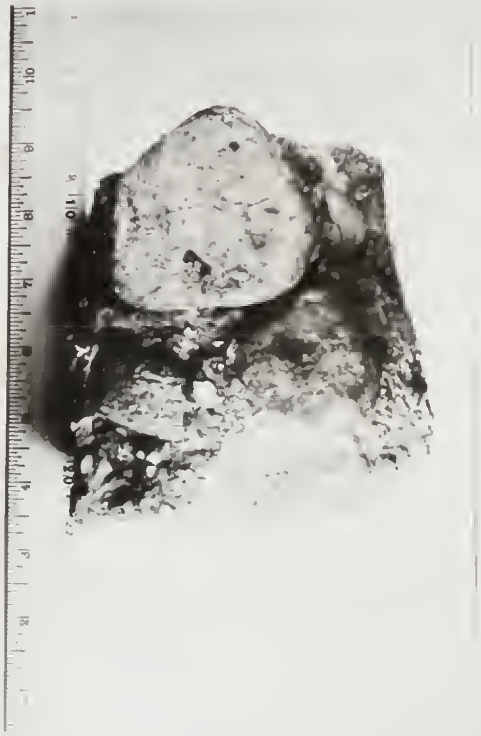

4

PLATE II

B29784